DOKUZ EYLÜL UNIVERSITY
GRADUATE SCHOOL OF NATURAL AND APPLIED SCIENCES

NUMERICAL ANALYSIS OF ABSORBERS USED IN LiBr / H_2O ABSORPTION REFRIGERATION

by
Sercan ACARER

August, 2010
İZMİR

NUMERICAL ANALYSIS OF ABSORBERS USED IN LiBr / H_2O ABSORPTION REFRIGERATION

A Thesis Submitted to the
Graduate School of Natural and Applied Sciences of Dokuz Eylül University
In Partial Fulfillment of the Requirements for the Degree of Master of Science
in Mechanical Engineering, Thermodynamics Program

by

Sercan ACARER

August, 2010
İZMİR

M.Sc THESIS EXAMINATION RESULT FORM

We have read the thesis entitled **"NUMERICAL ANALYSIS OF ABSORBERS USED IN LiBr / H_2O ABSORPTION REFRIGERATION"** completed by **SERCAN ACARER** under supervision of **PROF. DR. NURİ KAYANSAYAN** and we certify that in our opinion it is fully adequate, in scope and in quality, as a thesis for the degree of Master of Science.

Prof. Dr. Nuri KAYANSAYAN

Supervisor

(Jury Member)

(Jury Member)

Prof.Dr. Mustafa SABUNCU
Director
Graduate School of Natural and Applied Sciences

ACKNOWLEDGMENTS

I would like to thank Prof. Dr. Nuri Kayansayan for his unfailing guidance, support and supervision throughout this study. I am deeply grateful to my jury members; Dr. Moghtada Mobedi and Dr. Serhan Küçüka, who encouraged and helped me to improve my thesis. I would like to thank Dr. Ünver Özkol for his support and Dr. V. D. Papaefthimiou for sending a valuable paper. Also I would like to thank my friends Ersen and Çağlar and my labmates; Orçun, Gürcan, Necati, İbrahim, Shankaransh and Ali for their support. My parents; Faruk and Leyla, and my sister Ecem have always encouraged and supported my decisions.

Sercan ACARER

NUMERICAL ANALYSIS OF ABSORBERS USED IN LiBr / H_2O ABSORPTION REFRIGERATION

ABSTRACT

Vapour absorption of LiBr-H_2O solution flowing over water cooled vertical and horizontal tubes in the form of falling film is investigated numerically. Although only LiBr-H_2O solution is investigated, the present model can be applied to any other absorbent-absorbate pairs as long as the absorbent is nonvolatile. Because ammonia is volatile, the present model is not appropriate for NH_3-H_2O pair. As analytical investigation of the process without many assumptions is impossible due to the complex and coupled nature of the problem, numerical models using finite volume formulations are created for both geometries. Nusselt's solution is used for film hydrodynamics for both geometries, however it is modified slightly to allow for a change in film thickness with absorption of vapour and change in physical properties. It is observed that this modification improves accuracy of the simulation by reducing error greatly in conservation of species. Rectangular Eulerian grid is used for vertical absorber model, and body-fitted physical Eulerian grid is used for horizontal absorber model by performing a coordinate transformation. Coupled energy and species transport equations are solved numerically. Because the boundary conditions at the tube wall and film surface are not known, a multi iterative process is employed. Also one dimensional energy balance was employed for the cooling water side and bulk temprature distribution of the cooling water is obtained by an iterative procedure. Local physical properties are updated at each iteration. Results for both models are compared with experimental data available in the literature and it is shown that agreement is very good under most common conditions.

Keywords: Absorber, LiBr, mass transfer, absorption refrigeration.

LiBr / H_2O ABSORPSİYONLU SOĞUTMA SİSTEMİ ABSORBER NÜMERİK ANALİZİ

ÖZ

Bu çalışmada su soğutmalı yatay ve dikey borular üzerinden film tabakası şeklinde akan LiBr-H_2O çözeltisinin buharı emme işlemi nümerik olarak incelenmiştir. Sadece LiBr-H_2O çözeltisi incelenmiş olmasına karşılık, üretilen model emici madde uçucu olmadığı sürece herhangibir çözelti-gaz çiftine de uygulanabilir. Amonyak uçucu olduğu için bu model NH_3-H_2O çiftine uygun değidir. Analitik çözümleme problemin karmaşıklığı ve ısı-kütle transferinin birbirine çok güçlü bir şekilde bağlı olması sebebiyle birçok basitleştirici varsayım yapmadan mümkün değildir. Bu sebeple her iki geometri için kontrol hacmi metoduna dayalı nümerik modeller oluşturulmuştur. Film hidrodinamiği için Nusselt'in analitik çözümü kullanılmıştır, ancak bu çözüm, film kalınlığının buhar emilimi ve fiziksel özelliklerin yerel değişimine bağlı olarak değişmesine imkan verecek şekilde değiştirilmiştir. Bu değişikliğin sistemin kütle dengesinde önemli iyileşmeler sağladığı gözlemlenmiştir. Nümerik ayrıştırma için kullanılan ızgara yapısı uzayda sabit olup dikey absorber modeli için dikdörtgen yapıda, yatay absorber modeli için geometri uyumlu yapıdadır. Enerji ve kütle taşınım denklemleri bu ızgara yapıları kullanılarak nümerik olarak ayrıştırılmış ve film yüzeyinde ve boru duvarında sınır şartları bilinmediği için çoklu iteratif yöntemlerle çözülmüştür. Yerel fiziksel özellikler her iterasyon öncesi güncellenmiştir. Boru içinde akan soğutucu su için bir boyutlu enerji dengesi kurulmuştur ve iteratif yolla bir boyutlu soğutucu su sıcaklık dağılımı elde edilmiştir. Her iki modelden elde edilen sonuçlar literatürdeki deneysel sonuçlarla kıyaslanmış ve yaygın olarak kullanılan şartlarda deneysel sonuçlarla çok iyi derecede anlaşma gözlemlenmiştir.

Anahtar sözcükler: Absorber, LiBr, kütle aktarımı, absorpsiyonlu soğutucular.

CONTENTS

Page

CHAPTER ONE
INTRODUCTION

1.1 LiBr/H_2O Based Absorption Refrigeration Systems

Absorption cooling systems, which use heat as the driving force, are an alternative to electrical or mechanical-driven conventional gas compression cooling systems. Although absorption cooling technology has been known and used for over a hundred years, gas compression systems have usually been more economical, maintenance-free and more effective especially for small-scale applications.

As the cost of conventional energy sources and the demand to alternative energy sources have increased in recent decades, and as the gas compression systems contain chlorofluorocarbons which is harmful to environment; absorption cooling systems became a more competitive and environmentally friendly (Tsai & Perez-Blanco, 1998) alternative especially if there is a cheap heat source exists such as geothermal energy, waste heat, solar energy, etc.

1.1.1 Pairs in Absorption Refrigeration

An absorption cooling cycle utilizes a working pair, one of them is the refrigerant (or absorbate) and the other one is the absorbent. The most common used pairs are the LiBr / water and ammonia / water pairs but other pairs also exist.
For the LiBr / water pair, water is the refrigerant and the LiBr salt is the absorbent; For the ammonia / water pair, ammonia is the refrigerant and the water is the absorbent.

The use of ammonia as a refrigerant is advantegeous over water because evaporation temperature of ammonia is lower than that of water at the same pressure. On the other hand; nonvolatileness and high affinitiness to vapour of the LiBr salt

with additives is advantegeous over ammonia-water pair because absorption performance is higher. However, solubility of LiBr salt in water is limited which makes crystallisation possible when the temperature falls (Florides, Kalogirou, Tassou, & Wrobel, 2003).

Although the basic working principle of all kinds of absorption refrigerators are very similar to each other, each must be investigated seperately because of some minor differences. Hence absorption cycles using pairs other than LiBr/H_2O will not be in the scope of this study and the expression "absorption refrigerator" will refer to a LiBr/H_2O based absorption refrigerator.

1.1.2 Working Principle of LiBr/H_2O Based Absorption Refrigerators

Instead of compressing the gas as done in gas compression systems, an absorption refrigerator produces the same compression effect by absorbing and consequently desorbing the refrigerant.

In the absorption refrigerators, vapour is absorbed at low pressure in the absorber and consequently desorbed at high pressure in the generator by a heat source. The desorbed vapour is condensed in the condenser by rejecting heat to ambient and consequently evaporates in the evaporator at low temperature and refrigerates process water. Consequently it is absorbed in the absorber (rejects heat to ambient), and dilutes the concentrated solution (in terms of LiBr) supplied from the generator. The diluted solution is pumped to the generator and concentrated there by boiling water component in it using a heat source. The boiled vapour again goes to the condenser, and the concentrated solution goes to the absorber to be diluted again.

Performance and efficiency of the system can be increased by using the heat of the already boiled vapour to boil more refrigerant vapour from the weak solution as the main heat source does, then the cycle is named as double-effect absorption cycle (see Figure 1.5) (Qu, 2008).

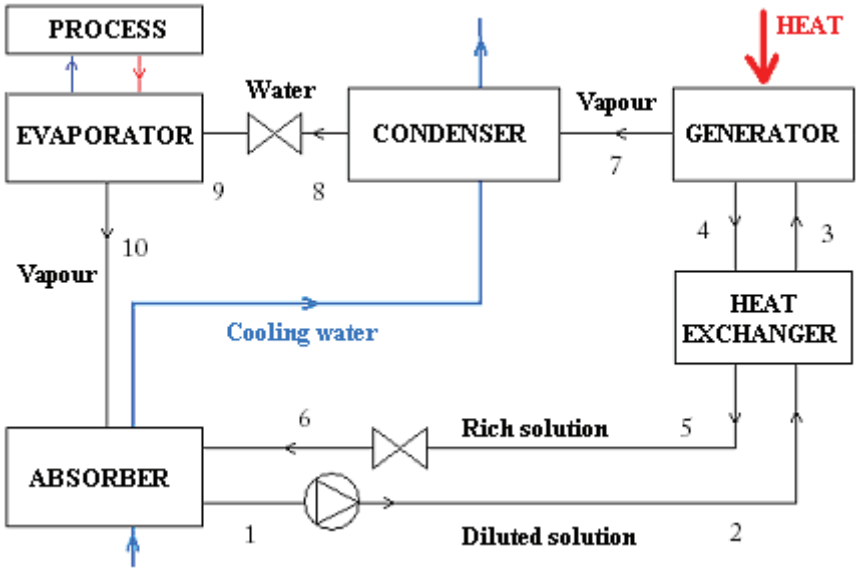

Figure 1.1 Flow diagram for a single-stage absorption cycle.

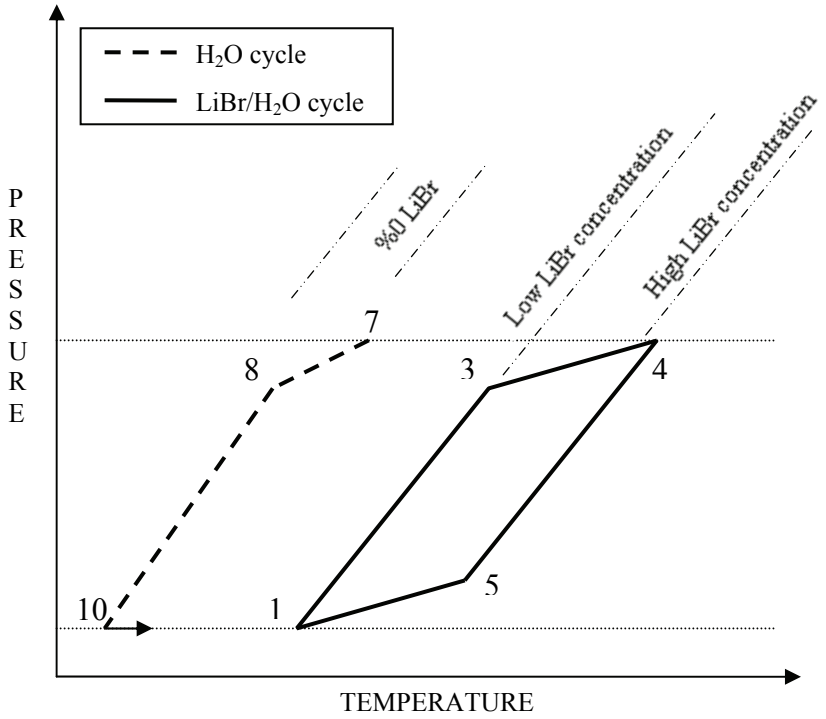

Figure 1.2 Pressure- temperature diagram of a single-stage absorption cycle.

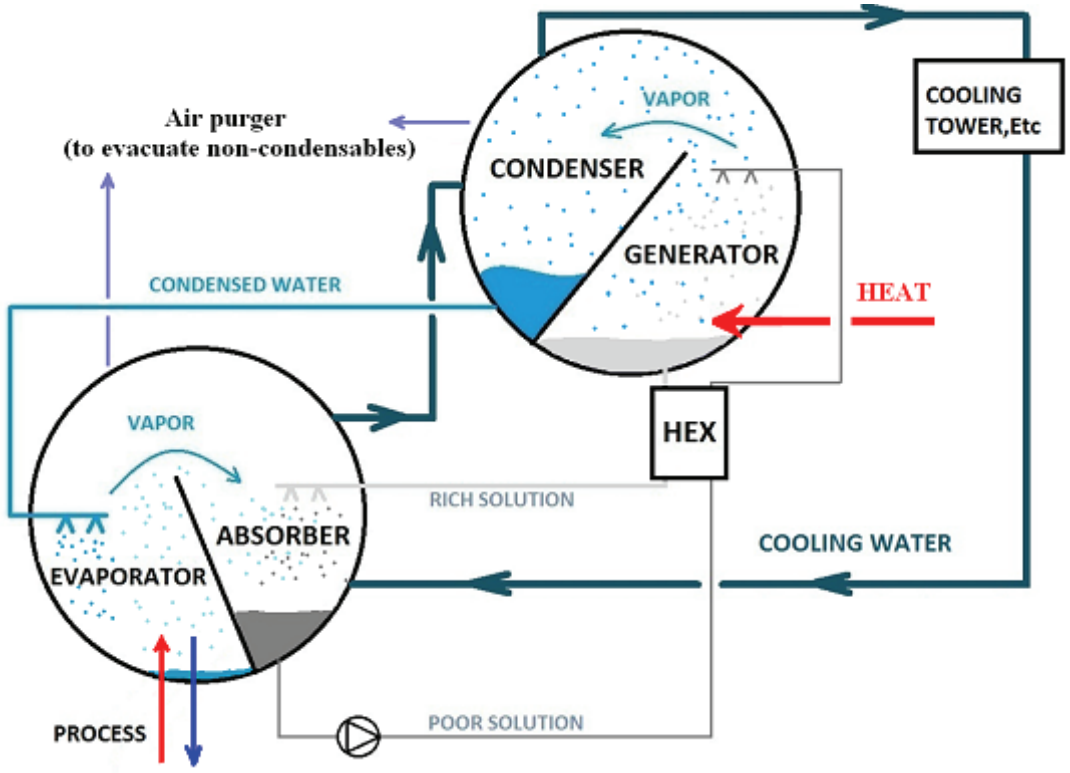

Figure 1.3 Schematic diagram of a typical single-stage absorption refrigerator design.

Figure 1.4 A single-stage absorption chiller driven by hot water or steam (picture was taken from official website of "Johnson Controls Inc.").

For a LiBr/H_2O based absorption refrigerator, water is the refrigerant and LiBr is the absorbent. The defect of this pair is that LiBr can crystallize in the heat exchanger between the generator and the absorber when the temperature decreases under a critical value.

The crystallisation problem becomes much more important for compact systems designed for small scale applications where temperature drops are raised to use smaller surface areas in heat exchangers. Many additives are added to the LiBr salt to decrease crystallization temperature (by increasing solubility), prevent corrosion, increase absorption performance, increase thermal&chemical stability, etc (Bourois, Valles, Medrano, & Coronas, 2005).

Devices in the absorption refrigerators that consume electrical energy are limited to pumps and vacuum pump, whose consumption is very low compared to that of a compressor of a gas compression refrigerator.

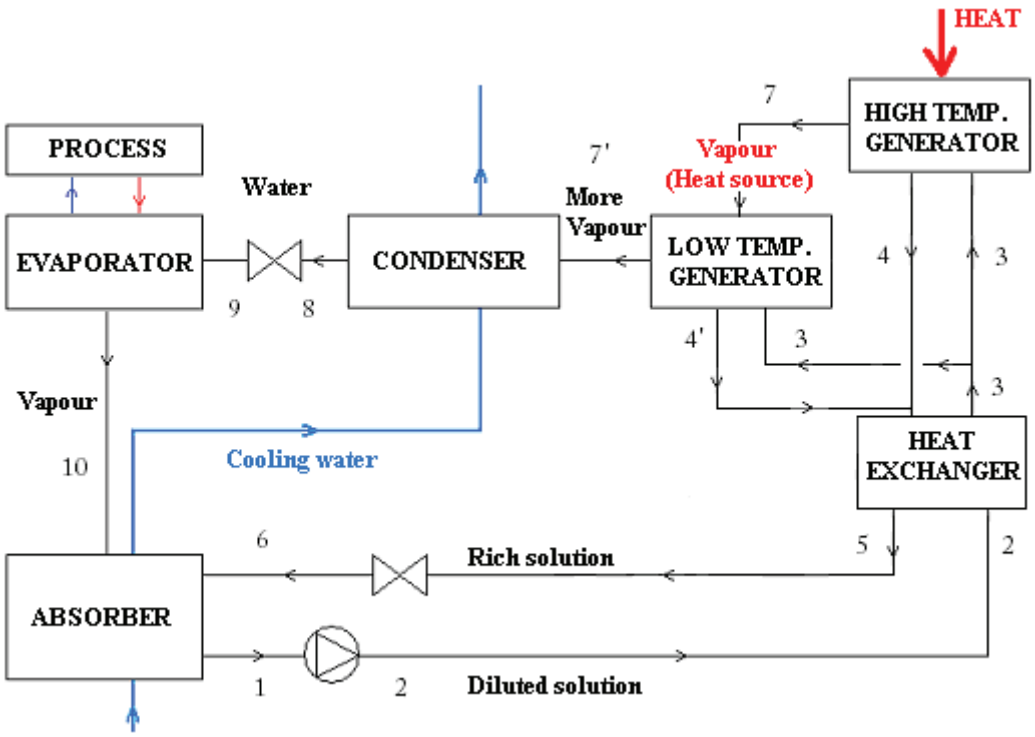

Figure 1.5 Flow diagram of a double-stage absorption cycle.

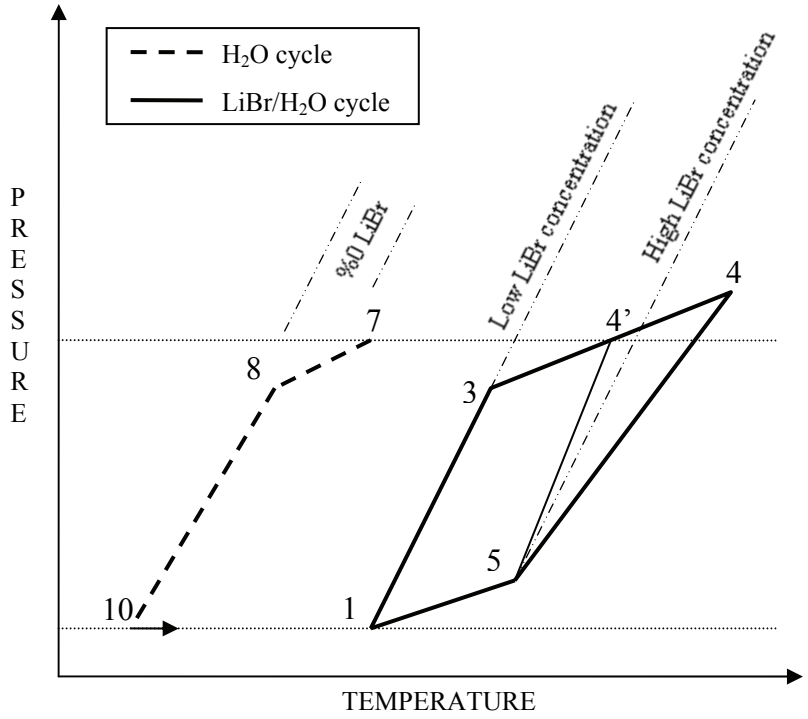

Figure 1.6 Pressure-temperature diagram of a double-stage absorption cycle.

Figure 1.7 A double-stage absorption chiller driven by gas or high-pressure steam (picture was taken from official website of "Johnson Controls Inc.").

1.1.3 Major Components of an Absorption Cycle

There are five major components of an absorption cycle (see Figures 1.1 and 1.3): the evaporator, condenser, generator, absorber and heat exchanger; and other components such as solution and water pumps, air purge system, etc.

1.1.3.1 Evaporator

Refrigerant supplied from condenser evaporates under vacuum conditions which absorps heat of process water flowing on the other side of the heat exchanger.
Because water is used as a refrigerant, evaporation temperature cannot be lower than about 5-6^{o}C which is a main drawback for LiBr/H_2O systems. However hybrid systems overcome this defect.

1.1.3.2 Condenser

High pressure superheated vapour supplied from the generator rejects heat to the ambient and condenses in the condenser and becomes ready for evaporation.

1.1.3.3 Generator

Diluted solution supplied from the absorber by a solution pump is heated by a heat source in the generator.
The solution is concentrated in terms of LiBr by the boiling of water which is continuously supplied to the condenser. The concentrated solution goes to the absorber to be diluted by the vapour supplied from the evaporator.

1.1.3.4 Solution Heat Exchanger

As mentioned in the previous title, lowering the solution temperature increases absorption rates unless solubility limit is reached. The temperature of concentrated solution supplied from the generator is usually over absorption temperature limit which means evaporation (desorption) instead of absorption occurs, hence the absorber partially or completely (depending on cooling water temperature) acts as a low temperature generator (see Fig. 1.5).

A heat exchanger between the generator and the absorber prevents the situation explained above. In the heat exchanger, cooler dilute solution (moving from the absorber) precools the hotter concentrated solution (moving from the generator) to a reasonable degree. Furthermore, preheating for the dilute solution decreases heat load of the generator.

The main problem faced in the heat exchanger is that crystallisation of LiBr salt can occur when temperature falls below a critical temperature. This is the chronical problem of a $LiBr/H_2O$ absorption cycle. Many research is done on this area by improving the additives which are added into the solution to increase solubility of LiBr in water (and of course to improve other properties of the solution), and by carefully designing the heat exchanger.

1.1.3.5 Absorber

Concentrated solution supplied from the generator absorps vapour and is diluted in the absorber, it is then collected and pumped to the generator to be concentrated and extract high pressure vapour again. Absorber can be considered as the heart of the system, however it is usually the least efficient component of an absorption machine (Raisul Islam, Wijeysundera, & Ho, 2006), hence absorption rates can be considered as a direct measurement for overall system performance.

Falling film absorbers are the most commonly used absorbers, because absorption surface is very large compared to the solution volume and rejection of heat of absorption to the ambient is easier. Heat of absorption is released at the absorption surface and presence of this heat decreases absorption performance, hence it should be removed from the system to enhance absorption performance. Bubble absorption, in which vapour is supplied from bottom of a pool, which is filled of solution, is not practical, because pressure of vapour supplied from the evaporator is very low (about 0.01 bar). Absorber performance is affected by large number of parameters such as (Tsai et al., 1998):

1.1.3.5.1 Presence of Non-condensables. As the absorbers operate under vacuum conditions, there shouldnot be presence of any gases other than refrigerant vapour. However corrosion and passivation generate non-condensable gases which cause resistance to mass flow. These non-condensables are removed from the system by the purge system.

1.1.3.5.2 Solution Distribution. Because the solution is usually sprayed over tubes arranged vertically or horizontally, instabilities, which prevents uniform film flow, can arise. However, these instabilities usually improve absorption performance.

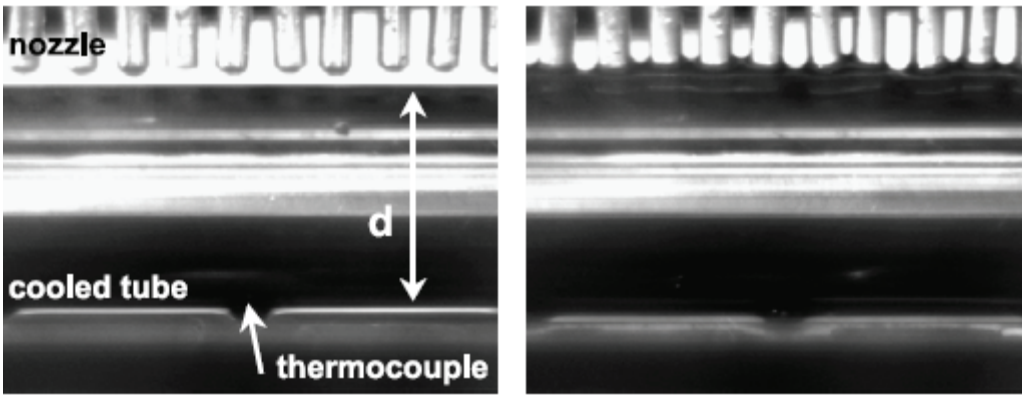

Figure 1.8 Solution spray and distribution over a horizontal tube (Seol & Lee, 2005).

1.1.3.5.3 Heat of Absorption. Heat, generated during absorption process, must be removed, otherwise absorption performance falls; hence, lowering solution temperature increases absorption rates unless solubility limit for LiBr is not reached. If temperature increases over a critical value, vapour desorption instead of absorption occurs.

The released heat of absorption is generally removed by water for large-scale applications, which completes its cycle by flowing through the condenser and consequently rejecting its heat in a cooling tower. However, air cooled systems are preferred for middle and low-scale residential and commercial applications, to be more economical (Bourouis et al., 2004). Commonly, there are two types of falling film absorbers:

- Vertical tubular absorber (see Figure 1.9),
- Horizotal tube bundle absorber (see Figure 1.10).

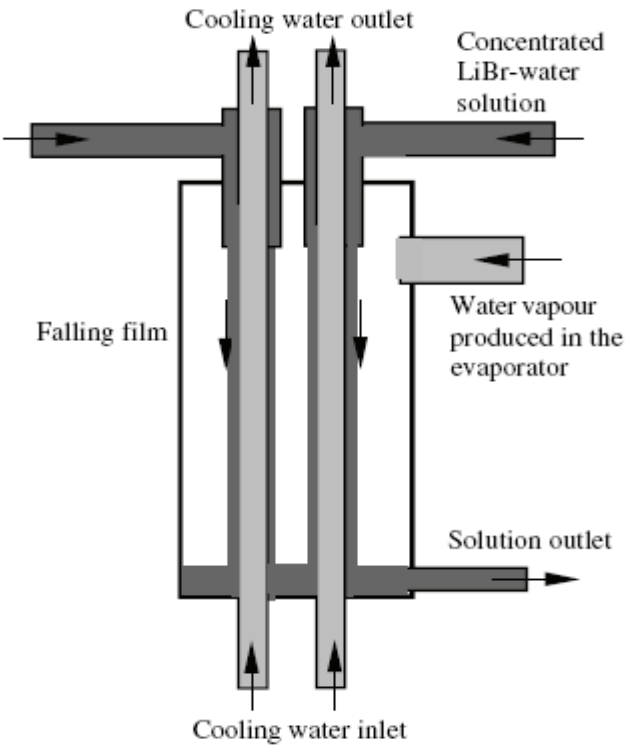

Figure 1.9 A traditional vertical tubular absorber construction (Florides et al., 2002).

Vertical absorber is made of a number of vertical tubes, where the rich solution (position 6 in Figure 1.1) is supplied from the top of the vertical tubes, and flows down in the form of thin falling film. Vapour is supplied from the evaporator and is absorbed by the solution while the solution is flowing down. Heat of absorption is rejected to cooling water, which is flowing inside the tube. However for air-cooled small scale applications, the solution flows down inside the tube (so also the vapour is supplied from inside of the tube) and cooling air flows outside the finned tube (Bourouis et al., 2004).

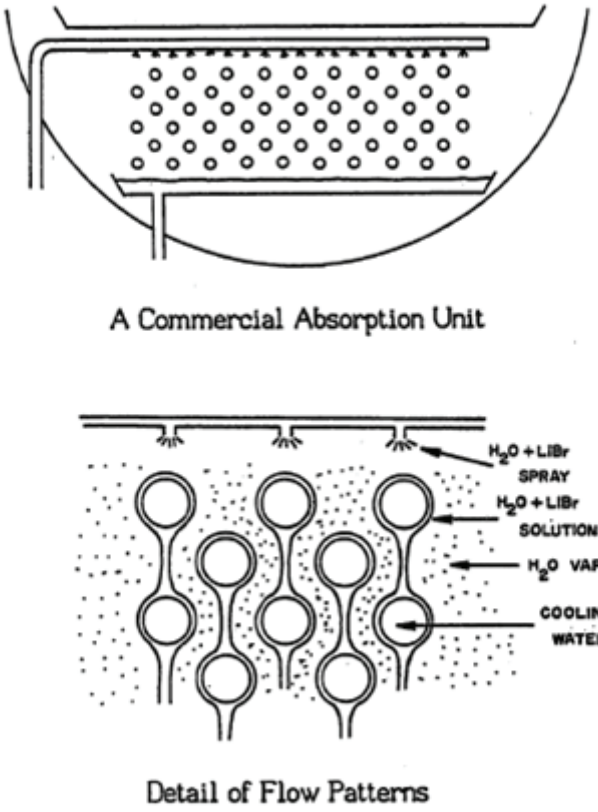

Figure 1.10 A traditional horizontal tubular absorber construction (Andberg, 1986).

Horizontal absorber is made of a number of horizontal tubes arranged vertically. The rich solution (position 6 in Figure 1.1) is sprayed over the top of the top tubes, and flows down in the form of thin falling film on the tubes. Similar to the vertical

absorber, vapour is supplied from the evaporator and is absorbed by the solution while the solution is flowing down. Heat of absorption is rejected to cooling water, which is flowing inside the tube.

1.2 Introduction to Numerical Absorber Modeling

Description of the problem will be introduced for absorption on a vertical plate, which is the simplest geometry for an absorber, where LiBr/H_2O solution film flows down a vertical cooled plate while the refrigerant supplied from the evaporator is absorbed at the film surface.. In the following chapters, detailed numerical modeling will be shown for tubular geometries.

Vapour pressure of the solution at the film surface should be less than the absorber vapour pressure, for absorption of vapour into the falling film. However typical velocity magnitudes of absorbed vapour are very low, so vapour pressure of the surface is very close to the absorber vapour pressure. Hence they can be taken equal to each other. So a thermodynamic equilibrium can be established between temperature and concentration at the film surface with a small error such that surface LiBr concentration varies with local surface temperature to match absorber vapour pressure (see Figure 1.12). This is one of the film surface boundary conditions. Absorption of vapour into liquid solution film produces latent heat at the solution/vapour interface, which is mostly transferred into the solution. This is the second film surface boundary condition.

The process is governed by three main partial differential equations:

- Hydrodynamics of the film flow is governed by the Navier-Stokes equations.,
- Energy balance for a differential control volume is governed by the energy equation,

- Species balance for a differential control volume is governed by the species transport equation.

These three equations are coupled with each other, however coupling between the energy and the species transport equations is much stronger than that between the Navier-Stokes equations and the energy or the species transport equations.

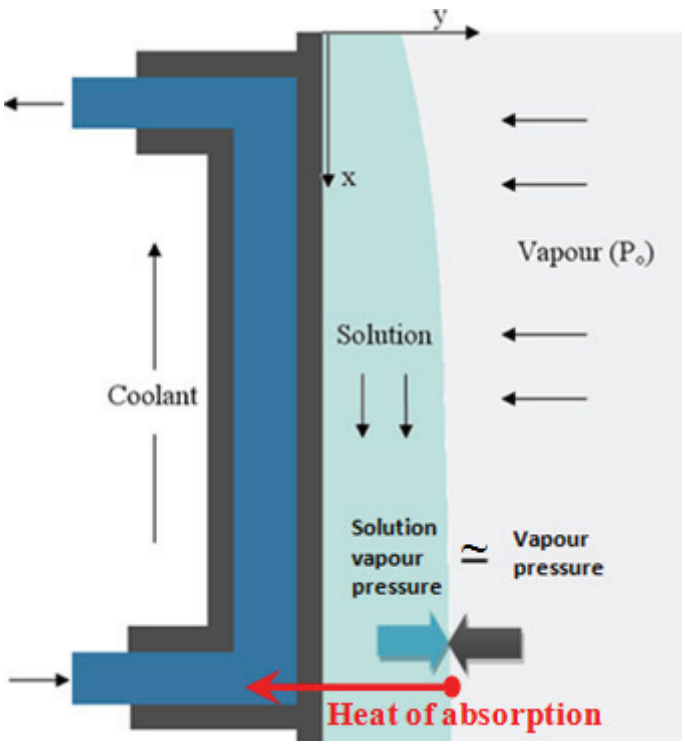

Figure 1.11 Physical domain for absorption process for falling film flowing down a vertical cooled plate.

In the present study, absorption of vapour into the $LiBr/H_2O$ solution is considered and modeled numerically using the finite volume approach. Vapour absorption rates for variety of conditions are predicted, performance trends are outlined. Two kinds of absorber geometries are investigated and compared with each other and accuracy of the models are verified by experimental data avaiable in the literature.

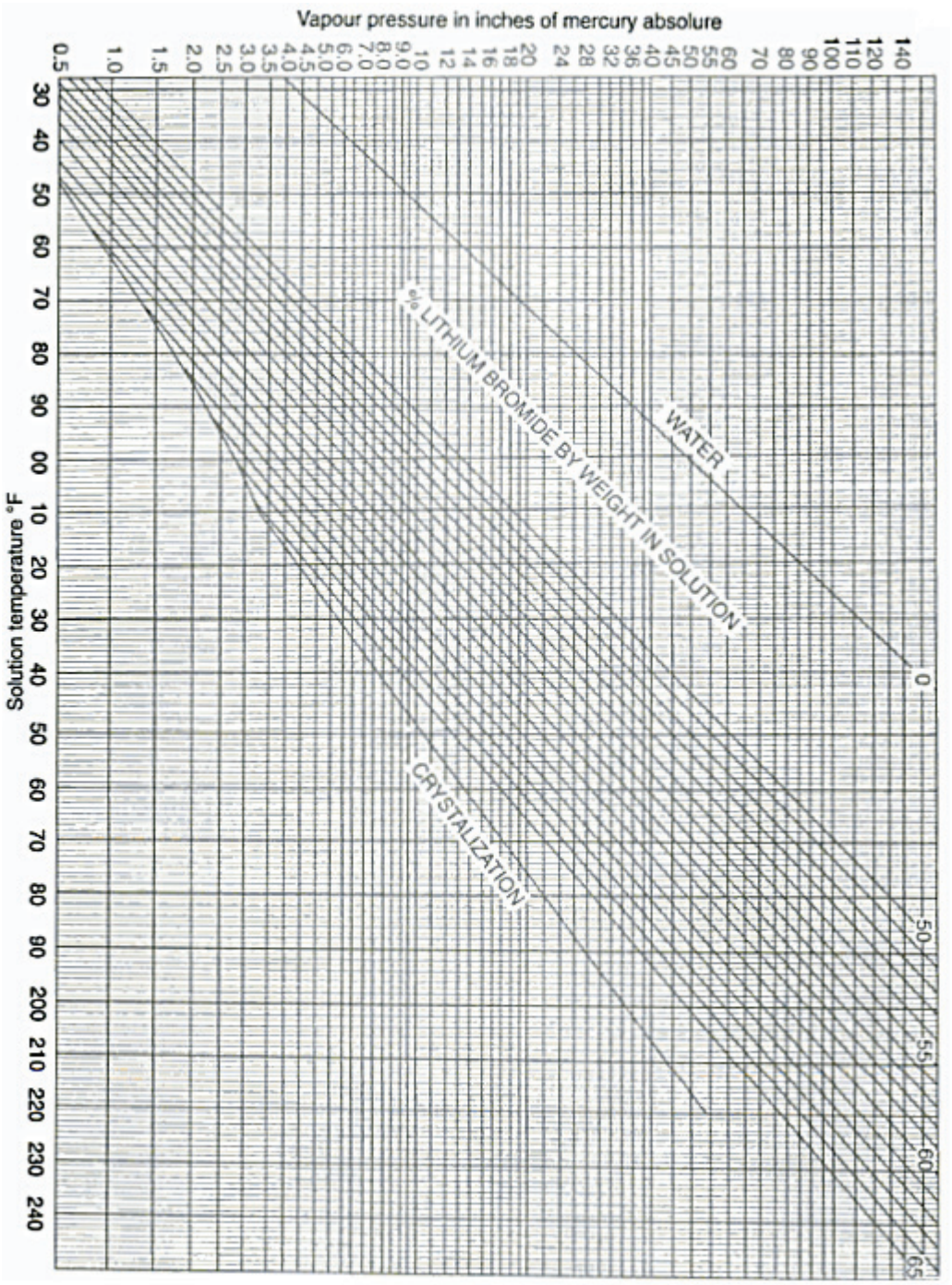

Figure 1.12 LiBr-H_20 pressure equilibrium diagram (was taken from Ananthanarayanan, 2005.).

CHAPTER TWO
RESEARCH EFFORTS ON
SIMULATING SIMULTANEOUS HEAT&MASS TRANSFER PHONEMEA

Simultaneous heat and mass transfer occuring in absorbers is a very complex process, which can be affected from variety of conditions (Tsai et al., 1998); among these variables flow unsteadiness, imperfect distribution of solution which may cause dry surfaces on the tubes, presence of non-condensables which creates resistance to mass transfer, geometry of the absorber, temperature distribution, etc., can be considered.

Various research has been done on simulating simultaneous heat and mass transfer process analytically and numerically (Killion & Garimella, 2001), however, analytical solutions are avaiable only after many simplifying assumptions which may not be necessary for numerical models.

2.1 Analytical Solutions

Grigor'eva & Nakoryakov (1977a) were the first to solve combined heat and mass transfer problem. They solved two-dimensional absorption process for smooth steady laminar film flowing down an isothermal vertical plate.

Their assumptions were:

a) Slug flow,
b) The vertical plate is completely wetted,
c) Constant physical properties,
d) Diffusion of temperature and concentration in the flow direction is negligible compared to convection of them,

e) The transverse velocity component is negligible,
f) Film thickness is constant,
g) Linearized vapour pressure equilibrium function at the interface,
h) Constant absorber vapour pressure,
i) No shear stress or surface tension at the solution-vapour interface,
j) Heat transfer to the vapour is negligible,
k) Inlet temperature and concentration profiles are uniform,
l) Local absorption rate is computed assuming the film is infinitely dilute in water (and mass fraction of LiBr is equal to one) or net mass flux in the transverse direction is zero.

Fick's first law of binary diffusion for a fixed coordinate system can be written as ("y" is the transverse direction):

$$C_{H_2O}\dot{m}_{LiBr} - C_{LiBr}\dot{m}_{H_2O} = -\rho_s D \frac{\partial C_{LiBr}}{\partial y} \tag{2.1}$$

However it is assumed that:

$$\dot{m}_{H_2O} = -\rho_s D \frac{\partial C_{LiBr}}{\partial y} \tag{2.2}$$

It can clearly seen that this assumption is not reasonable enough.

After these assumptions, the resulting equations are solved using Fourier seperation of variables techniques, temperature and concentration fields, heat transfer at the wall and solution-vapour interface and bulk temperature and concentrations are presented. The result of the solution depends only on four non-dimensional variables (except boundary conditions and pressure equilibrium function coefficients):

a) the Lewis number ($Le_s = D/\alpha_s$), which is the ratio of mass diffusivity to thermal diffusivity,

b) the Prandl number ($Pr_s = \nu_s / \alpha_s$), which is the ratio of momentum diffusivity to thermal diffusivity,

c) the Reynolds number ($Re_s = 4u_{mean}\delta / \nu_s$), which is the ratio of inertia forces to viscous forces,

d) the dimensionless group $h_{abs}a / c_{p-s}$, where h_{abs} is the heat of absorption and a is the pressure equilibrium coefficient at the interface with the dimension Kelvin^{-1} ($C_{if} = a\ T_{if} + b$).

Because evaluation of the exact solution mentioned above is complex, Nakoryakov & Grigor'eva (1977b, 1980a, 1980b) presented approximated solutions valid for special regions. Nakoryakov et al. (1995) developed a approximate model in which the film thickness increases as the mass is absorbed. Their results show that even for relatively large downstream distances, film thickness growth is small (a few percent).

Kholpanov, Malyusov, & Zhavoronkov (1982) solved the same approximated problem of Nakoryakov et al. (1980a, 1980b), which are valid for near inlet regions, but took surface shear stress effects into account.

Grossman (1983), used the same assumptions found in Grigor'eva et al. (1977), but assumed a fully-developed, laminar, Nusselt solution for the velocity profile. It is also shown that the linear relationship for temperature and concentration at the interface for satisfying vapour pressure equilibrium is valid for a wide range of temperatures and concentrations. Also he utilized a numerical model based on finite difference method, and compared the results with the results of his analytical solution.

Brauner, Moalem Maron, & Mayerson (1989) considered the similar simplified problem of Nakoryakov et al. (1980a, 1980b), but they relaxed the assumption of infinite dilution of water (Eq. 2.2).

It is known that falling film is not usually steady and smooth, as the vapour is absorbed, waves at the film surface appears (Seol et al., 2005). There are various research on wavy films, the first are the studies of Nakoryakov, Burdukov, Bufetov, Grigor'eva, & Dorokhov (1982). Waves at the film surface has a mixing effect (Islam, Miyara, & Setoguchi, 2009) , hence it is assumed that, just below each wave, temperature and concentration profiles are uniform. Charasteristic wavelengths are obtained from photographic techniques. Hence temperature and concentration fields between the waves are solved analytically assuming uniform field after each wave. Their results agree with experimental data at least predicts the trends.

2.2 Numerical Solutions

Andberg & Vliet (1983) were probably the first to develop a fully numerical model for absorption process. They investigated absorption process for a laminar film flow flowing down a vertical isothermal plate. Their assumptions were similar to that of investigators above, however they didnot neglect energy change due to diffusion of the species and the film thickness to increase as the vapour is absorbed.

Andberg (1986) is probably the first to model horizontal tube absorber in his PhD Thesis. He utilized finite difference formulation to solve momentum, energy and species transport equations. He assumed planar jet (sheet) between the successive tubes which does not contribute to the absorption process. Secondly he assumed the LiBr/H_2O solution mixes perfectly in the planar jet such that the solution enters the next tube uniformly. Contrary to the previous study (Andberg et al., 1983), he neglected energy transfer due to diffusion of the species because it was seen that the effect of it on the results are very small. Also he eliminated the assumption of infinite dilution of water (see Eq. 2.1 and 2.2) by using the expression:

$$\dot{m}_{H_2 0} = -\rho_s D \frac{1}{C_{LiBr}} \frac{\partial C_{LiBr}}{\partial y} \tag{2.3}$$

The results revealed that hydrodynamic charasteristics of the numerical model is very similar to that of Nusselts' solution except the inlet (jet impingement) region (see Figure 2.1). He presented a simplified model in which the Nusselt's solution is used for the hydrodynamics and an analytical method is employed for determining the concentration field. Only the energy equation is solved numerically.

He compared the results of the more complex model with the simplified model and concluded that the difference in terms of overall concentration change is on average within %3 and on maximum within %10.5.

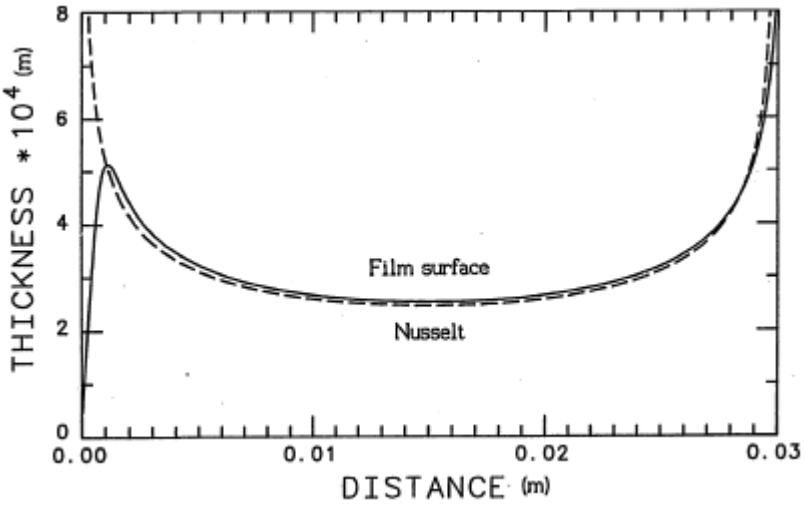

Figure 2.1 Film thickness distribution along the tube circumference calculated by Andberg (1986) and from the Nusselt's solution.

Choudhury, Hisajima, Ohuchi, Nishiguchi, Fukushima, & Sakaguchi (1993) investigated the problem similar to that of Andberg (1986), however they assumed constant physical properties, Nusselt's solution for the film hydrodynamics and isothermal tube wall. They also assumed that the solution inlet conditions are in equilibrium with the vapour. As a result of this study, optimum tube diameters and film flow rates are predicted for maximum absorption rates.

Lu, Li, Li and Yu-Chi (1996) developed a model which is very similar to that of Choudhury et al. (1993), however they included two empirically derived coefficients to the model that take surface wetting ratio and tube spirality into effect.

Yüksel and Schlünder (1987) solved absorption process for averaged (steady) turbulent film flowing over a vertical wall. Turbulence is taken into account by adding empirically derived eddy diffisuvity profiles to the thermal and mass diffusivity coefficients. They also assumed a polynomial function for concentration at the inlet instead of an uniform profile.

Rogdakis, Papaefthimiou, & Karampinos (2003) calculated heat of absorption in their vertical absorber model in the range of temperature between 0 to 180^{o}C and LiBr concentration between %20 and %70, by substracting partial enthalphy of water in the LiBr-H_2O solution from superheated vapour enthalphy. Heat of absorption varied in their model, however they assumed constant physical properties and constant film thickness. Papaefthimiou, Karampinos, & Rogdakis (2006) created a numerical model very similar to that of Choudhury et al. (1993), however they used variable heat of absorption as was done in their previous study. They used Nusselt's solution for the film hydrodynamics, and investigated a single horizontal tube. Effects of solution mass flow rate, coolant inlet temperature and tube radius on mass absorption performance was investigated, the results are compared with experimental data avaiable in the literature. Their results on heat of absorption field is presented in Fig. 2.2.

Patnaik & Perez-Blanco (1996) numerically modeled wavy falling film flowing over a vertical plate at Reynolds numbers between 200 and 1000. They divided wave into four parts such as wave front, wave back, trail and substrate and utilized photographic techniques and semi-analytical methods to obtain information about wave hydrodynamics. They also assumed isothermal wall, constant physical properties, no heat transfer to the vapour phase. Results of the model was compared with experimental data avaiable in the literature, it is shown that at the model predicts performance correctly in some situations.

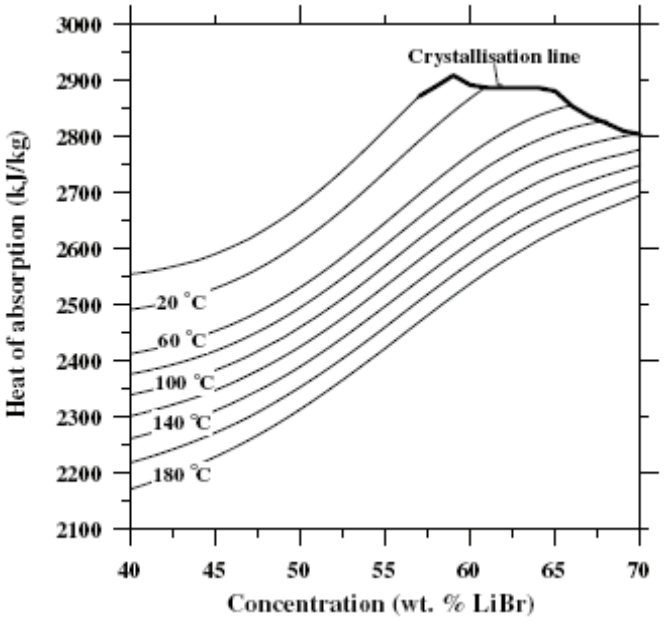

Figure 2.2 Heat of absorption of LiBr-H_2O solution (Figure was taken from Papaefthimiou et al. 2006).

Islam et al. (2009) considered wavy film flowing over a isothermal vertical plate. Finite difference formulation was utilized to solve combined transient momentum, energy and species transport equations. Film thickness is periodically distributed at the inflow boundary to ensure film waviness, hence by removing disturbance, smooth film can also be simulated. It is shown that wavy film structure increases absorption rates considerably.

In the present study, an extensive model for both vertical and horizontal tubular absorbers that eliminates many common assumptions simultaneously (such as variation of physical properties locally, model for counter-flow cooling water flowing inside the tubes, variation of wall temperature and variation of film thickness with absorption of vapour and change in physical properties) is created and results are presented in detail. Although some advanced features such as simulation of waves are missing, the present model can predict the process in excellent detail under certain common conditions where effect of the waves are small.

CHAPTER THREE
A NUMERICAL MODEL FOR VERTICAL TUBULAR ABSORBER

The $LiBr/H_2O$ solution is distributed from the top of a number of vertical tubes and flows down in the form of falling film at the outer surface of the tube. Vapour is supplied from the evaporator continiously under vacuum conditions. As the solution absorps vapour, heat of absorption is generated which must be rejected to the ambient by water or air. Schematic view of the vertical absorber is demonstrated in Figure 3.1.

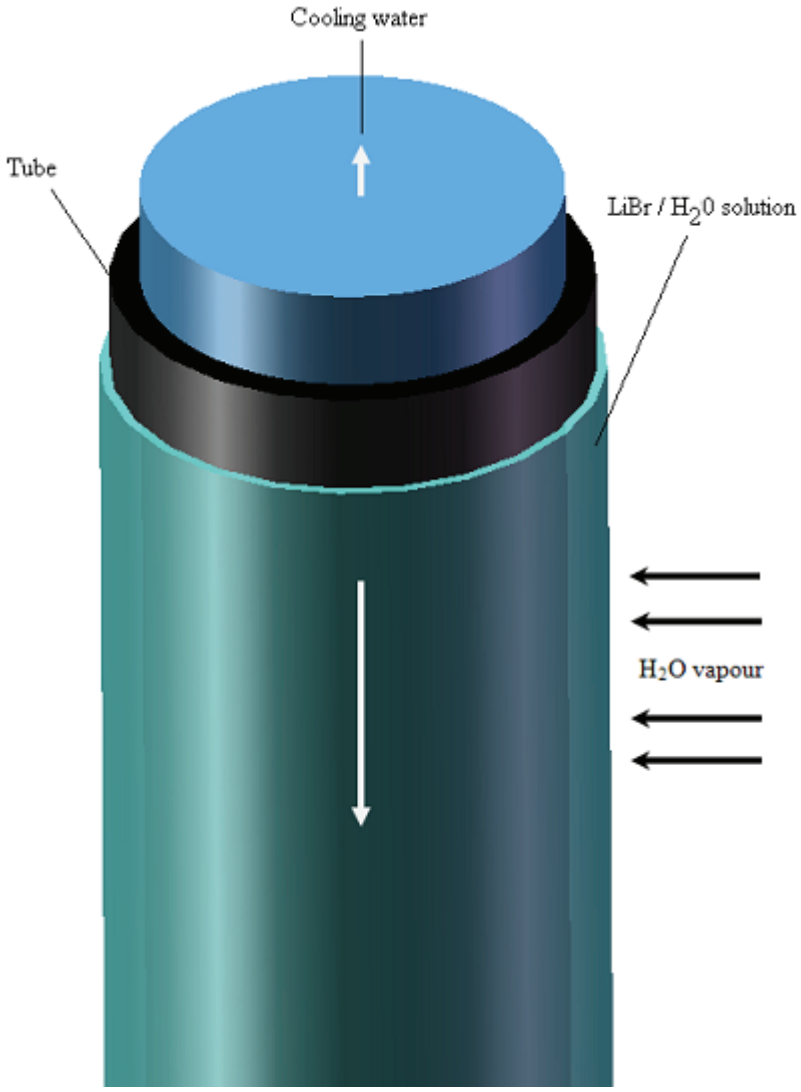

Figure 3.1 Simplified view of a vertical tubular absorber.

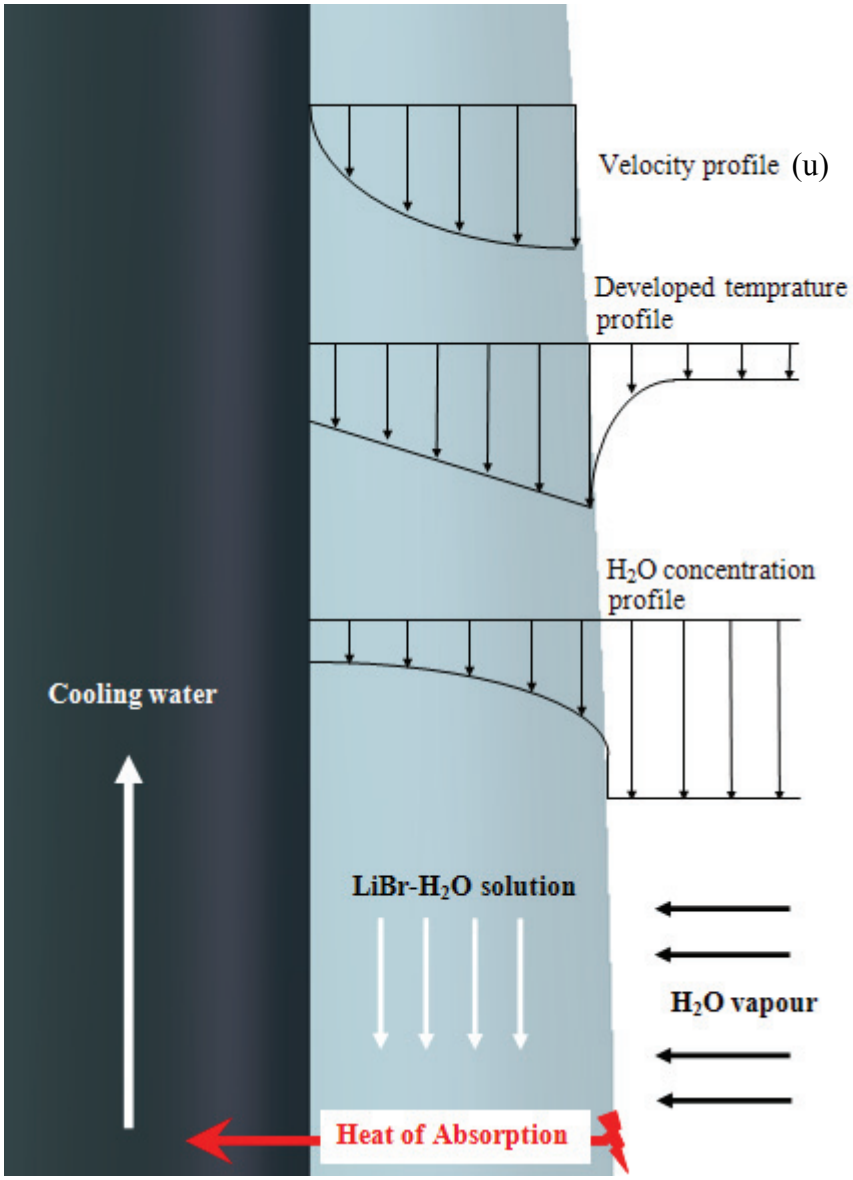

Figure 3.2 Typical cross-stream velocity, temperature and concentration profiles.

In the present study, water is used as the cooling fluid, and enters the copper tube from the bottom and exits from the top of the tube. Counter flow arrangement is advantegeous because absorption performance falls considerably at the end of the tube, hence a cooler water at the bottom of the tube limits this performance drop and as a consequence the whole tube surface can be used more efficiently.

To model the absorber, a two dimensional section of the falling film is divided a number of non- overlapping fixed (Eulerian) control volumes (see Fig. 3.3). These control volumes represent differential volumes on which conservation of mass, momentum, energy and species are investigated simultaneously. Details of the finite volume approach is discussed in section 3.3.

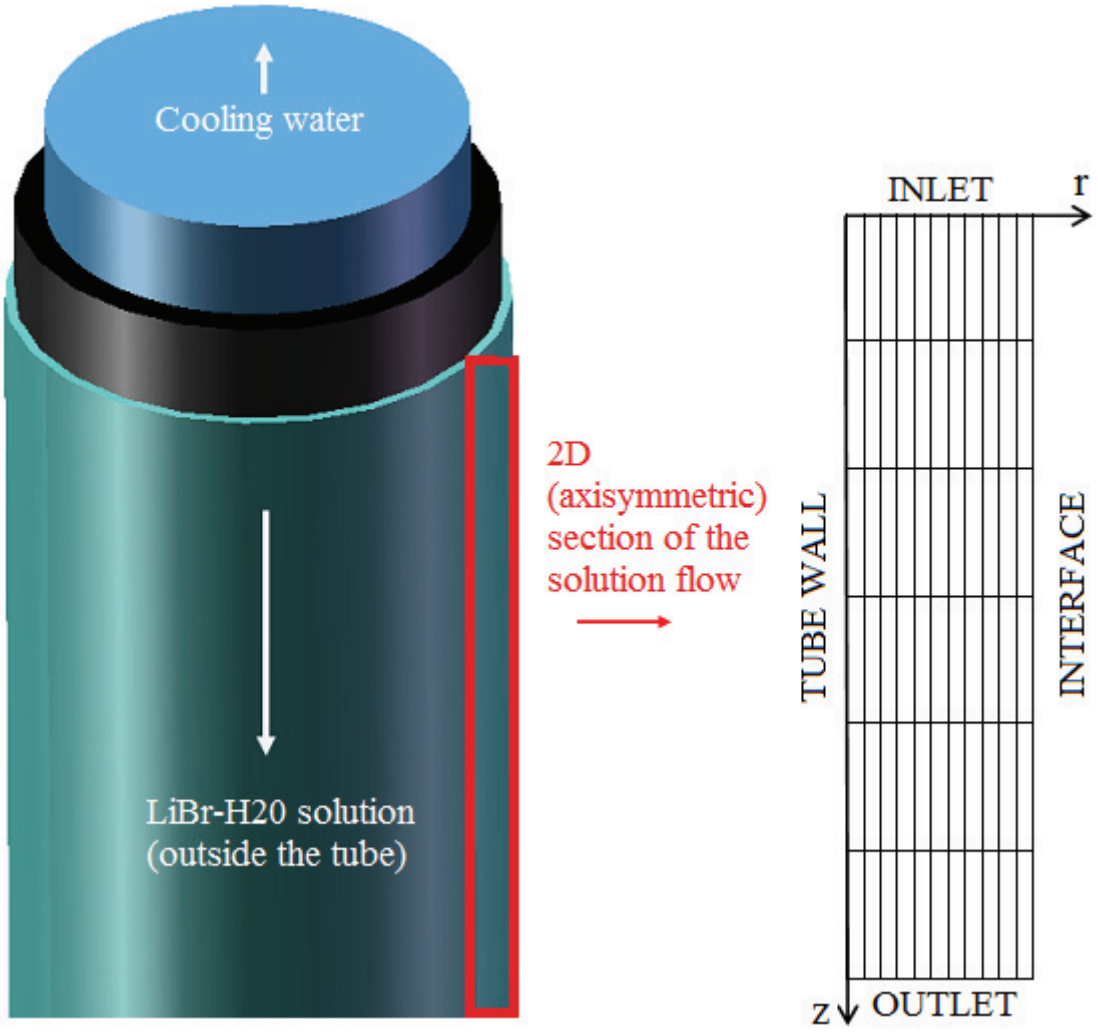

Figure 3.3 Physical calculation domain, the finite volumes and the physical coordinate system.

Properties of the model can be listed as follows:

- Physical properties vary with local temperature and concentration,
- The massflow rate increases with the absorption of vapour into the liquid film, hence the film thickness varies as the vapour is absorbed
  (But variations within the differential control volume are neglected).

Assumptions can be listed as follows:

- Tube is completely wetted by the solution,
- Vapour pressure equilibrium exists at the vapour & solution interface,
- The flow is laminar and non-wavy throughout,
- Heat transfer in the vapour phase is negligible compared to that in the solution, so the heat of absorption is fully transferred into the solution,
- No shear stress is exerted on the film flow by the vapour,
- Diffusion in the flow direction is negligible,

3.1 Governing Equations

Velocity profiles can be calculated from Navier-Stokes equations assuming that the viscous forces are dominant over the inertia and pressure forces, and physical properties within a differential volume are constant:

$$u(r) = \frac{\rho_s g \delta^2}{2\mu_s}\left(2\left(\frac{r - r_o}{\delta}\right) - \left(\frac{r - r_o}{\delta}\right)^2\right) \tag{3.1}$$

From continuity, transverse (radial) component of the velocity is zero:

$$v(r, z) = 0 \tag{3.2}$$

The film thickness for a known mass flow rate can be expressed as:

$$\delta = \left(\frac{3\mu_s \Gamma_s}{\rho_s^2 g} \right)^{1/3} \tag{3.3}$$

Where Γ_s is the solution mass flow rate per length of tube outer circumference.

Energy balance for a differential control volume in the cylindrical coordinates can be expressed as (Andberg, 1986):

$$\frac{\partial(\rho_s h_s)}{\partial t} + \frac{\partial(\rho_s u h_s)}{\partial z} + \frac{\partial(\rho_s v h_s)}{\partial r} = \frac{1}{r}\frac{\partial}{\partial r}\left(k_s r \frac{\partial T}{\partial r} \right) + \frac{\partial}{\partial z}\left(k_s \frac{\partial T}{\partial z} \right)$$
$$+ \frac{1}{r}\frac{\partial}{\partial r}\left(\sum_{i=LiBr}^{H_2O} \rho_s D r \frac{\partial C_i}{\partial r} H_i \right) + \frac{\partial}{\partial z}\left(\sum_{i=LiBr}^{H_2O} \rho_s D \frac{\partial C_i}{\partial z} H_i \right) + \frac{\mu_s}{J}\frac{\partial P}{\partial r} + \frac{\mu_s}{J}\frac{\partial P}{\partial z} + \phi \tag{3.4}$$

Andberg et al. (1983) have shown that the transport of energy by mass diffusion is negligible comprared to other transpor mechanisms, hence these terms (third and fourth terms in the RHS) can be ignored. Also an order of magnitude analysis easily shows that typical values of film thickness are very small compared to the tube diameter, hence radius within the film can be taken constant. Apart from these, assuming $dh=c_p\, dT$, steady state, constant properties inside a single cell, no pressure gradients within the film, no diffusion along the flow direction and viscous dissipation; energy equation reduces to:

$$u\frac{\partial T}{\partial z} = \alpha_s \frac{\partial^2 T}{\partial r^2} \tag{3.5}$$

Species balance for a differential control volume in the cylindrical coordinates assuming ordinary diffusion, constant solution density (then concentration can be

expressed in terms of mass fraction of a species within the solution) can be expressed as (Bejan, 1993):

$$\frac{\partial(\rho_s C)}{\partial t}+\frac{\partial(\rho_s u C)}{\partial z}+\frac{\partial(\rho_s v C)}{\partial r}=\frac{1}{r}\frac{\partial}{\partial r}\left(\rho_s D r\frac{\partial C}{\partial r}\right)+\frac{\partial}{\partial z}\left(\rho_s D\frac{\partial C}{\partial z}\right) \tag{3.6}$$

Similar assumptions that are done for energy equation (3.5) can also be made for species transport equation (3.6):

$$u\frac{\partial C}{\partial z}=D\frac{\partial^2 C}{\partial r^2} \tag{3.7}$$

3.1.1 Energy Balance in the Cooling Water Side

Typically, the solution film has very small mass flow rate compared to the cooling water mass flow rate. Thus, the specific heat of the LiBr-water solution is smaller than that of cooling water. Hence, heat capacity of the cooling water is much larger than that of the solution, which means the overall temperature increase of the cooling water is much smaller than that of the solution. So a one dimensional description for the cooling water is reasonable for describing the process by assuming a constant heat transfer coefficient from tube wall to the cooling water (see Figure 3.4).

In the present study, the heat transfer coefficient for the cooling water side is calculated from $Nu_b = 0.023\,Re_b^{0.8}\,Pr_b^{0.4}\left(\mu_b/\mu_w\right)^{0.262}$ correlation which is valid for incompressible turbulent flow flowing inside a pipe (Kakaç & Liu, 1998).

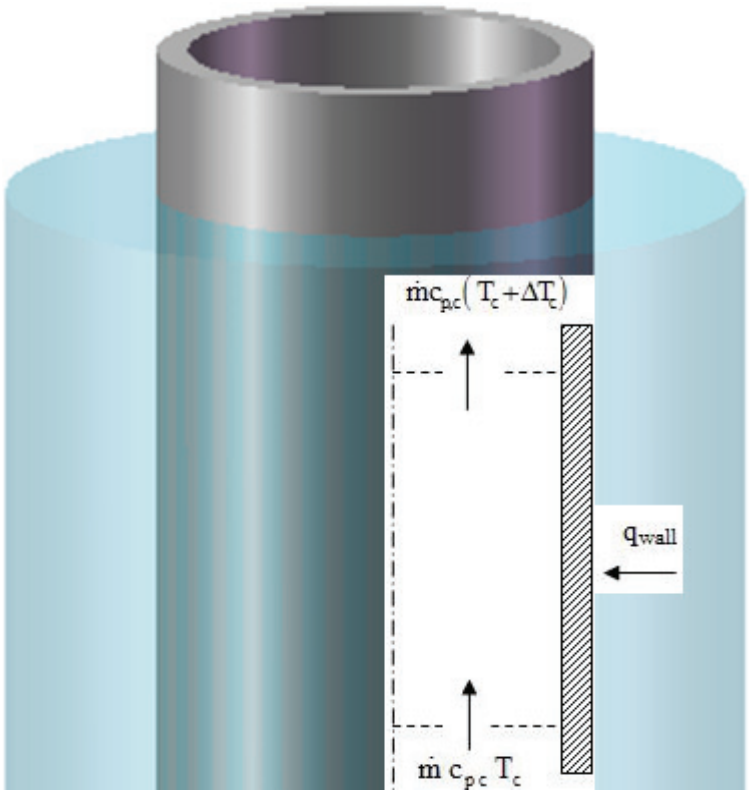

Figure 3.4 Differential control volume for the cooling water flowing inside the tube.

An expression for the cooling water temperature field can be derived from the one dimensional energy balance:

$$\frac{\partial T_c}{dz} = -\frac{2\pi(r_o+\delta)\,q_{wall}}{\dot{m}_c c_{pc}} \tag{3.8}$$

3.1.2 Initial & Boundary Conditions

Because the problem is a steady spatial marching problem, the calculation procedure must start from solution inlet, hence the boundary conditions at the inlet are categorized under “initial conditions”. Also calculation of the cooling water side starts from inlet, so it is also spatial marching problem.

Initial conditions for the LiBr/H_2O solution at the inlet (see Figure 3.3) are:

$$\left.\begin{array}{l} z = 0 \\ r_o \le r \le r_o + \delta \end{array}\right\} \quad \begin{array}{l} T = T_{in} \\ C = C_{in} \end{array} \tag{3.9}$$

An initial temperature for the cooling water at the top of the tube must be specified (because actually the cooling water enters the domain from the bottom of the tube, later it will be corrected by an iterative procedure.):

$$\left.\begin{array}{l} z = 0 \\ 0 \le r \le r_i \end{array}\right\} \quad T_c = T_{c-inlet-estimated} \tag{3.10}$$

Boundary conditions (see Figure 3.3) for the LiBr/H_2O solution are as follows:

At the tube wall:

$$\left.\begin{array}{l} 0 \le z \le L \\ r = r_o \end{array}\right\} \quad \begin{array}{l} T = T_c + \dfrac{q_{wall}}{U} \\ \dfrac{\partial C}{\partial r} = 0 \end{array} \tag{3.11}$$

U is the overall heat transfer coefficient calculated at the outer surface of the tube:

$$U = \left[\frac{r_o}{r_i h_c} + \frac{r_o}{k_{wall}} \ln\left(\frac{r_o}{r_i}\right) \right]^{-1} \tag{3.12}$$

At the solution-vapour interface:

$$\left.\begin{array}{l} 0 \le z \le L \\ r = r_o + \delta \end{array}\right\}$$

Nodal mass flux of the vapour for a fixed coordinate system can be calculated from Fick's first law (Incorpera & DeWitt, 2002):

$$C_{H_20}\dot{m}_{LiBr} - C_{LiBr}\dot{m}_{H_20} = -\rho D\frac{\partial C_{LiBr}}{\partial y} \tag{3.13}$$

Because LiBr is a nonvolatile absorbent, it does not mix with the vapour phase at the interface surface ($\dot{m}_{LiBr} = 0$ at the interface), hence Eq. 3.13 reduces to:

$$\dot{m}_{H_2O} = -\rho D\frac{1}{C_{LiBr-if}}\frac{\partial C_{LiBr}}{\partial r} \tag{3.14}$$

Vapour pressure equilibrium condition can be expressed as (see Figure 1.12) (Ananthanarayanan, 2005):

$$T_{if} = f(p, C_{if}) \tag{3.15}$$

Raisul Islam et al. (2006) linearized this equilibrium relationship in the range of pressure values of 0.8 to 2 kPa, temperature values of 20 to 50°C and LiBr concentration values of 0.55 to 0.65 (pressure is given in terms of kPa):

$$C_{if} = \left(4.8688 \text{ x } 10^{-3} \text{ x } p^{-0.188}\right) T_{if} + 0.37794 \tag{3.16}$$

Specific heat of absorption, which is the heat released at the film surface (or absorption surface) per unit mass, is defined as the difference between the entalphy of vapour and partial entalphy of water within the solution:

$$h_{abs} = h_v - h_w \tag{3.17}$$

It should be noted that this heat is not released inside the solution because the vapour phase cannot travel inside the solution without being absorbed. Hence absorption only occurs at the film surface. Total heat rate released at the surface is defined as the product of specific heat of absorption and mass absorption flux:

$$q_{if} = h_{abs}\dot{m}_{H_2O} \tag{3.18}$$

The released heat at the interface is transferred into the solution:

$$q_{if} = -k_s \frac{\partial T}{\partial r} \tag{3.19}$$

At the outlet, axial gradients of temperature and concentration are set to zero.

3.2 Partial Nondimensionalization of the Governing Equations

The velocity profile (Eq. 3.1) and the governing equations (Eq. 3.5 and 3.7) are nondimensionalized (see Figure 3.5). However, to satisfy pressure equilibrium condition, the temperature dimension is not nondimensionalized because local temperature values are necessary to obtain local interfacial concentration values at the film surface. Following dimensionless spatial variables are considered:

$$Z = \frac{z}{L} \tag{3.20}$$

$$R = \frac{r - r_o}{\delta} \tag{3.21}$$

By substituting (3.20-21) into the equations (3.1), (3.5), (3.7) and (3.8);

The velocity profile (Eq. 3.1) becomes:

$$u(R) = \frac{3}{2} u_{mean} \left(2R - R^2\right) \tag{3.22}$$

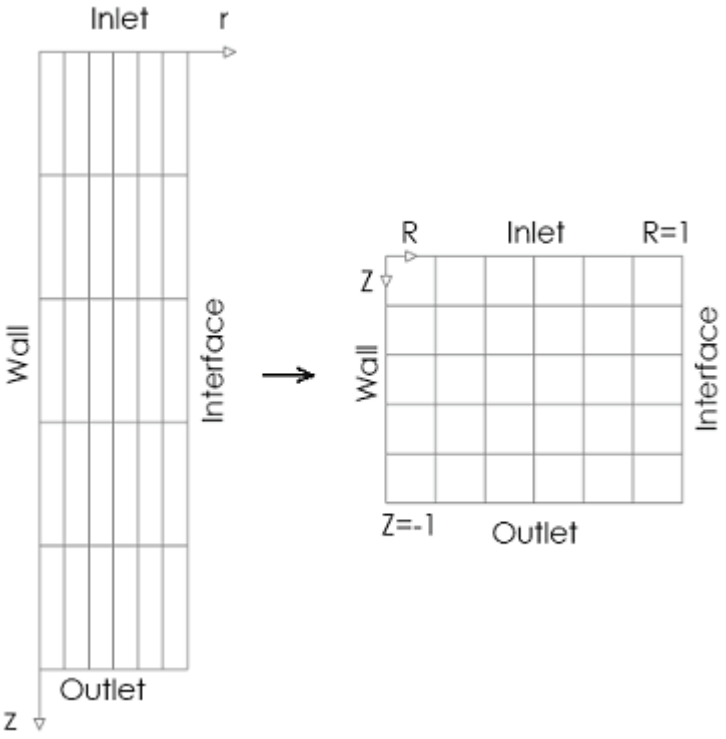

(a) (b)

Figure 3.5 The physical (a), and the dimensioless (b) calculation domain.

If Reynolds, Prandl and Schmidt numbers are defined as (respectively):

$$Re_s = \frac{4\Gamma_s}{\mu_s} \tag{3.23}$$

Where Γ_s is the solution mass flow rate per length of tube outer circumference.

$$Pr_s = \frac{\mu_s c_{ps}}{k_s} \tag{3.24}$$

$$Sc_s = \frac{\mu_s}{\rho_s D} \tag{3.25}$$

The energy equation (Eq. 3.5) becomes:

$$\frac{\partial T}{\partial Z} = \left(\frac{2}{3(2R - R^2)} \frac{1}{Re_s Pr_s} \frac{L}{\delta} \right) \frac{\partial^2 T}{\partial R^2} \tag{3.26}$$

The species transport equation (Eq. 3.7) becomes:

$$\frac{\partial C}{\partial Z} = \left(\frac{2}{3(2R - R^2)} \frac{1}{Re_s Sc_s} \frac{L}{\delta} \right) \frac{\partial^2 C}{\partial R^2} \tag{3.27}$$

Cooling water energy balance (Eq. 3.8) becomes:

$$\frac{\partial T_c}{dZ} = -\left(\frac{2\pi (r_o + \delta) L}{\dot{m}_c c_{pc}} \frac{k_s}{\delta} \right) \frac{\partial T_{(s)}}{\partial R} \tag{3.28}$$

The term ' $-2\pi (r_o + \delta)$ L k / $(\dot{m}_c c_{pc} \delta)$ ' is named as "gradcool"

3.2.1 Initial&Boundary Conditions for the Nondimensionalized Equations

Boundary conditions for the physical governing equations can be written for the nondimensional equations (3.26 and 3.27) as follows:

Initial conditions for the LiBr/H_2O solution at the inlet (see Figure 3.5) are:

$$\left.\begin{array}{l} Z = 0 \\ 0 \le R \le 1 \end{array}\right\} \quad \begin{array}{l} T = T_{in} \\ C = C_{in} \end{array} \tag{3.29}$$

For the cooling water:

$$\left.\begin{array}{l} Z = 0 \end{array}\right\} \quad T_c = T_{c-inlet-estimated} \tag{3.30}$$

Boundary conditions (see Figure 3.5) for the LiBr/H_2O solution are as follows:

At the tube wall:

$$\left.\begin{array}{l} 0 \le Z \le 1 \\ R = 0 \end{array}\right\} \quad \begin{array}{l} T = T_c + \dfrac{q_{wall}}{U} = T_c + \left(\dfrac{k_s}{U\delta}\right)\dfrac{\partial T}{\partial R} \\ \dfrac{\partial C}{\partial R} = 0 \end{array} \tag{3.31}$$

The term '$k_s / (U\delta)$' is named as 'CW' in the code.

At the solution-vapour interface:

$$\left.\begin{array}{l} 0 \le Z \le 1 \\ R = 1 \end{array}\right\}$$

Heat of absorpton is transferred into the solution:

$$\frac{\partial T}{\partial R} = -\frac{\rho D h_{abs}}{k_s}\frac{1}{C_{if}}\frac{\partial C}{\partial R} \tag{3.32}$$

The term "$\rho D h_{abs} / k_s$" is named as the mass coefficient in the code.

Vapour pressure equilibrium condition exists at the interface (see equations 3.15 and 3.16, and section 3.1.2):

$$C_{if} = \left(4.8688 \text{ x } 10^{-3} \text{ x } p^{-0.188}\right) T_{if} + 0.37794 \tag{3.33}$$

At the outlet, gradients of temperature and concentration with respect to R are set to zero.

3.3 Deriving the Discretization Equations

The control volume method is used for deriving the discretization equations (Patankar, 1980). Simply, the solution domain is divided into a number of nonoverlapping control volumes such that each control volume surrounds one node point, then the governing equations are integrated over each control volume. The discretization equation obtained by the control volume method expresses the conservation principle for the dependent variables for a finite control volume, just as the original governing equations expresses it for a differential control volume.
This property is specially very attractive because conservation of mass, momentum, energy, species balance, etc. is exactly satisfied over any group of control volumes, hence over the overall calculation domain.

In Figure 3.6; P is the currently investigated node, N, S, W and E are the neighbour nodes at north, south, west and east respectively; n, s, w and e are the center of control surfaces at north, south, west, and east respectively. Note that the derivatives in the circumferencial (θ) direction is neglected. As done in the finite difference method; in the control volume approach, values of the dependent variables (velocity, temperature, concentration, etc.) are only necessary at the node points (P,

N, S, W, E, etc.) to calculate the solution, however the values at the control surfaces (n, s, e and w, etc.) emerges in the discretization equation. To express these values in terms of the values at the node points (P, N, S, W, E, etc.), it is required to assume profiles expressing the variation of the values between the node points.

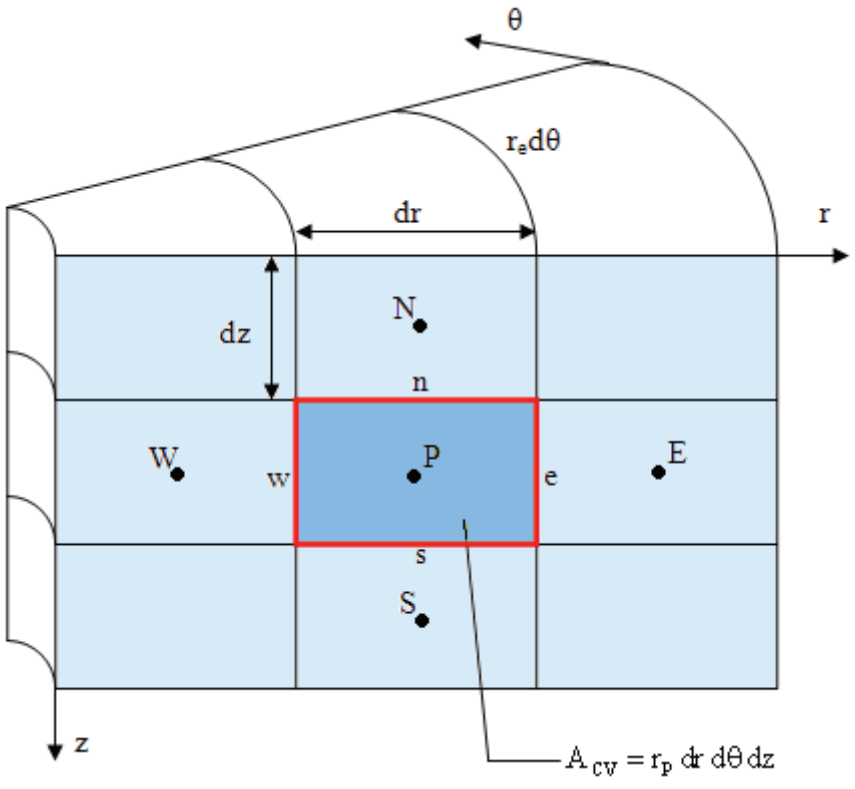

Figure 3.6 Schematic view of a two dimensional cylindrical domain with nine control volumes.

For complex control volume geometries, where direct integration of equations over a control volume is not possible, Gauss' divergence theorem can be applied to each control surface of a control volume in any shape; such that $\int_{C.V.} \mathrm{div}(\vec{f})dV = \int_{C.S.} \vec{f}\,\vec{n}dA$, where C.V. is the control volume, C.S. is the control surface (n, s, e, w, etc.), $\vec{f}$ is the flux vector at the control surface and $\vec{n}$ is the surface normal direction. However, because the problem presently considered has a rectangular grid structure, directly integrating the governing equation over a control volume without using the theorem is possible.

Integrating the energy equation over a C.V. (from north to the sourth in the axial direction and from west to the east in the radial direction) can be expressed as:

$$\int_{n}^{s}\frac{\partial T}{\partial Z}dRdZ=\int_{w}^{e}\left(\frac{2}{3(2R-R^{2})}\frac{1}{Re_{s}\,Pr_{s}}\frac{L}{\delta}\right)\frac{\partial^{2}T}{\partial R^{2}}dRdZ \tag{3.34}$$

Carrying out the integral yields:

$$\left(T_{s}-T_{n}\right)=\frac{\Delta Z}{\Delta R}\left(\frac{2}{3(2R-R^{2})}\frac{1}{Re_{s}\,Pr_{s}}\frac{L}{\delta}\right)\left(\left.\frac{\partial T}{\partial R}\right|_{e}-\left.\frac{\partial T}{\partial R}\right|_{w}\right) \tag{3.35}$$

Similarly, integrating the species transport equation over a C.V. can be expressed as:

$$\int_{n}^{s}\frac{\partial C}{\partial Z}dRdZ=\int_{w}^{e}\left(\frac{2}{3(2R-R^{2})}\frac{1}{Re_{s}\,Sc_{s}}\frac{L}{\delta}\right)\frac{\partial^{2}C}{\partial R^{2}}dRdZ \tag{3.36}$$

Carrying out the integral yields:

$$\left(C_{s}-C_{n}\right)=\frac{\Delta Z}{\Delta R}\left(\frac{2}{3(2R-R^{2})}\frac{1}{Re_{s}\,Sc_{s}}\frac{L}{\delta}\right)\left(\left.\frac{\partial C}{\partial R}\right|_{e}-\left.\frac{\partial C}{\partial R}\right|_{w}\right) \tag{3.37}$$

3.4 Solution Method

T_s, T_n, C_s and C_n terms represent values at control surfaces of any control volume (see Figure 3.6). As the convective effects in the downstream direction is very strong compared to the diffusion effects, using upwind scheme (Patankar, 1980) is appropriate for these terms. Solution flows down with the effect of gravity, hence

$T_s \simeq T_P$, $T_n \simeq T_N$, $C_s \simeq C_P$ and $C_n \simeq C_N$ (see Figure 3.6). Derivatives in Eq. 3.35 and 3.37 for inner nodes are evaluated using central difference formulation as follows:

$$\left.\frac{\partial T}{\partial R}\right|_e = \frac{T_E - T_P}{\Delta R}, \quad \left.\frac{\partial T}{\partial R}\right|_w = \frac{T_P - T_W}{\Delta R} \tag{3.38a}$$

$$\left.\frac{\partial C}{\partial R}\right|_e = \frac{C_E - C_P}{\Delta R}, \quad \left.\frac{\partial C}{\partial R}\right|_w = \frac{C_P - C_W}{\Delta R} \tag{3.38b}$$

Special treatments are necessary for discretizing equations 3.35 and 3.37 for boundaries (wall, inlet, surface and outlet), but the method is the same as the one discussed above. The resulting equation system are arranged in matrix form, and solved 'line-by-line' (iteratively) using the 'Three Diagonal Matrix Algorithm' (Patankar, 1980). The matrix that will be solved for a column in a two-dimensional domain for temperature field is shown in Figure 3.7:

$$\begin{bmatrix} a_{P_1} & -a_{E_1} & & & & \\ -a_{W_2} & a_{P_2} & -a_{E_2} & & & \\ & \ddots & \ddots & \ddots & & \\ & & & -a_{W_{n-1}} & a_{P_{n-1}} & -a_{E_{n-1}} \\ & & & & -a_{W_n} & a_{P_n} \end{bmatrix} \begin{Bmatrix} T_{1,j} \\ T_{2,j} \\ \vdots \\ T_{n-1,j} \\ T_{n,j} \end{Bmatrix} = \begin{Bmatrix} a_{N_1} T_{N_1} + a_{S_1} T_{S_1} + Source_1 \\ a_{N_2} T_{N_2} + a_{S_2} T_{S_2} + Source_2 \\ \vdots \\ a_{N_{n-1}} T_{N_{n-1}} + a_{S_{n-1}} T_{S_{n-1}} + Source_{n-1} \\ a_{N_n} T_{N_n} + a_{S_n} T_{S_n} + Source_n \end{Bmatrix}$$

Figure 3.7 Matrix form of the discretization equations for a column in the 2D domain.

In Figure 3.7, 'a' coefficients that belong to P, W, E, N and S nodes are coeficients of T_P, T_W, T_E, T_N and T_S. See Figure 3.6 for definitions of w, e, n, s, W, E, N and S.

The column (line) scans all the two dimensional domain by traveling to a successive position in a selected direction. Because, the values outside the line is assumed to be known, a sufficient number of line scans are necessary for convergence in rectangular domain. The same procedure is valid for calculating concentration field. Readers are referred to Versteeg & Malalasekera (1995) for further details.

It should be noted that the above procedure is to calculate temperature and concentration fields for 'known' boundary conditions. However boudary conditions at the wall and film surface are not known. Hence calculations are performed for guessed boundary conditions.

A special iterative algorithm is necessary to calculate boundary conditions for coupled energy and species balance equations. Hence the procedure described above is a sub procedure for the solution algorithm.

3.4.1 Solution Algorithm

After specifying pyhsical variables, the program converts them to real dimensionless inputs and writes to file for future investigations. However, the difficulty arise at the film surface and tube wall because temperature and concentration values are not known at these surfaces. Besides from these, energy and species transport equations are coupled at the film surface. To deal with these difficulties, an iterative procedure must be employed for both the film surface and tube wall.

After guessing the temperature field, concentration field, mass absorption rates at the interface (from which the temperature gradient can also be calculated by eq. 3.32), wall temperature and coolant outlet temperature; the calculation starts from computing a new temperature field.

Depending on the new temperature field, a new concentration distribution at the interface boundary are evaluated from Eq. 3.16. Once the concentration values at the interface are known, a new concentration field can be obtained. Physical properties are updated locally before each calculation cycle. As the new temperature and concentration fields are known, a new mass absorption rate distribution at the interface can be obtained from the new concentration field, from which a new temperature gradient profile at the interface can be obtained. Once the new temperature gradient profile is known, a new temperature field then can be calculated.

The procedure continues until a reasonable convergence between the new and old mass absorption rates is achieved. But this convergency is valid for the old tube wall temperature, hence the above calculations must be updated each time a new wall temperature distribution is obtained.

Convergence criteria at the interface is defined as follows:

$$\frac{\left|\dot{m}_{abs/new} - \dot{m}_{abs/old}\right|}{m_{abs/new}} < \text{convergence criteria}$$

Convergence criteria at the tube wall is defined as follows:

$$\frac{\left|q_{wall/new} - q_{wall/old}\right|}{q_{wall/new}} < \text{convergence criteria}$$

A convergence criteria of 10^{-12} was chosen for the interface calculations with underrelaxation factors between 0.1 and 0.5, and a convergence criteria of 10^{-6} was chosen for the wall calculations with underrelaxation factors between 0.1 and 0.6. Underrelaxation factors are selected depending on the operating conditions.

Once convergence is achieved at the interface boundary, a new iterative algorithm must be employed for the wall boundary condition. Each iteration starts with the calculation of heat flux distribution at the tube wall, from which a new cooling water bulk temperature distribution along the axial direction can be obtained. Once the cooling water bulk temperature distribution is known, local tube wall temperature distribution can be calculated by using constant transfer coefficient at the cooling water side. The computation continues until convergence is achieved between the old and new wall temperature profiles. If these converges, then the solution is complete. The flowchart of the algorithm is presented in Figure 3.8.

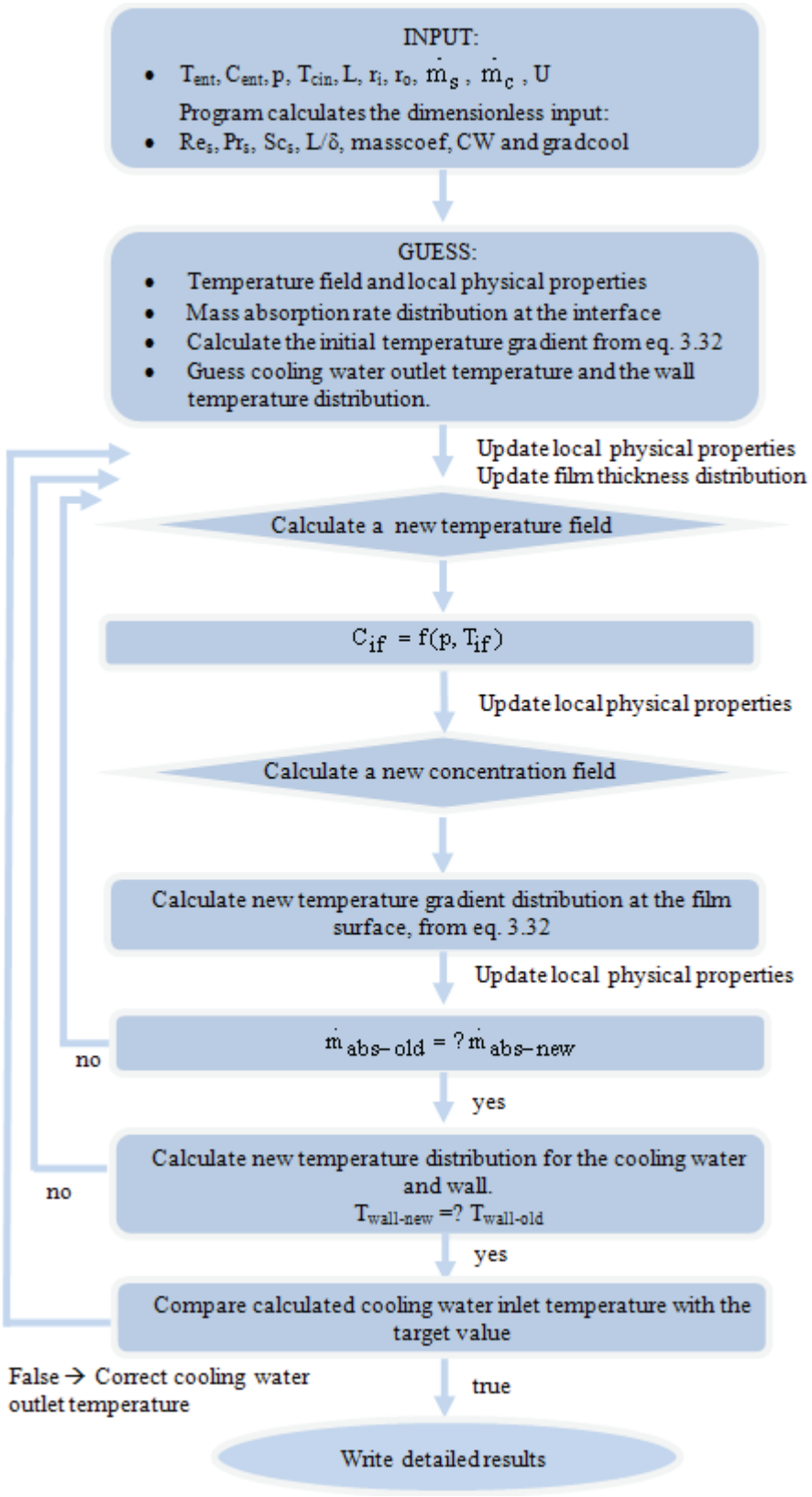

Figure 3.8 Flowchart for the computational algorithm of the vertical absorber model.

CHAPTER FOUR
A NUMERICAL MODEL FOR HORIZONTAL TUBULAR ABSORBER

The LiBr / H_2O solution is sprayed from the top of the horizontal tubes and flows down a number of horizontal tubes arranged vertically while vapour is supplied from the evaporator continiously under vacuum conditions (Figure 4.1). The flow is in the form of falling film on the tubes, and unsteady droplets or long tails between the tubes. As the solution absorps vapour, heat of absorption is generated which must be rejected to the ambient by a cooling water or air.

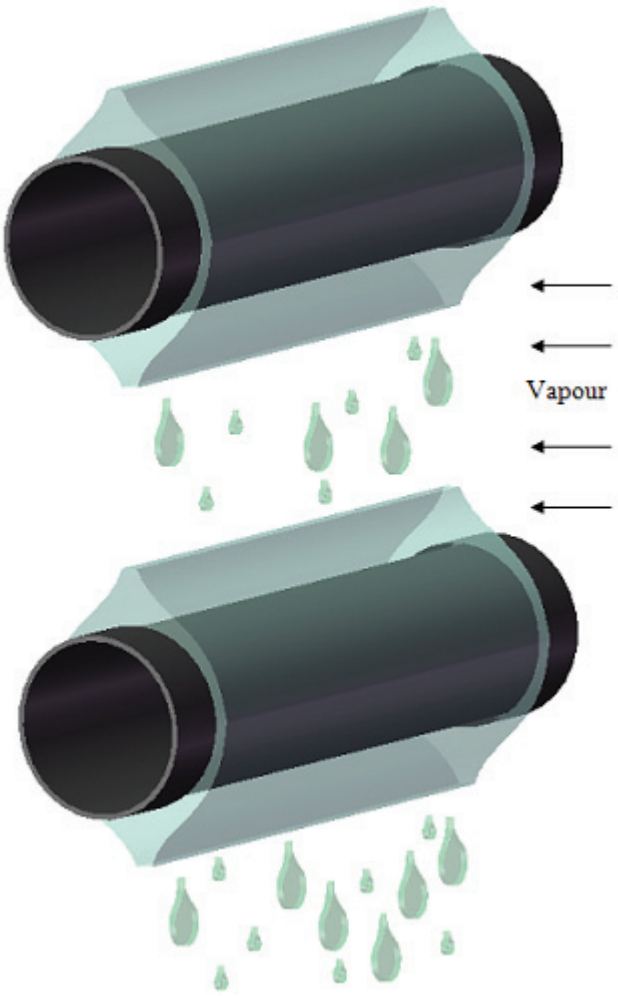

Figure 4.1 Schematic view of a horizontal absorber.

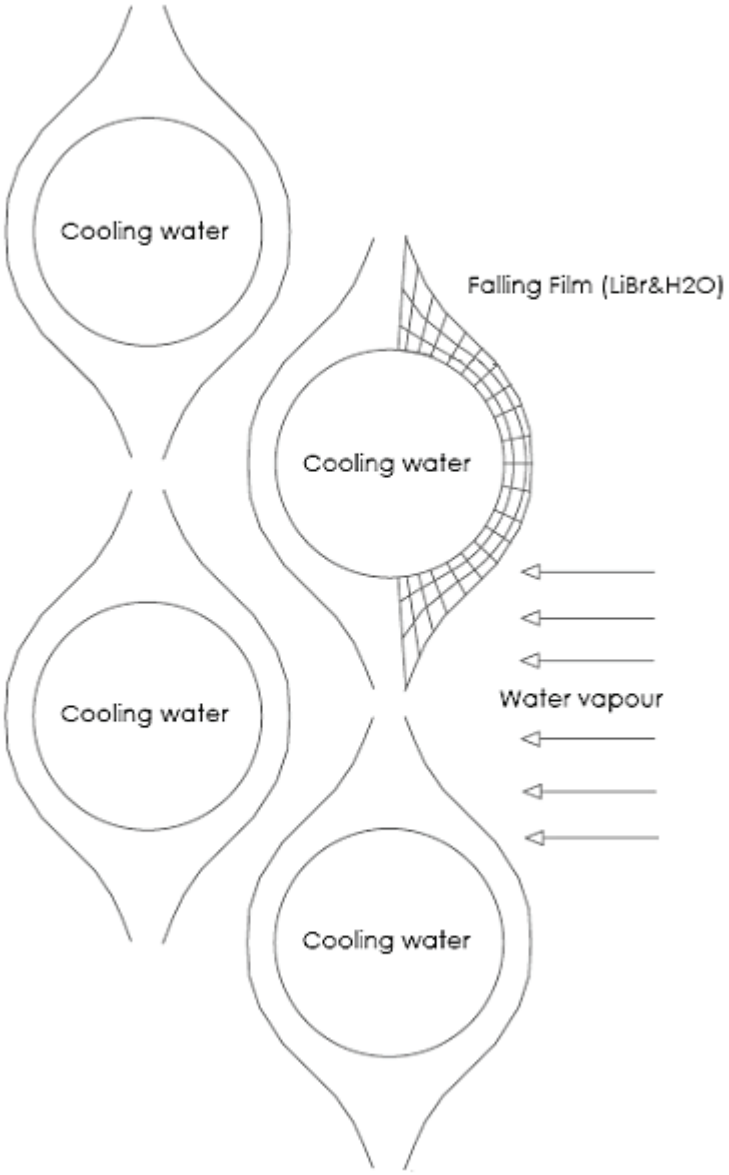

Figure 4.2 The physical domain and mesh used to model the falling film.

To model the absorber, a two dimensional section of the film flow is divided into a number of non-overlapping Eulerian control volumes (see section 3.3). However because the film thickness varies with downstream position, body fitted mesh is created (see Fig. 4.2). Coordinate transformation is performed to convert the physical domain into a rectangular domain to simplify programming.

Properties of the model can be listed as follows:

- Physical properties vary with local temperature and concentration (but variation within the differential control volume is neglected),
- The massflow rate increases as the vapour is absorbed into the liquid film, hence the film thickness distribution varies in the successsive tubes.

Assumptions can be listed as follows:

- Tube is completely wetted by the solution,
- Vapour pressure equilibrium exists at the vapour & solution interface,
- The flow is laminar and non-wavy throughout,
- Heat transfer in the vapour phase is negligible compared to that in the solution, so all of the heat generated at the interface is transferred into the solution,
- No shear stress is exerted on the film flow by the vapour,
- Diffusion in the flow direction is negligible,

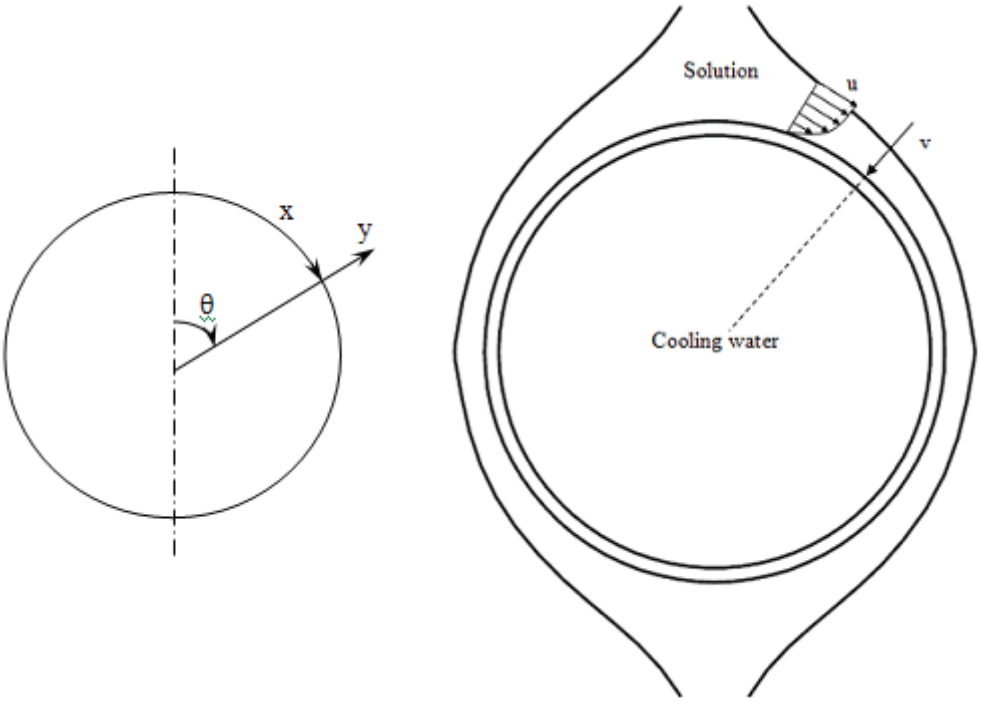

Figure 4.3 The physical coordinate system (left) and the velocity components (right).

4.1 Governing Equations

Film velocity profile can be calculated from the Navier-Stokes Equations. Because the film thickness is very small compared to the tube radius, cartesian coordinate system for film flow can be used and because viscous forces are dominant, inertia forces can be neglected. It's also assumed that pressure throughout the film is constant and the driving force is the gravity force.

Steady Navier-Stokes Equation in the flow direction (see the x axis in Figure 4.3) under these assumptions becomes:

$$\mu_s \frac{\partial^2 u}{\partial y^2} = -\rho_s g \sin\theta \tag{4.1}$$

Assumig no shear stress is exerted on the film by the vapour; velocity profile in the flow direction (see 'u' in Figure 4.3) can be derived as:

$$u(x,y) = \frac{\rho_s\, g\, \delta^2}{2\mu_s} \sin\theta \left(2\frac{y}{\delta} - \left(\frac{y}{\delta}\right)^2 \right) \tag{4.2}$$

The velocity profile in the transverse direction (see 'v' in Figure 4.3) can be determined from continuity:

$$v(x,y) = -\frac{\rho_s g}{2\mu_s} y^2 \left[\frac{d\delta}{dx} \sin\theta + \frac{1}{r_o}\left(\delta - \frac{y}{3}\right)\cos\theta \right] \tag{4.3}$$

Local film thickness can be derived from u-velocity (Eq. 4.2) for a known solution mass flow rate (Sultana, Wijeysundera, Ho, & Yap, 2007):

$$\delta(\theta) = \left(\frac{3\mu_s \Gamma_s}{\rho_s{}^2 g \sin\theta} \right)^{1/3} \tag{4.4}$$

Where Γ_s is the solution mass flow rate per length and side of tube ($\Gamma_s = \dot{m}_s / 2L$).

Steady energy balance for a differential control volume can be expressed in cartesian coordinates, because typical values of film thickness are very small compared to the tube diameter. By making the same assumptions that are already made in vertical absorber model (Eq. 3.5), it can be expressed as:

$$\frac{\partial(uT)}{\partial x} + \frac{\partial(vT)}{\partial y} = \alpha_s \frac{\partial^2 T}{\partial y^2} \tag{4.5}$$

Steady species balance for a differential control volume under the same assumptions that are already made in vertical absorber model (Eq. 3.7) can be expressed as:

$$\frac{\partial(uC)}{\partial x} + \frac{\partial(vC)}{\partial y} = D \frac{\partial^2 C}{\partial y^2} \tag{4.6}$$

4.1.1 Energy Balance in the Cooling Water Side

As in the case of vertical absorbers, typically, the solution film has very small mass flow rate compared to the cooling water mass flow rate. Thus, the specific heat of the LiBr-water solution is smaller than that of cooling water and typical length of a tube for a horizontal absorber is even smaller than typical length of vertical absorber. Hence, heat capacity of the cooling water is much larger than that of the

solution, combining this with typical small tube length means the overall temperature increase of the cooling water is much smaller than that of the solution.

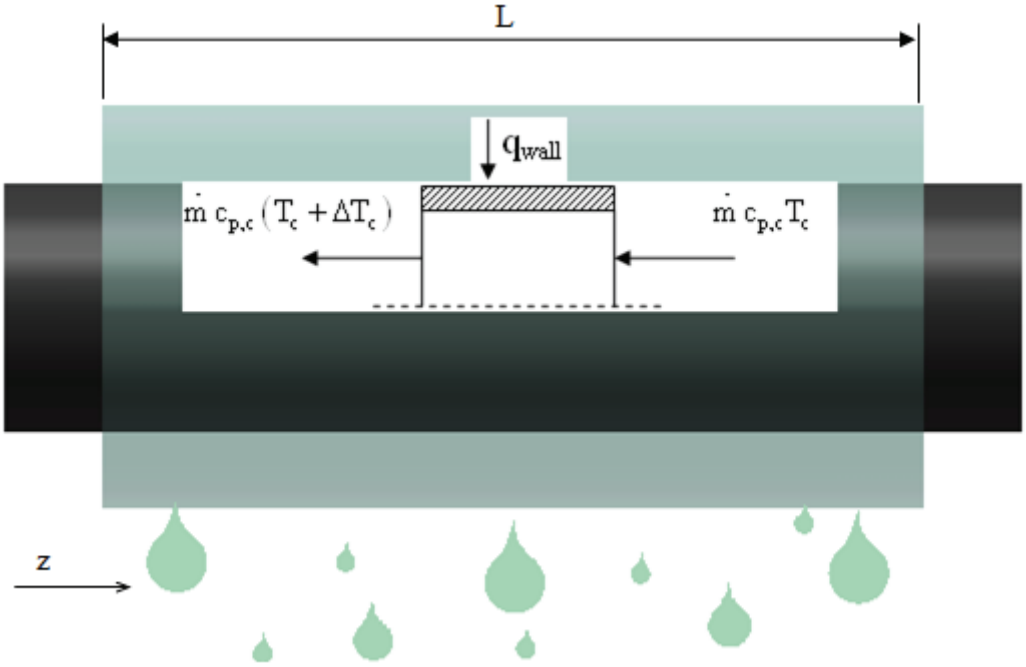

Figure 4.4 One dimensional differential control volume for the cooling water flowing inside the tube.

It can be concluded from a previous investigation (Papaefthimiouet al. 2006) that the temperature increase of the cooling water is linear in the axial direction of the tube. Hence cooling water temperature can be calculated at the half length of each tube, and this will represent the mean cooling water temperature for the tube. Heat transfer coefficient in the cooling water side is calculated from $Nu_b = 0.023\,Re_b^{0.8}\,Pr_b^{0.4}\left(\mu_b/\mu_w\right)^{0.262}$ correlation which is valid for incompressible turbulent flow flowing inside a pipe (Kakaç et al., 1998).

Cooling water temperature gradient expression for the cooling water can be derived from the one dimensional energy balance:

$$\frac{dT_c}{dz} = \frac{\left(2\pi r_o\right) q_{wall-average}}{m_c\, c_{p,c}} \tag{4.7}$$

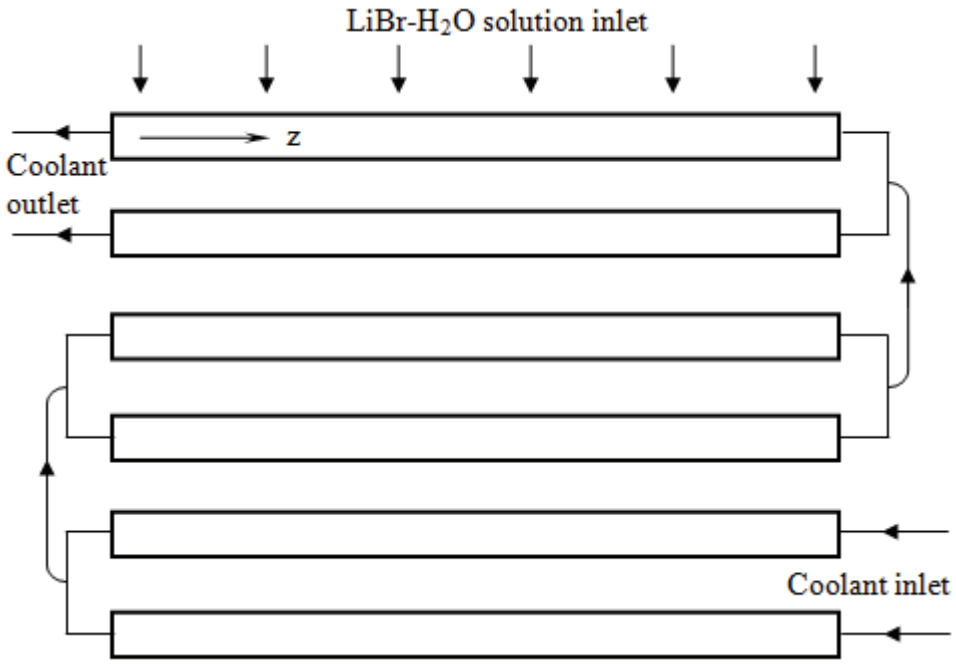

Figure 4.5 Tubes and the cooling water arrangement.

4.1.2 Initial&Boundary Conditions

Because the problem is a steady spatial marching problem, the calculation procedure must start from solution inlet, hence the boundary conditions at the inlet are categorized under "initial conditions".

Initial conditions for the LiBr-H_2O solution at the inlet are (see Figure 4.6):

$$\left.\begin{array}{l} x = x_{in} \\ 0 \le y \le \delta(x) \end{array}\right\} \quad \begin{array}{l} T = T_{in} \\ C = C_{in} \end{array} \tag{4.8}$$

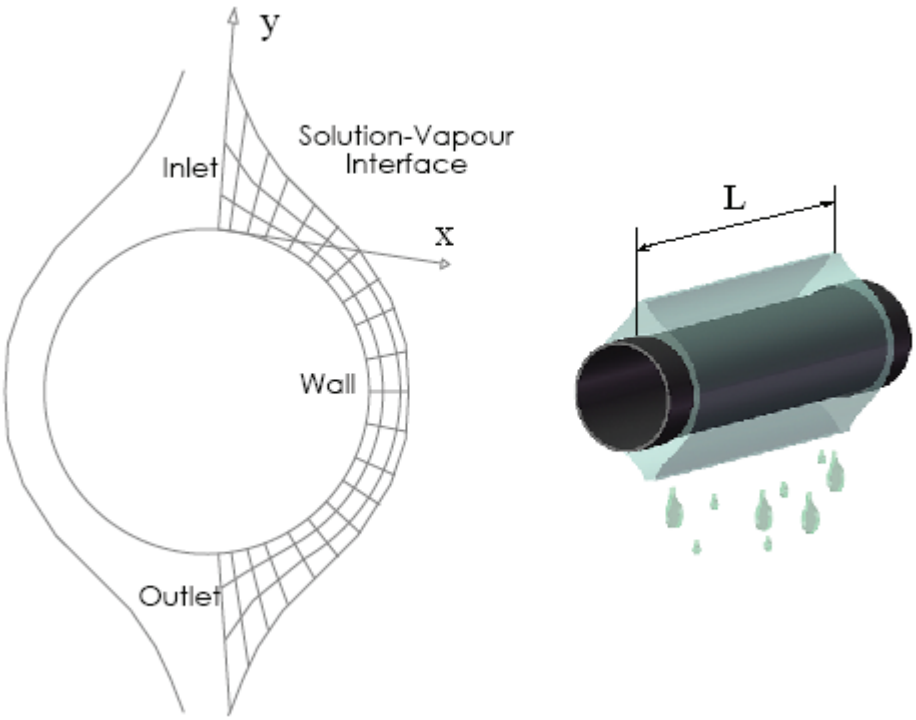

Figure 4.6 Boundaries of the physical domain (right) and demonstration of tube length (right).

The boundary conditions for the LiBr-H_2O solution are as follows:

At the tube surface:

$$\left.\begin{array}{l} y = 0 \\ x_{in} \le x \le x_{out} \end{array}\right\} \quad \begin{array}{l} U\left(T - T_c\right) = k_s \dfrac{\partial T}{\partial y} \\ \dfrac{\partial C}{\partial y} = 0 \end{array} \tag{4.9}$$

U is the overall heat transfer coefficient calculated at the outer surface of the tube (see Eq. 3.12).

At the solution-vapour interface:

$$\left.\begin{array}{l} y=\delta(x) \\ x_{in} \le x \le x_{out} \end{array}\right\}$$

Mass flux is calculated from Fick's first law (see Eq. 3.14):

$$\dot{m}_{H_2O} = -\rho_s D \frac{1}{C_{if}} \frac{\partial C}{\partial y} \tag{4.10}$$

Vapour pressure equilibrium condition function is (see equations 3.15 and 3.16, and section 3.1.2):

$$T_{if} = f(p, C_{if}) \tag{4.11}$$

Heat generation at the interface can be expressed as the product of mass absorption rate and heat of absorption per unit mass flow rate (see Section 3.1.2):

$$q_{if} = h_{abs} \dot{m}_{H_2O} \tag{4.12}$$

And heat of absorption is transferred into the solution:

$$q_{if} = -k_s \frac{\partial T}{\partial y} \tag{4.13}$$

At the outlet, gradients of temperature and concentration in the flow direction are set to zero.

4.2 Coordinate Transformation

Because the film thickness changes with the circumferential position (see Figure 4.3), a coordinate transformation process is needed in order to convert the complex domain into a nondimensional square domain (see Figure 4.7), hence derivatives are normalized. This generally increases complexity of the governing equations, however simplifies the code considerably. Hence we are considering the following non-dimensional variables:

$$X = \frac{\theta}{\pi} = \frac{x}{\pi r_o} \tag{4.14a}$$

$$Y = \frac{y}{\delta(x)} \tag{4.14b}$$

$$Z = \frac{z}{L} \tag{4.14c}$$

Because the film thickness is infinite at the top and bottom of the tube for the Nusselt's solution, hence Y becomes infinite in these extreme points. Hence regions close to X=0 and X=1 are omitted from the solution domain in order to prevent this situation (see Figure 4.7).

By substituting 4.14 into governing equations;

Film thickness expression (Eq. 4.4) becomes:

$$\delta(\theta) = \left(\frac{3\mu_s \Gamma_s}{\rho_s{}^2 g \sin(\pi X)} \right)^{1/3} \tag{4.15}$$

Where Γ_s is the solution mass flow rate per length and side of tube ($\Gamma_s = \dot{m}_s / 2L$).

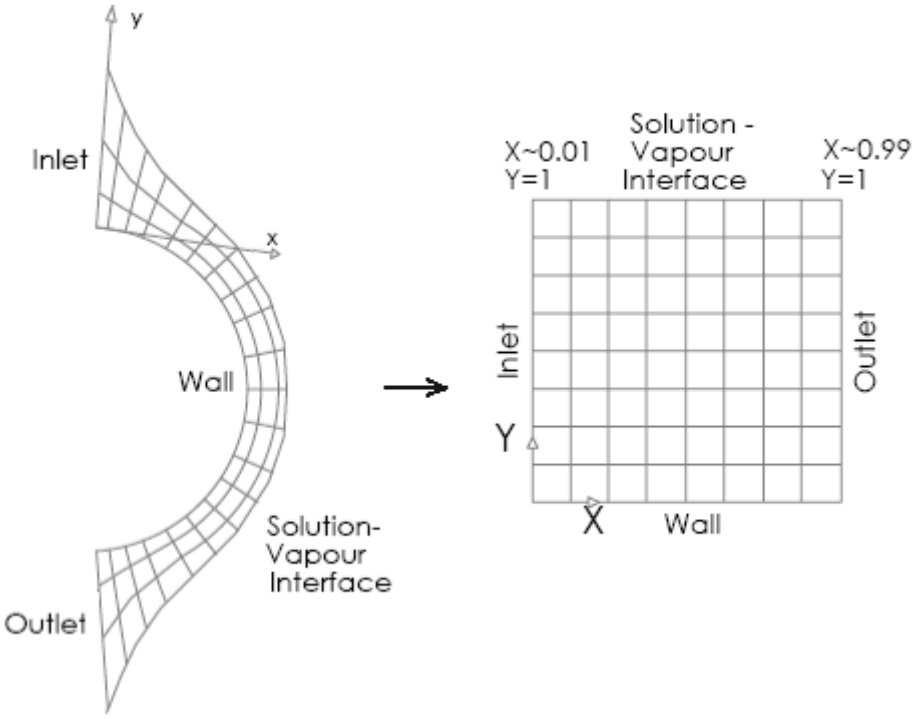

(a) (b)

Figure 4.7 The physical calculation domain (a), and the transformed calculation domain (b).

The velocity profiles (Eq. 4.2 and 4.3) become:

$$u(X,Y) = \frac{\rho_s\, g\, \delta^2}{2\mu_s} \sin(\pi X)\left(2Y - Y^2\right) \tag{4.16}$$

$$v(X,Y) = -\frac{\rho_s g}{2\mu_s} Y^2\ \delta^2 \frac{1}{r_o}\left[\frac{1}{\pi}\frac{d\delta}{dX}\sin(\pi X) + \delta\left(1 - \frac{Y}{3}\right)\cos(\pi X)\right] \tag{4.17}$$

If the solution Reynolds, Prandl and Schmidt numbers are defined as (respectively):

$$\mathrm{Re}_s = \frac{4\Gamma_s}{\mu_s} \tag{4.18}$$

Where Γ_s is the solution mass flow rate per length and side of tube ($\Gamma_s = \dot{m}_s / 2L$).

$$\mathrm{Pr}_s = \frac{\mu_s c_{ps}}{k_s} \tag{4.19}$$

$$\mathrm{Sc}_s = \frac{\mu_s}{\rho_s D} \tag{4.20}$$

Energy equation (4.5) becomes:

$$\frac{\partial T}{\partial X} - \left[\frac{v}{u}\frac{\pi r_o}{\delta} - \frac{Y}{\delta}\frac{d\delta}{dX}\right]\frac{\partial T}{\partial Y} - \left[\frac{8}{3}\frac{1}{\mathrm{Pr}_s}\frac{\pi r_o}{\delta_{90}}\frac{\sin(\pi X)^{1/3}}{\mathrm{Re}_s\left(2Y - Y^2\right)}\right]\frac{\partial^2 T}{\partial Y^2} = 0 \tag{4.21}$$

Species transport equation (4.6) becomes:

$$\frac{\partial C}{\partial X} - \left[\frac{v}{u}\frac{\pi r_o}{\delta} - \frac{Y}{\delta}\frac{d\delta}{dX}\right]\frac{\partial C}{\partial Y} - \left[\frac{8}{3}\frac{1}{\mathrm{Sc}_s}\frac{\pi r_o}{\delta_{90}}\frac{\sin(\pi X)^{1/3}}{\mathrm{Re}_s\left(2Y - Y^2\right)}\right]\frac{\partial^2 C}{\partial Y^2} = 0 \tag{4.22}$$

In the equations 4.21 and 4.22, δ_{90} is the film thickness at the middle of the tube (X=0.5).

4.2.1 Initial & Boundary Conditions for the Transformed Equations

The boundary conditions for the transformed governing equations (Eq. 4.21 and 4.22) can be derived from the boundary conditions of the physical governing equations as follows:

At the entrance (see Figure 4.7):

$$\left.\begin{array}{l} X = X_{in} \\ 0 \le Y \le 1 \end{array}\right\} \quad \begin{array}{l} T = T_{in} \\ C = C_{in} \end{array} \tag{4.23}$$

At the tube wall:

$$\left.\begin{array}{l} Y = 0 \\ X_{in} \le X \le X_{out} \end{array}\right\} \quad \begin{array}{l} T_{wall} = T_c + \left(\dfrac{k_s}{\delta_{mean} U} \right) \dfrac{\partial T}{\partial Y} \\ \dfrac{\partial C}{\partial Y} = 0 \end{array} \tag{4.24}$$

The term ' $k_s / (\delta_{mean} U)$ ' is named as "CW".

At the solution-vapour interface:

$$\left.\begin{array}{l} Y=1 \\ X_{in} \le X \le X_{out} \end{array}\right\}$$

Heat of absorption is transferred into the solution (see Section 3.1.2):

$$\frac{\partial T}{\partial Y} = -\frac{\rho_s Dh_{abs}}{k_s} \frac{1}{C_{if}} \frac{\partial C}{\partial Y} \tag{4.25}$$

The term ' $\rho_s Dh_{abs} / k_s$ ' is named as "the mass coefficient".

Vapour pressure equilibrium condition (see equations 3.15 and 3.16, and section 3.1.2):

$$T_{if} = f(p, C_{if}) \tag{4.26}$$

At the outlet, gradients of temperature and concentration with respect to X are set to zero.

4.3 Deriving the Discretization Equations

The control volume method is used for deriving the discretization equations (see section 3.3). The transformed governing equations (4.21-22) are integrated over a control volume respectively by assuming constant Y, δ(X), u and v inside a control volume:

$$\frac{\Delta Y}{\Delta X}\left(T_e - T_w\right) - \left[\frac{v}{u}\frac{\pi r_o}{\delta} - \frac{Y}{\delta}\frac{d\delta}{dX}\right]\left(T_n - T_s\right) - \left[\frac{8}{3}\frac{1}{Pr_s}\frac{\pi r_o}{\delta}\frac{\sin(\pi X)^{1/3}}{Re_s\left(2Y - Y^2\right)}\right]\left.\frac{\partial T}{\partial Y}\right|_s^n = 0 \tag{4.27}$$

$$\frac{\Delta Y}{\Delta X}\left(C_e - C_w\right) - \left[\frac{v}{u}\frac{\pi r_o}{\delta} - \frac{Y}{\delta}\frac{d\delta}{dX}\right]\left(C_n - C_s\right) - \left[\frac{8}{3}\frac{1}{Sc_s}\frac{\pi r_o}{\delta}\frac{\sin(\pi X)^{1/3}}{Re_s\left(2Y - Y^2\right)}\right]\left.\frac{\partial C}{\partial Y}\right|_s^n = 0 \tag{4.28}$$

Definitions of w, e, n, s, W, E, N and S points are illustrated in Figure 4.8.

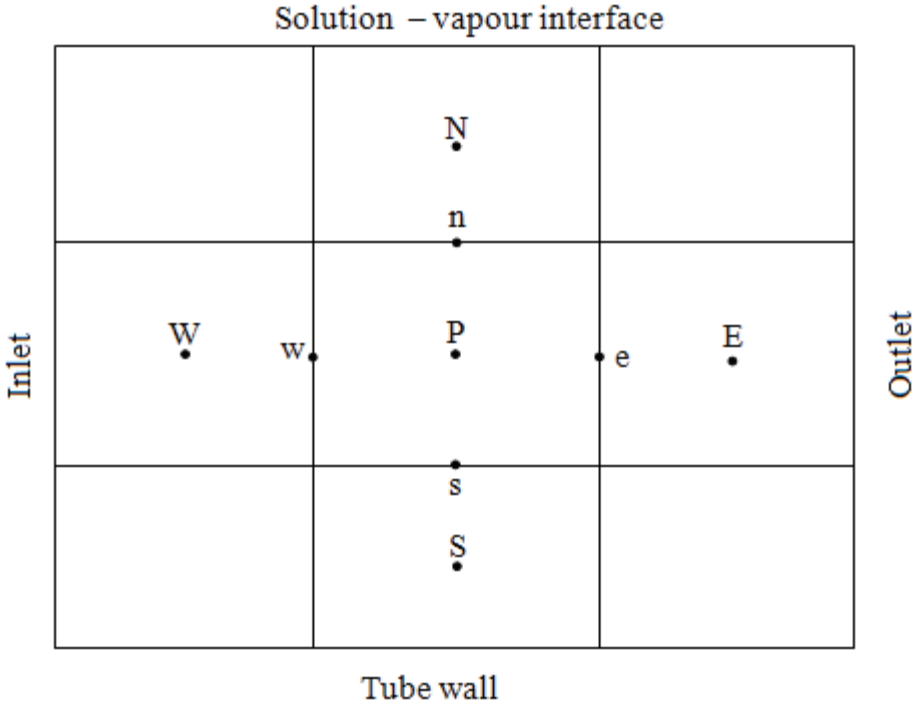

Figure 4.8 Schematic view of the grid structure, and definitions of the west, east, south and north nodes and control surfaces.

Cooling water energy balance becomes:

$$\frac{dT_c}{dZ} = -\left(\frac{(2\pi r_o) L k_s}{m_c c_{p,c} \delta_{mean}}\right) \left.\frac{\partial T}{\partial Y}\right|_{mean} \tag{4.29}$$

The term ' $-2\pi r_o L k_s / \left(\dot{m}_c c_{pc} \delta_{mean}\right)$ ' is named as "gradcool".

4.4 Solution Method

Calculating temperature and concentration fields for known boundary conditions are discussed is section 3.4. However there are some differences, because transverse (v) velocity component arises in the horizontal geometry (see Figure 4.3). However because the transverse velocity component is very small, diffusion is stronger and

upwind scheme is not appropriate. Hence central differencing scheme is used in the transverse (y) direction. Hence $T_n = (T_N + T_P)/2$ and $T_s = (T_P + T_S)/2$. Upwind scheme (Patankar, 1980) is used in the downstream direction as is done in the vertical absorber model. Hence, $T_w \simeq T_W$, $T_e \simeq T_P$, $C_w \simeq C_W$ and $C_e \simeq C_P$ (see Figure 4.8).

Derivatives in Eq. 4.27 and 4.28 for inner nodes are evaluated using central difference formulation as follows:

$$\left.\frac{\partial T}{\partial Y}\right|_n = \frac{T_N - T_P}{\Delta Y}, \quad \left.\frac{\partial T}{\partial Y}\right|_s = \frac{T_P - T_S}{\Delta Y} \tag{4.30a}$$

$$\left.\frac{\partial C}{\partial Y}\right|_n = \frac{C_N - C_P}{\Delta Y}, \quad \left.\frac{\partial C}{\partial Y}\right|_s = \frac{C_P - C_S}{\Delta Y} \tag{4.30b}$$

4.4.1 Solution Algorithm

The solution algorithm for the horizontal absorber model is very similar to that of the vertical absorber model, however there are slight differences for the cooling water side (see Figures 4.4 and 4.5). Cooling water temperature is known at the inlet of the last tube, on the other hand, the calculation procedure starts from the first tube. Hence a cooling water outlet temperature must be predicted.

A sufficient number of two dimensional sections (see Figures 4.2, 4.4 and 4.6) must be solved consecutively to observe the decrease of the cooling water temperature. This adds some three dimensional effects to the solution. However because of long computational time, three axial positions are selected by assuming linear decrease in cooling water temperature. Cooling water bulk temperatures at the middle and end (cooling water enters from the end of the tube because of the counter-flow heat exchanger - like design) of each tube are recorded. The cooling water temperature at the half length of the tube is taken as the mean value for the

considered tube. The cooling water temperature at the end of the tube is taken as the exit temperature for the successive tube.

The other difference between the vertical absorber model and horizontal absorber model is that, in the horizontal absorber model, LiBr-H_2O exit bulk temperature and concentration for a tube is the uniform inlet temperature and concentration for the successive tube. Absorption between two tubes is neglected. Also the film mass flow rate increases as the vapour is absorbed, however mass flow rate will be taken constant for a single tube, and the total absorbed mass in a single tube is added to the film mass flow rate at the exit of the tube, hence it increases at the inlet of the successive tube.

Apart from the differences mentioned above, the solution algorithm is very similar to that of the vertical absorber model, hence readers are referred to section 3.4 for more details about the algorithm. A flowchart of the algorithm is presented in Figure 4.9.

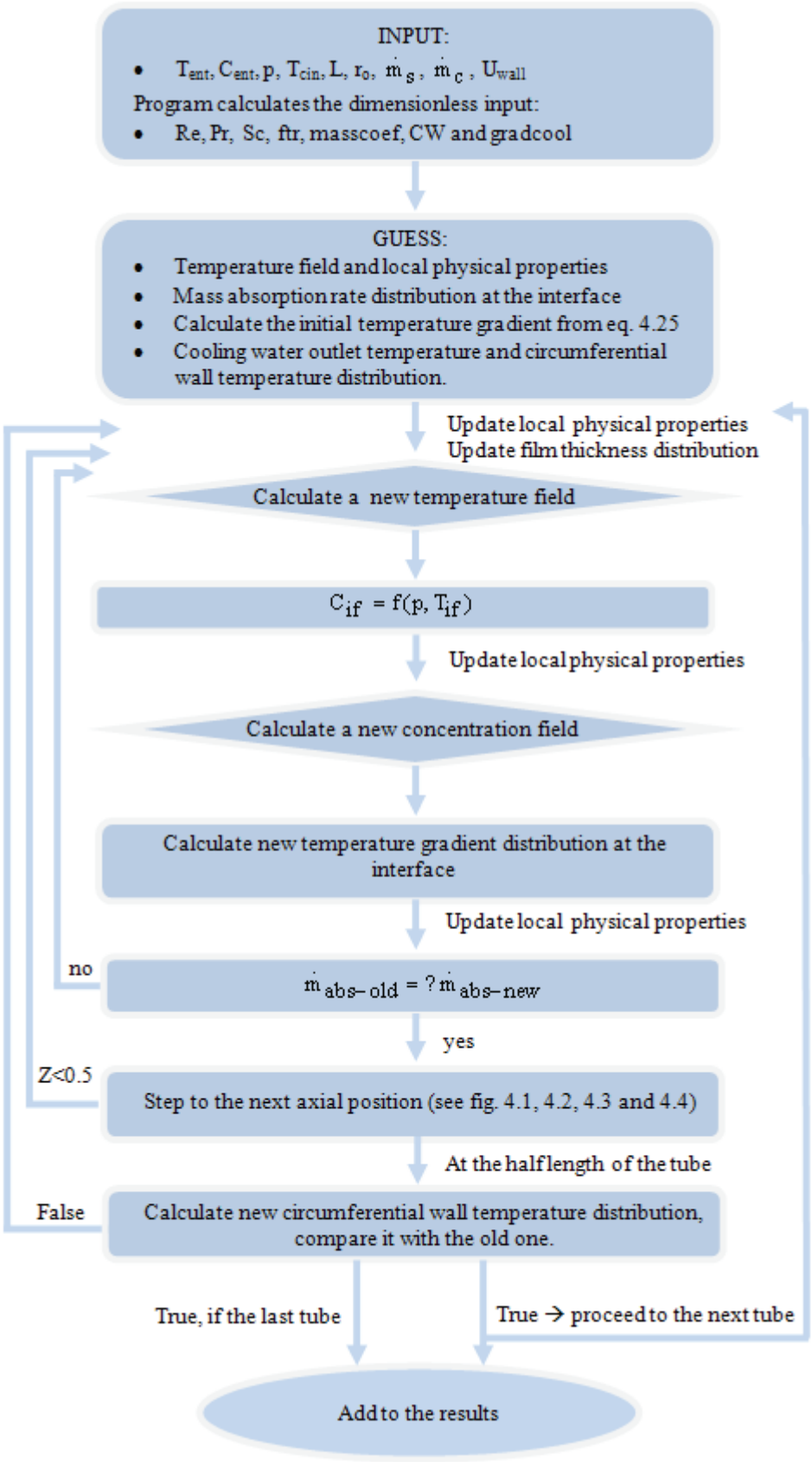

Figure 4.9 Flowchart for the algorithm of the horizontal absorber model.

CHAPTER FIVE
RESULTS

5.1 Introduction

Results for the vertical and the horizontal absorbers under various conditions such as the vapour pressure, solution inlet temperature, solution inlet concentration, cooling water inlet temperature, mass flow rate and tube geometry are given. Results are compared with experimental data avaiable in the literature and the limits of the present model are outlined (Section 5.5). To understand the geometry and dimensionless axes used in the simulations, please see Figures 3.1 and 3.5 for the vertical type absorber and see Figures 4.1 and 4.7 for the horizontal type absorber.

The distribution and mean value of vapour absorption flux is selected as the performance parameter. Because the film thickness is a function of film Reynolds number and some physical properties, the mass (and heat) flux distributions are valid for any physical system that satisfies the dimensionless numbers used as program inputs.

Heat flux distributions at the film surface and wall are also plotted which are also very important parameters, because mass transfer is strongly coupled with heat transfer, such that mass transfer is possible as long as heat of absorption is transferred from the interface to the cooling water.

5.1.1 Evaluation of Physical Properties

Physical properties of LiBr-H_20 are taken from various sources. Curve fits of experimental data for density, heat capacity, dynamic viscosity and thermal conductivity are taken from Kwang (1992):

$$\rho_s = 1000\,x\left((0.7086 + 1.691\ x\ C) - 0.0005\ x\ T\right) \quad \left[kg/m^3\right] \tag{5.1}$$

$$c_{ps} = 1000\,x\,19.458\,x\,T^{0.05}\ x\ \left(100\ x\ C\right)^{-0.609} \quad \left[J/kgK\right] \tag{5.2}$$

$$k_s = 1.163\,x\left(0.4945 + 0.002052\ x\ T - 0.000015\ x\ T^2 - 0.31xC\right) \quad \left[W/m^2K\right] \tag{5.3}$$

$$\mu_s = \left(1 + 0.686602333\ x\ e^{(0.107\ x\ 100\ x\ C)}\ x\ T^{-1.238}\right)\Big/ 1000 \quad \left[Ns/m^2\right] \tag{5.4}$$

The curve fit of Andberg (1986) for heat of absorption is modified by the author to match the more accurate data calculated by Papaefthimiou et al. (2006).:

$$\begin{aligned} h_{abs} = {} & 2.5124\ x\ 10^6 - \left(283.3 + 1177\ x\ T\right) \\ & + 20152\ x\ (1660.47\ *\ C^7 - 2550\,x\,C^8 + 1410.1xC^9) \quad [J/kgK] \end{aligned} \tag{5.5}$$

Surface pressure equilibrium function ($C_{if} = f(p, T_{if})$) is taken from Raisul Islam et al. (2006) which is linearized in the range of our interest:

$$C_{if} = \left(4.8688\ x\ 10^{-3}\ x\ p^{-0.188}\right) T_{if} + 0.37794 \tag{3.16}$$

Diffusivity was taken constant because curve fits in the above references are wrong, and no other appropriate curvefit can be found:

$$D = 1.52\ x\ 10^{-9} \quad \left[m^2/s\right] \tag{5.6}$$

5.1.2 Definitions

The local interfacial mass flux for vertical absorber can be obtained by the expression (see Figure 3.5 and Eq. 3.14):

$$\dot{m}(Z) = \rho D \frac{1}{C} \left. \frac{\partial C}{\delta(Z) \partial R} \right|_{R=1} \qquad \left[kg / m^2 s \right] \tag{5.7}$$

Where $\delta(Z) = \left(0.75 \, Re \, \upsilon_s^{\,2} / g \right)^{1/3}$ is the film thickness (see Eq. 3.3) evaluated at the local bulk conditions at any axial (downstream) position. Note that it is only dependent to the local Reynolds number, the temprature and the concentration (so to the solution viscosity and density). As the temperature is not nondimensionalized (see Section 3.2), the distribution of the flux is valid for partially nondimensionalized system.

Mean interfacial mass flux can be evaluated by directly averaging local mass fluxes:

$$\dot{m}_{mean} = \int_{Z=0}^{1} \dot{m}(Z) \, dZ \tag{5.8}$$

The local interfacial mass flux for the horizontal absorber can be obtained by the expression (see Figure 4.7 and Eq. 4.10) :

$$\dot{m}(X) = \rho D \frac{1}{C} \left. \frac{\partial C}{\delta(X) \partial X} \right|_{Y=1} \qquad \left[kg / m^2 s \right] \tag{5.9}$$

Where $\delta(X) = \left(0.75 \, Re \, \upsilon_s^{\,2} / g / \sin(\pi X) \right)^{1/3}$ is the film thickness (see Eq. 4.4) evaluated at the local bulk conditions at any circumferential position. Note that it is only dependent to the local Reynolds number, temprature and concentration (so the

solution viscosity and density). By this way, the massflux distribution can be evaluated for the partially nondimensional system as mentioned above.

Overall interfacial mass flux can be evaluated by directly averaging local mass fluxes:

$$\dot{m}_{mean} = \frac{\sum_{X_{in}}^{X_{out}} \dot{m}(X)}{n} \tag{5.10}$$

Where n is the number of cells in the downstream (x) direction (see Figure 4.6).

Bulk temperature (T_b) and concentration (C_b) for both vertical and horizontal absorber can be calculated as follows:

$$T_b = \frac{\sum_{\text{tube wall}}^{\text{film surface}} uT}{u_{mean}} \tag{5.11}$$

$$C_b = \frac{\sum_{\text{tube wall}}^{\text{film surface}} uC}{u_{mean}} \tag{5.12}$$

Where ‘u’ is the velocity component in the downstream direction (see Fig. 3.2 and 4.3). In nondimensional domain, ‘u’ can be replaced by the term ($2R-R^2$) for the vertical absorber (Eq. 3.22), and ($2Y-Y^2$) for the horizontal absorber (Eq. 4.16). R and Y are the axes normal to the tube surface for vertical and horizontal geometries respectively.

5.2 Results of the Vertical Absorber Model

The physical geometry of the vertical absorber considered consists of a single copper tube with an outer diameter of 19.05 mm, inner diameter of 16.6 mm and a length of 1.5m. LiBr / H_2O solution flows outside the tube with a mass flow rate of 0.00724 kg/s. Concentration of the solution at the inlet is %60 (wt) LiBr. Two inlet temperatures for the solution is considered: the high and low temperatures.

The high temperature is selected as 46^oC which is just 1^oC below the equilibrium temperature for %60 LiBr concentration and 1225Pa vapour pressure. This is a typical value of commercial absorbers, hence it is desired to investigate results for real absorbers.

The low temperature is selected as 31^oC which is just 1^oC above the cooling water inlet temperature. This is selected to see what happens if the solution temperature in the heat exchanger is reduced.

Cooling water mass flow rate is selected as 0.43 kg/s with an inlet temperature of 30^oC which is a reasonable value for mediterranean countries, also 25^oC cooling water inlet case was considered for comparison purposes.

Vapour pressure mostly depends on the chilled water temperature, minimum chilled water temperature that a LiBr absorption system practically can reach is about 4^oC, and practical value is about 7^oC which corresponds to a vapour pressure of about 800Pa. In the present study, a 1250 Pa vapour pressure was selected which corresponds to a water temperature of 10^oC. Although this may be a high temperature for cooling purposes, much experiments have done under vapour pressures close to that pressure.

Physical parameters are summarized in Table 5.1 and the corresponding dimensionless parameters (temperature is an exception which has a dimension) are shown in Table 5.2.

Table 5.1 Physical parameters which satisfies the dimensionless inputs.

	High solution inlet temperature	**Low solution inlet temperature**
T_{si}	46 ^{o}C	31 ^{o}C
C_{si}	0.6 (mass (or wt) fraction of LiBr)	
m_{si}	0.00724 kg/s	
$\delta_i = f(m_{si})$	0.39 mm	0.446 mm
p	1250 Pa	
r_o	9.525 mm	
r_i	8.3 mm	
L	1.5 m	
T_{ci}	30 ^{o}C	
m_c	0.43 kg/s	

Table 5.2 Program inputs at the inlet conditions.

	High solution inlet temperature	**Low solution inlet temperature**
T_{si}	46 ^{o}C	31 ^{o}C
C_{si}	0.6 (wt LiBr)	
p	1250 Pa	
Re_s	103.37	69.12
Pr_s	21.13	32.146
Sc_s	1812.68	2699
L/δ_i	3846	3363
masscoef (see page 35)	16.87	17.69
CW (see page 34)	0.1847	0.156
gradcool (see page 33)	-0.055	-0.04655

5.2.1 Results for High Temperature Solution Inlet

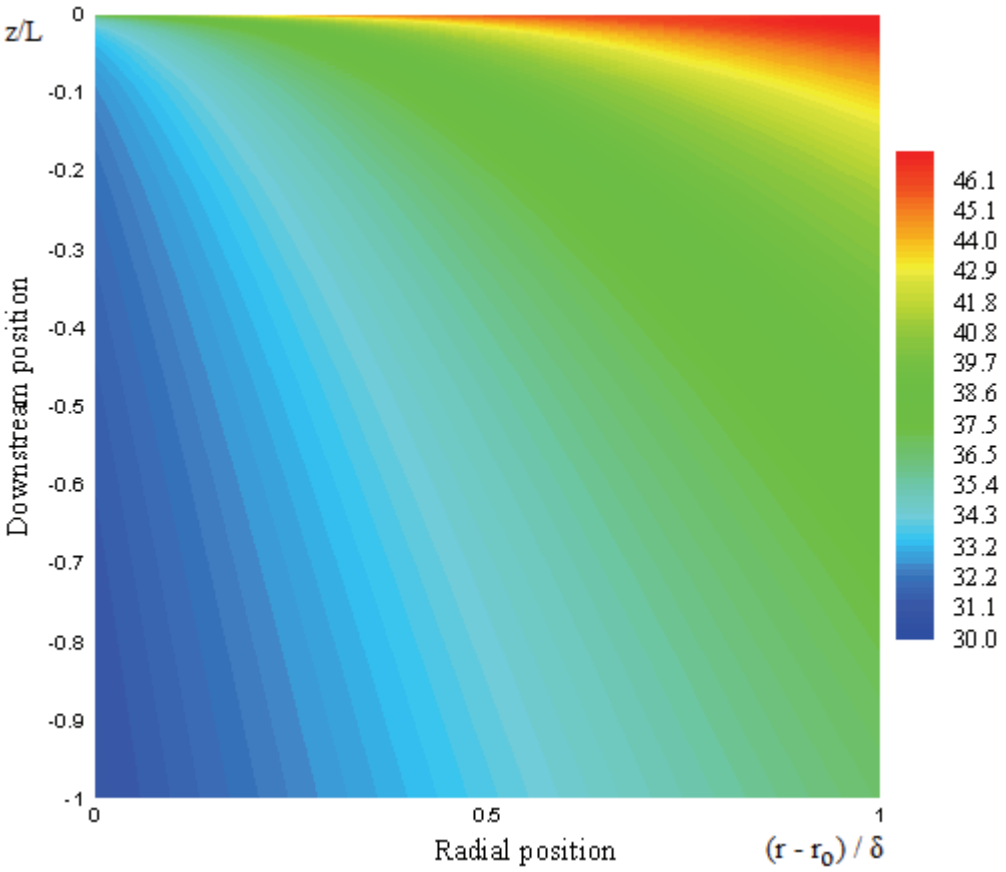

Figure 5.1 Temperature field of the falling film in dimensionless domain, high temperature inlet, vertical absorber.

Prandl number, which is the ratio of the solution viscous diffusivity to the solution thermal diffusivity, is about 21 at the inlet conditions. Schmidt number, which is the ratio of the solution viscous diffusivity to the mass diffusivity (of any species in the solution) is about 1813 at the inlet conditions. Hence it can be concluded that the ratio of the solution thermal diffusivity to the mass diffusivity is about 90. This means that the development of the thermal boundary layer is about 90 times faster than that of the concentration boundary layer. This fact can be observed in the results of the present model; the temperature and concentration fields are shown in Figures 5.1 and 5.2 respectively. A close look at these figures roughly reveals that the thermal boundary layer at the interface develops much faster than the development of the concentration boundary layer such that although the thermal boundary layer is

fully developed before % 10 of the tube length (see the deformation of flat free stream temperature profile between z/L=0.002 and z/L=0.01 in Figure 5.7); the concentration boundary layer can never reach to the tube wall for the present parameters. This becomes clearer when Figures 5.5 and 5.6 are analysed. As seen in Figure 5.5, the interface and wall temperature falls below the entrance temperature (46^{o}C) before the solution moves to %10 of the tube length (z/L=0.1). Hence the temperature profile is fully developed before z/L=0.1. On the other hand, Figure 5.6 reveals that the wall LiBr concentration never falls below %99 of the entrance concentration (0.6) for the present parameters.

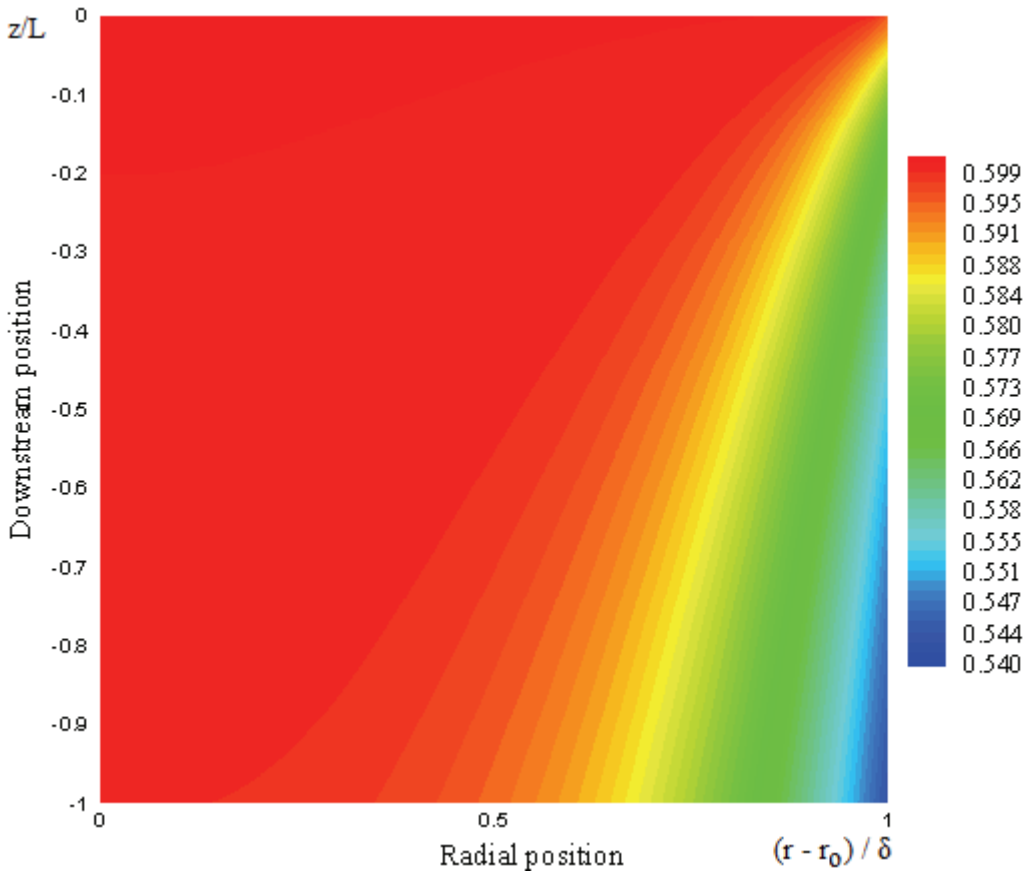

Figure 5.2 LiBr concentration field (weight ratio) of the falling film, high temperature inlet, vertical absorber.

Figure 5.5 reveals that the cooling water immediately effects the solution bulk temperature (because the film is very thin) which sharply falls at the entrance region. From this fact, it is expected that the solution inlet temperature should not effect overall absorption performance considerably, because the solution bulk temperatures are expected to become equal at z/L~0.1 for any inlet solution temperature case. Absorption performances of high and low solution inlet temperature cases (Figures 5.9 and 5.19) are compared in Section 5.2.3. Another important point is that the wall temperature sharply falls from 37^{o}C to 33^{o}C at the inlet (see the region z/L<0.05 in Figure 5.5). The reason of this is that the solution temperature is high at the inlet. However heat transfer rates are above average at these regions. The reasons of this is discussed below in details.

Investigating Figure 5.6 reveals that decrease rate of surface LiBr concentration (so increase rate of water concentration) is faster than the decrease rate of bulk LiBr concentration. This shows the fact that diffusivity of LiBr or water in the solution is very low such that an increase in water concentration at the surface does not effect bulk conditions at the same magnitude although the film surface velocity is higher than the near wall velocity, which makes bulk value to get closer to the surface value (see Eq. 5.12).

Figures 5.7 and 5.8 show the cross-stream temperature and concentration profiles. The solution enters the domain with uniform (or flat) temperature and concentration profiles (with 46^{o}C temperature and 0.6 LiBr concentration). However the tube wall is much cooler than the solution bulk and heat of absorption at the interface causes surface temperature to increase slightly. Hence just after the inlet point (at z/L=0.002 and z/L=0.01 in Figure 5.7) extremely high temperature gradients (relative to the average value) occur at the wall and film surface (see gradients at right (interface) and left (wall) at z/L=0.002 and z/L=0.01 in Figure 5.7). These high temperature gradients at the inlet are caused by the extremely high concentration gradients (see right side at z/L=0.002 and z/L=0.01 in Figure 5.8) at the film surface, which causes extremely high absorption fluxes at the entrance (see z/L<0.01 in Figure 5.9). Hence the released heat of absorption the film surface increases surface temperature which

causes high temperature gradients. Concentration gradients at the near inlet region is high because LiBr concentration is high in the regions near to the surface. Hence driving force for absorption is high.

However as observed in Figure 5.7; although temperature gradients at the wall (left side in the figure) and interface (right side in the figure) are very high at the inlet (z/L=0.002 and z/L=0.01 in Figure 5.7), in the middle of the film thickness (at positions close to $(r - r_o) / \delta = 0.5$), the temperature profile is still flat till the solution passes from z/L=0.01. Hence the released heat of absorption cannot be transferred into the cooling water. So the surface (and near surface) temperature increases at the inlet (1-2^oC above the inlet temperature in steady state). The increase of the temperature is balanced (or limited) by sharp fall of absorption flux (just after inlet) to equalize the solution vapour pressure to the absorber pressure (see position z/L=0.01 in Figure 5.9). However mass absorption rates start to increase sharply as the temperature profile develops to allow for a heat transfer from surface to the wall (the increase in mean temperature gradient from the interface to tube wall can be observed in Figure 5.7 after z/L=0.1), which also causes the wall temperature to drop because heat can be released to the cooling water more easily.

However as the vapour is absorbed with high amounts at the inlet (at z/L<0.01), the bulk and surface vapour concentrations starts to increase which decreases driving potential for vapour absorption. Hence heat of absorption falls (see interface heat flux at z/L>0.12 in Figure 5.10). This causes interface temperature to fall (see Figure 5.5). Although the decrease of the interface temperature has a positive effect on absorption performance (because it decreases the solution vapour pressure, which is balanced by increased mass absorption), the effect of increased vapour concentration (which decreases driving force for absorption) is dominant. As a consequence, mass absorption rates starts to fall gradually after % 10 of the tube length (see interface heat flux at z/L>0.12 in Figure 5.9).

Figure 5.3 shows that the film thickness increases as the solution moves from z/L=0 to z/L=1. This is why the bulk temperature decreases as the solution moves

(see the decrease of bulk temperature in Figure 5.5), hence the solution viscosity increases as the bulk temperature decreases. In addition to that, absorption of vapour also increases the film thickness, however its effect is small compared to the effect of the solution viscosity. In conclusion, overall increase in the film thickness is % 7.18, which is an increase that cannot be neglected.

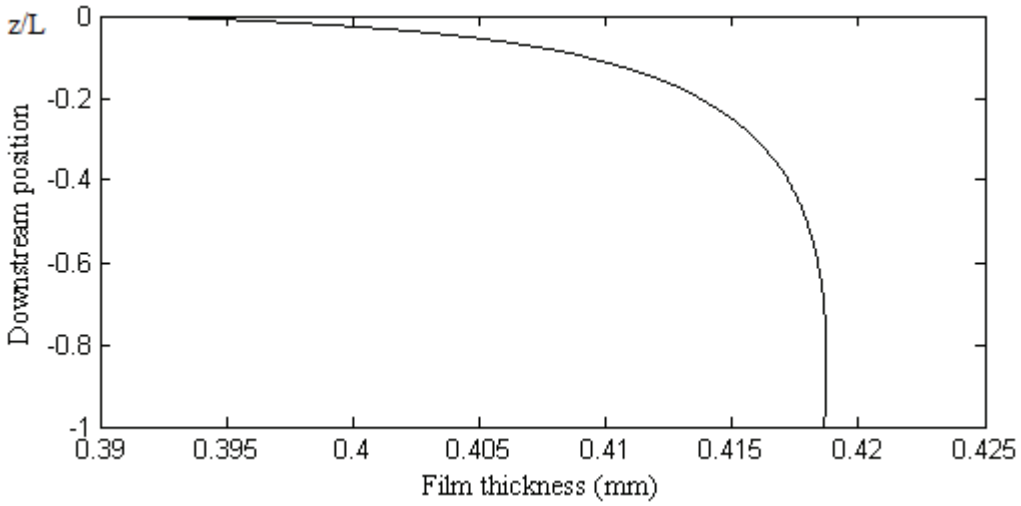

Figure 5.3 Variation of film thickness with the downstream position, high temperature inlet, vertical absorber.

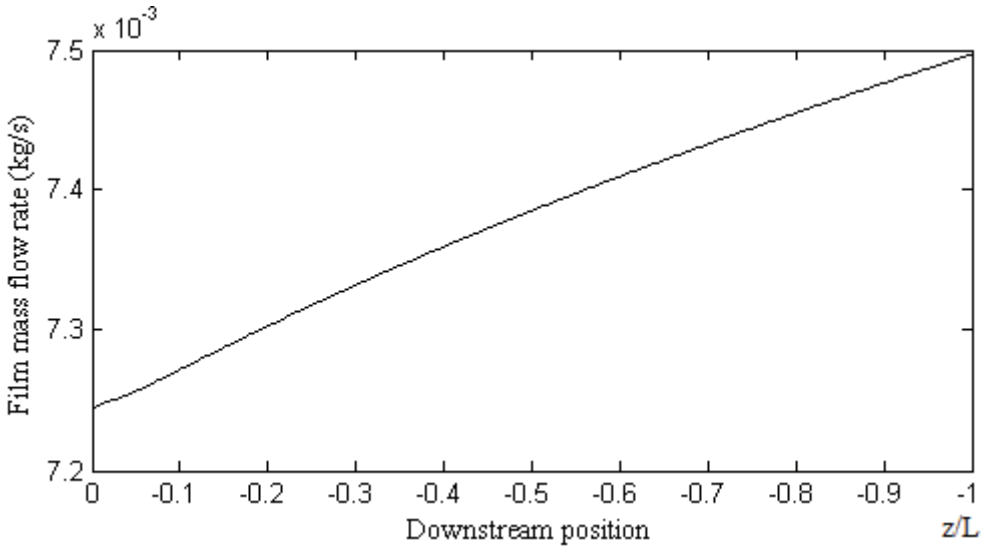

Figure 5.4 The increase of film mass flow rate by the absorption of vapour, high temperature inlet, vertical absorber.

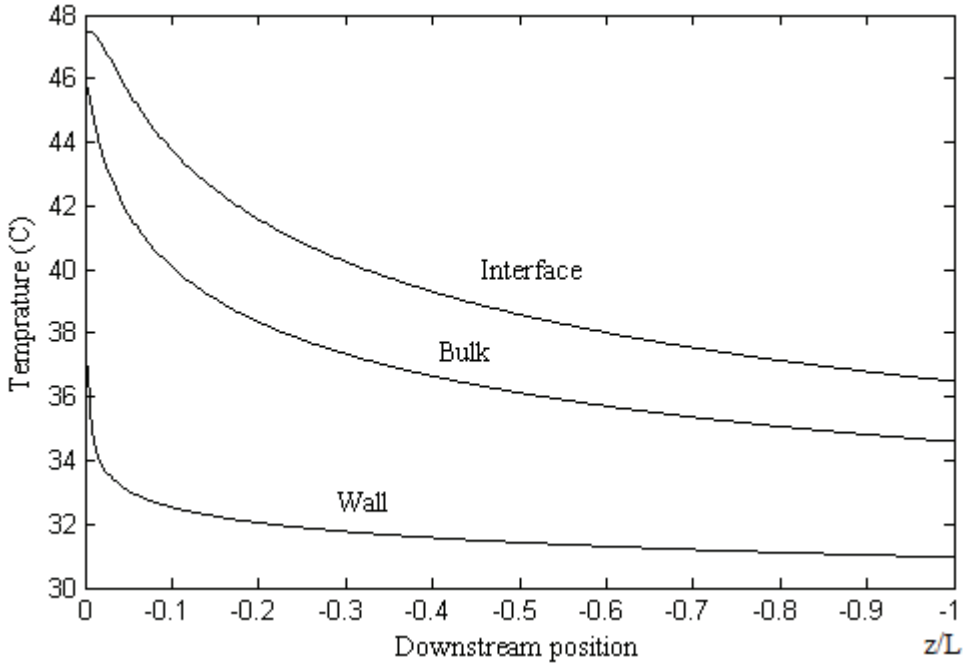

Figure 5.5 Variation of the interface, wall and bulk temperature with downstream position, high temperature inlet, vertical absorber.

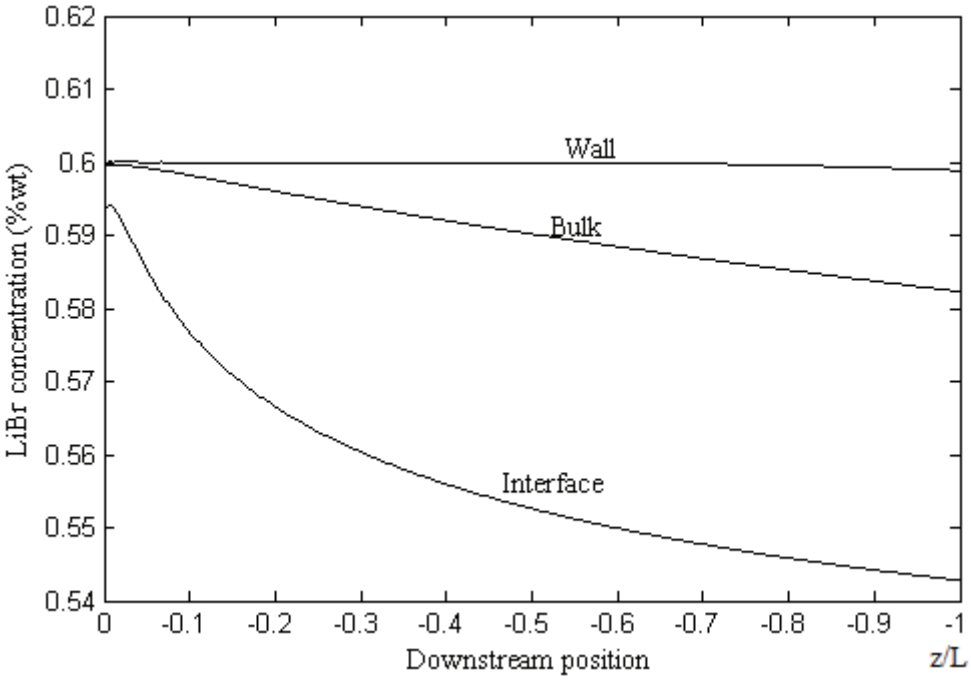

Figure 5.6 Variation of the interface, wall and bulk lithium bromide concentration with downstream position, high temperature inlet, vertical absorber.

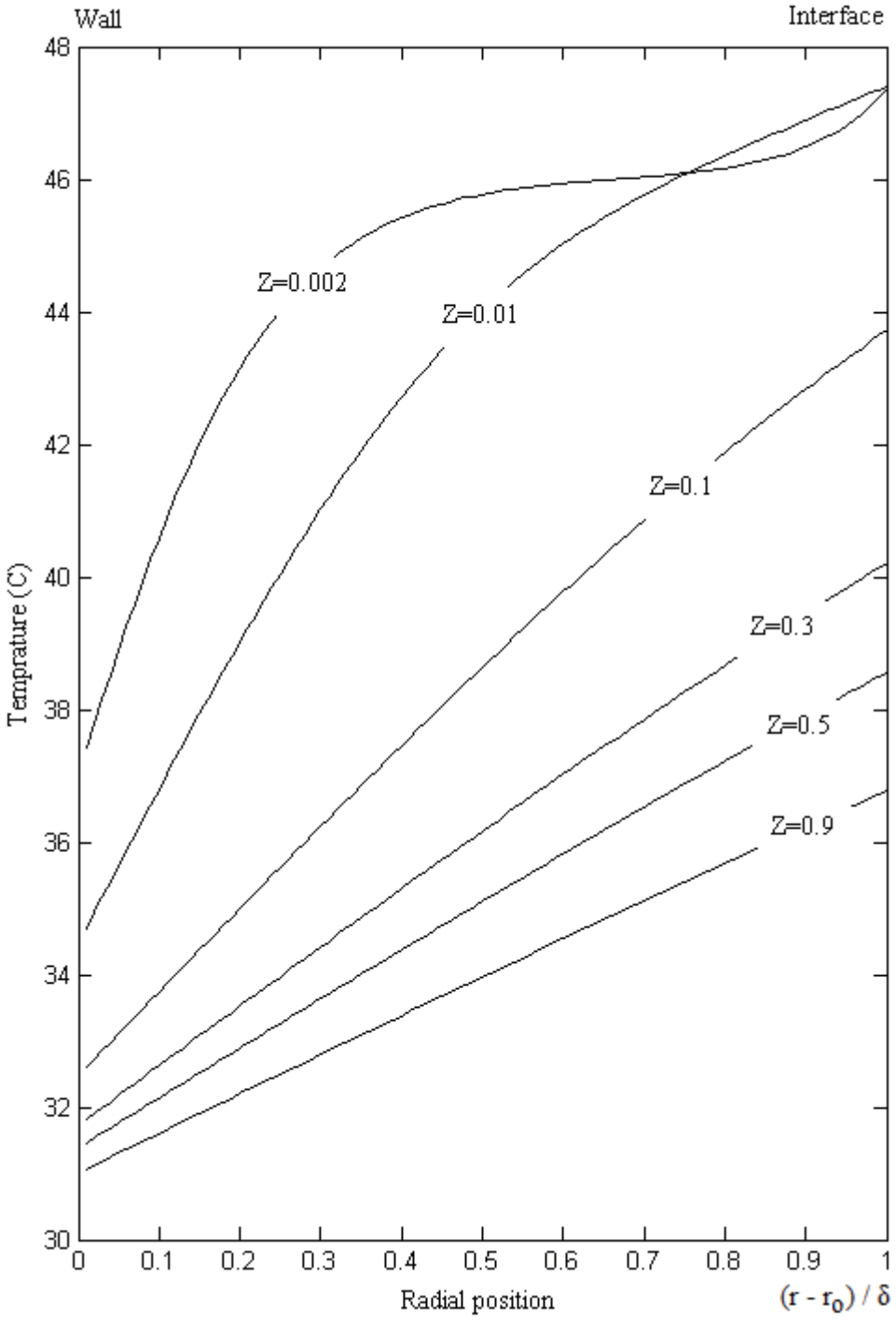

Figure 5.7 Cross stream temperature profiles at selected downstream positions, high temperature inlet, vertical absorber.

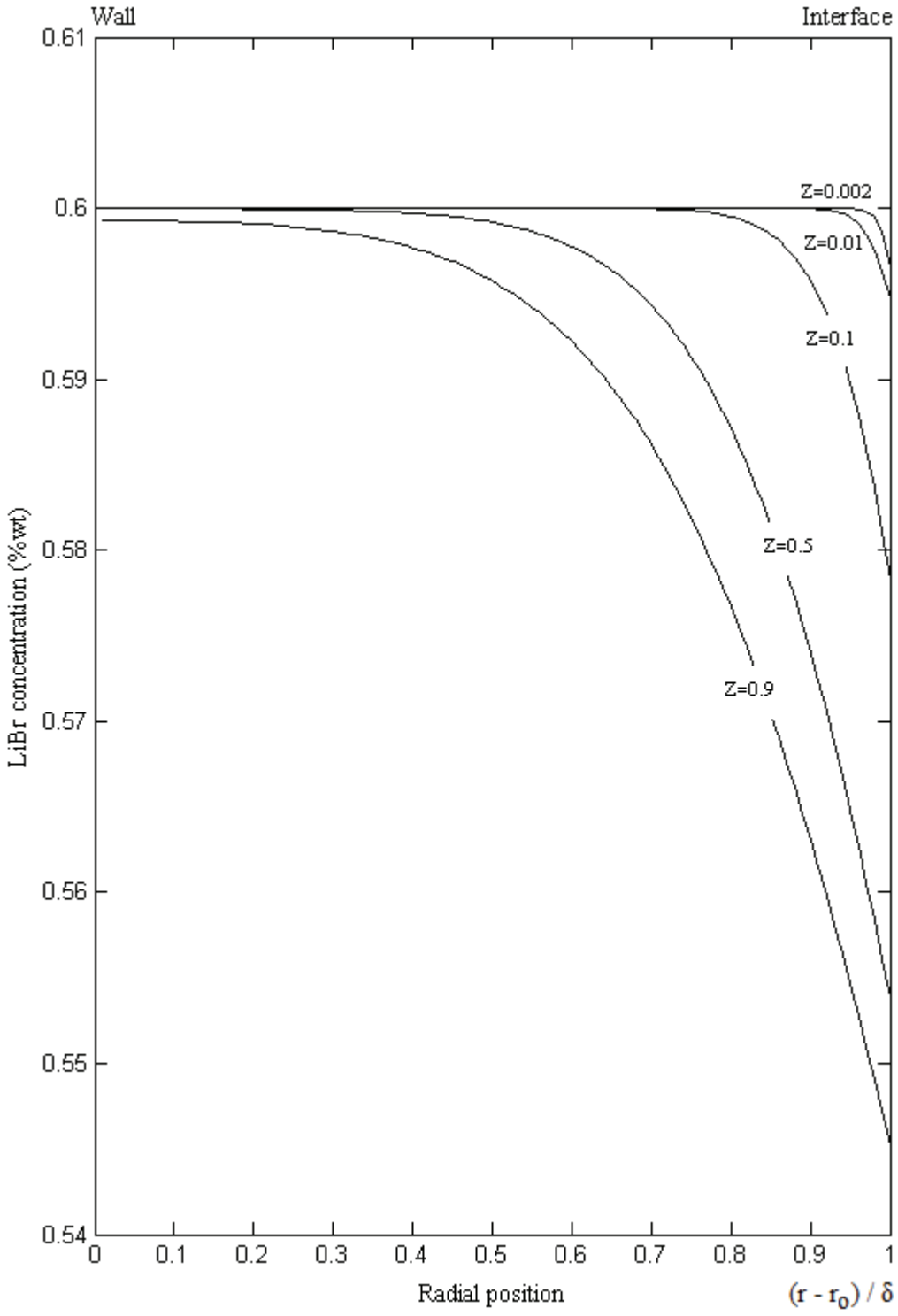

Figure 5.8 Cross stream LiBr concentration profiles at selected downstream positions, high temperature inlet, vertical absorber.

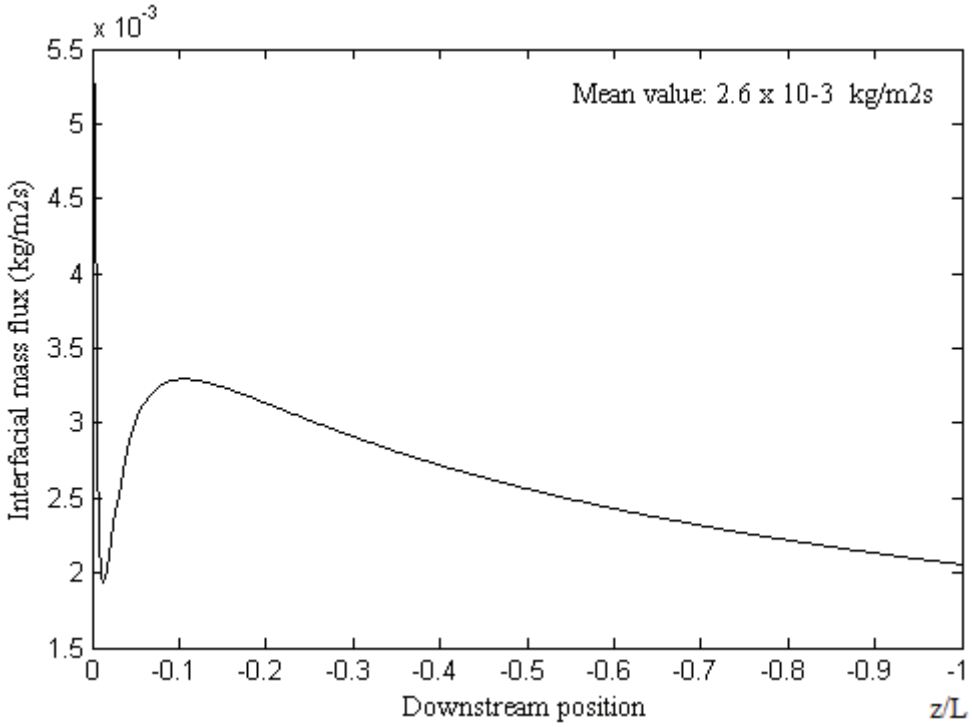

Figure 5.9 Variation of the surface vapour absorption flux with downstream position, high temperature inlet, vertical absorber.

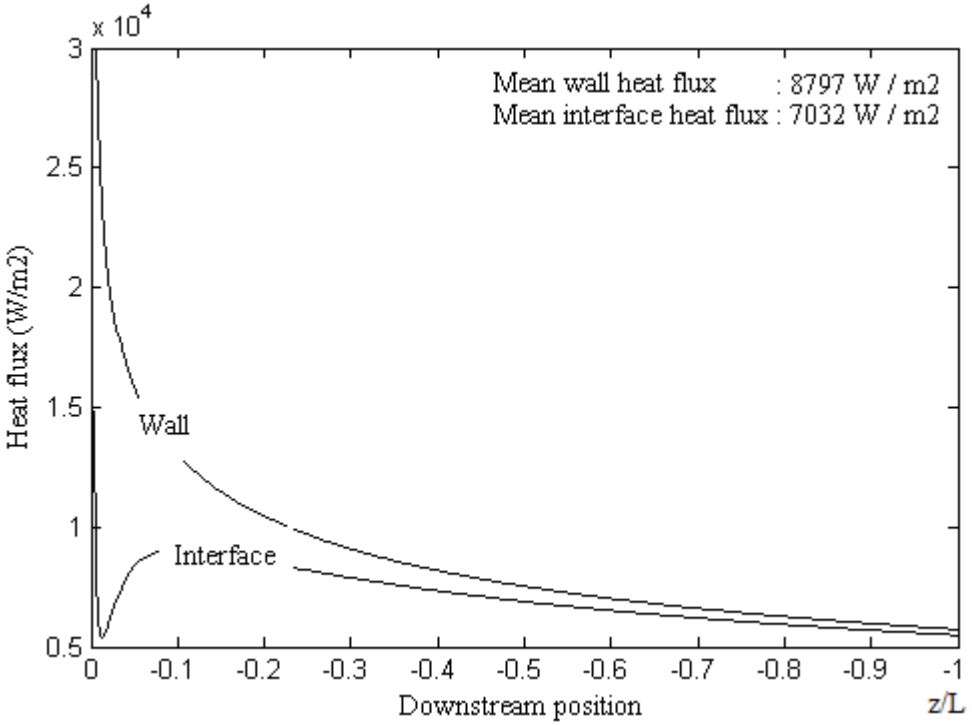

Figure 5.10 Variation of the surface and wall heat flux with downstream position, high temperature inlet, vertical absorber.

5.2.2 Results for Low Temperature Solution Inlet

The same mechanism that have already been discussed in Section 5.2.1 is also valid for the present case. However there are some differences: as the solution enters the domain with a lower temperature (compared to the high solution inlet case), a very high absorption flux at the inlet is observed (see Figure 5.19). This peak value is higher than the peak value of the high inlet temperature case (see peak of mass flux at z/L<0.01 in Figure 5.9). Hence high rates of heat of absorption causes bulk and surface temperature to increase sharply from 31°C to 37.56°C (see Figure 5.15). This can also be observed in Figure 5.11, where interface temperature remains high till z/L~0.2.

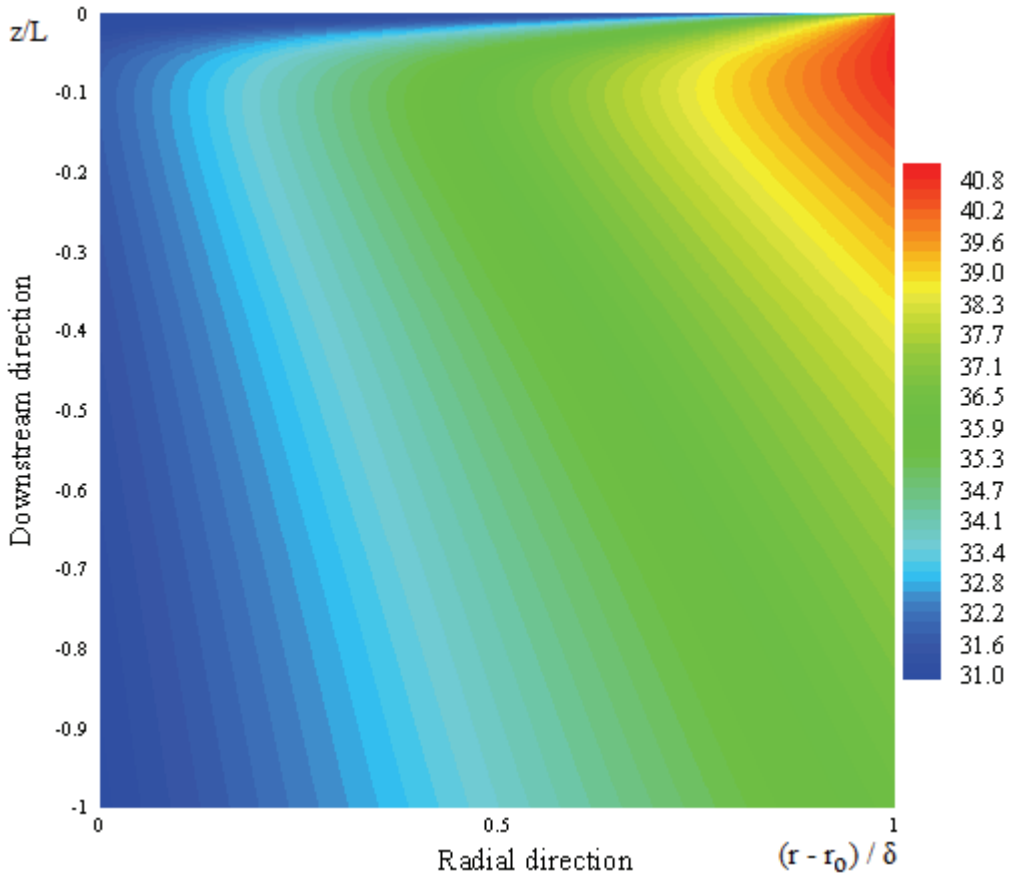

Figure 5.11 Temperature field of the falling film in dimensionless domain, low temperature inlet, vertical absorber.

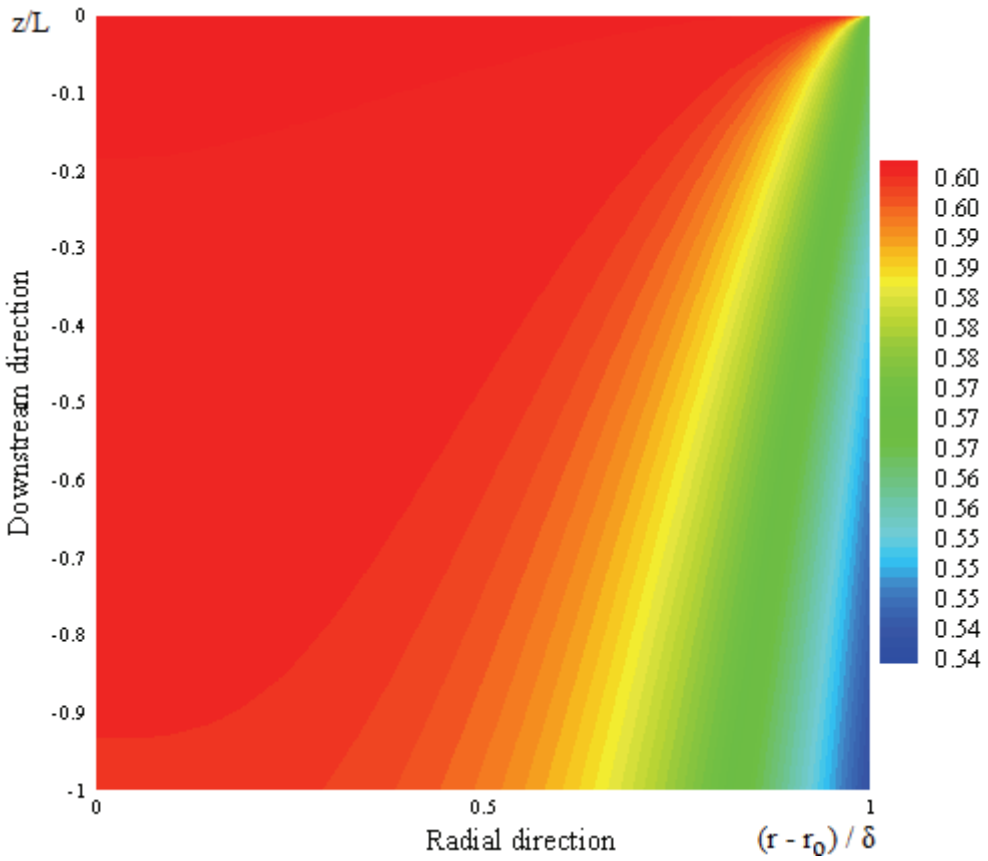

Figure 5.12 LiBr concentration field (weight ratio) of the falling film, low temperature inlet, vertical absorber.

As observed in Figure 5.17, the high heat flux discussed above causes interface temperature to increase greatly (also see Figure 5.15). Hence a high heat flux arises at the interface. However as observed in Figure 5.17, this heat of absorption cannot be transferred to the cooling water because the temperature profile is still flat at z/L=0.002 from tube wall to the middle regions of the film thickness. Hence solution temperature increases. At z/L=0.1, temperature gradient at the wall starts to develop, hence heat of absorption can be transferred into the cooling water. At z/L=0.1, temperature profile is fully developed and heat of absorption can easily be transferred to the cooling water.

There is not any obvious difference between concentration fields for high and low solution inlet temperature cases (see Figures 5.2 and 5.12) because the difference which is discussed above only occurs at the near inlet region (z/L<0.1). Hence these

difference in temperature fields do not effect overall absorption performance considerably (see Section 5.2.3). The concentration boundary layer still does not reach to the tube wall. However at the near inlet region (z/L<0.01), there is a significant difference between the mass fluxes of the two cases which can be seen by comparing Figures 5.8 and 5.18. In Figure 5.18, the concentration gradient at the inlet (z/L=0.002) is higher than that of the case of Figure 5.8.

As the temperature profile develops to allow for a heat transfer from the film surface to wall, the sudden fall in mass absorption stops. However as the surface and bulk vapour concentrations starts to increase, driving potential for absorption process starts to fall gradually after %10 of the tube length (see Figure 5.19) as observed in the previous case. Hence absorption rates starts to fall gradually at z/L>0.1.

Figure 5.20 shows the relationship between heat fluxes at the film surface and tube wall. At the inlet region, because of higher heat of absorption, heat flux at the film surface is higher than the heat transfer at the wall. Hence solution bulk temperature increases till z/L~0.1. After that point, decrease in absorption flux (because of increase in vapour concentration) decreases the heat of absorption, hence surface heat flux starts to decrease gradually. On the other hand also wall heat flux decreases gradually. However wall heat flux is slightly higher than the surface heat flux at this region. Hence solution bulk temperature starts to fall gradually at z/L>0.1 (this can also be observed in Figure 5.15).

Film thickness is relatively large at the inlet (Figure 5.13), because the solution viscosity is high in that region, however as the temperature increases, the solution viscosity decreases, which causes film thickness to decrease (about %5.3, see Figure 5.13). On the other hand, there is also an increase in the film thickness because of vapour absorption, as observed in Figure 5.14 (there is a % 3.44 increase in the film mass flow rate). This increase is quick at the inlet because of the peak value in absorption. However close examination to Figure 5.13 reveals that its effect is small compared to the effect of the solution viscosity.

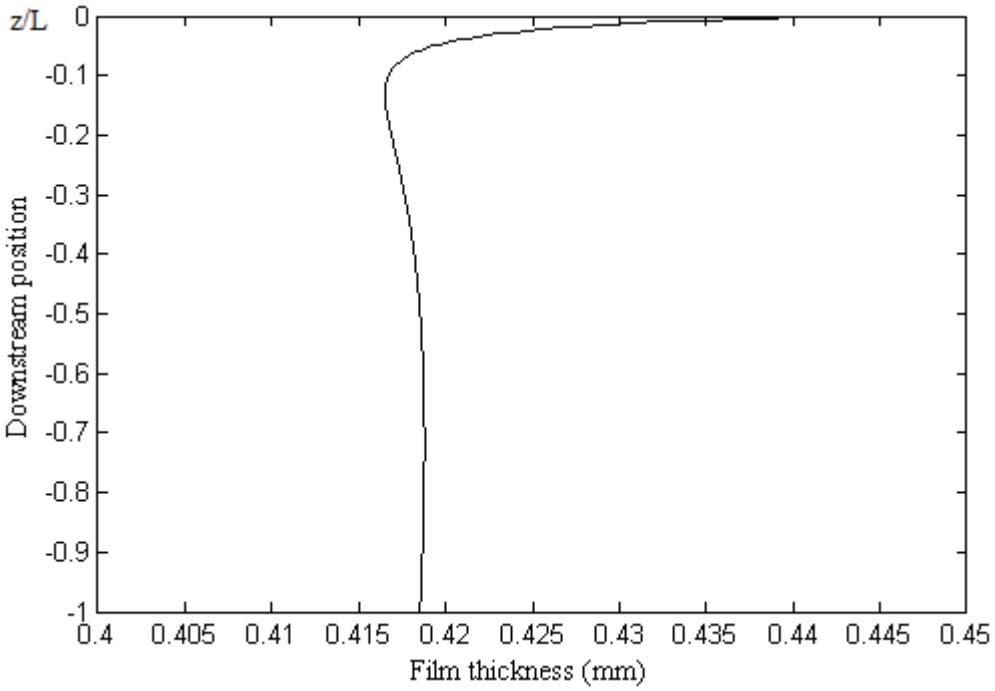

Figure 5.13 Variation of film thickness in the downstream direction, low temperature inlet, vertical absorber.

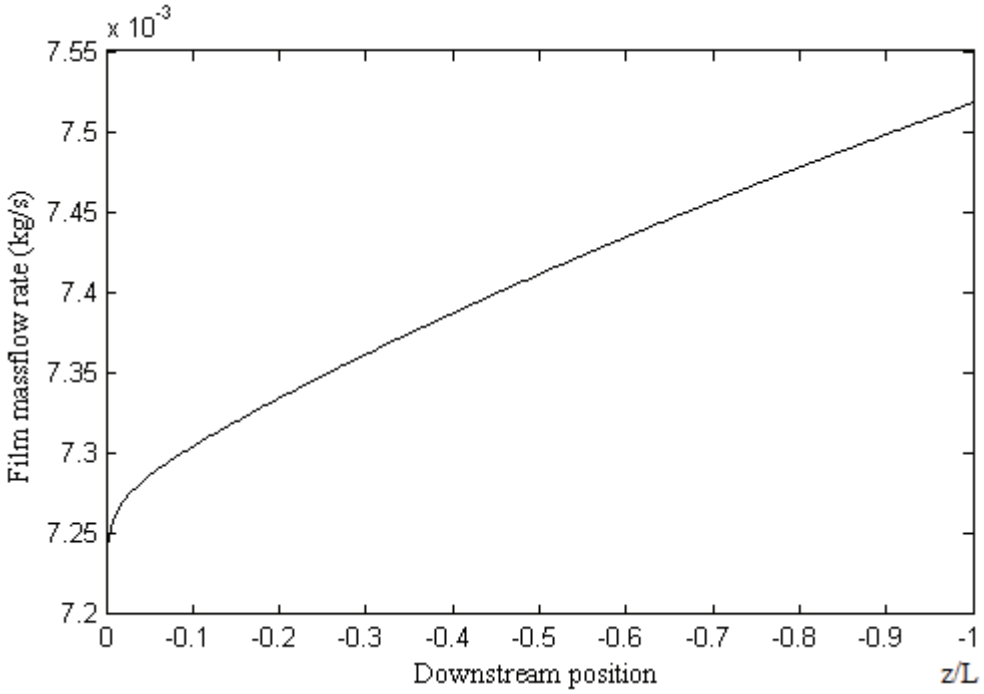

Figure 5.14 The increase of film mass flow rate by the absorption of vapour, low temperature inlet, vertical absorber

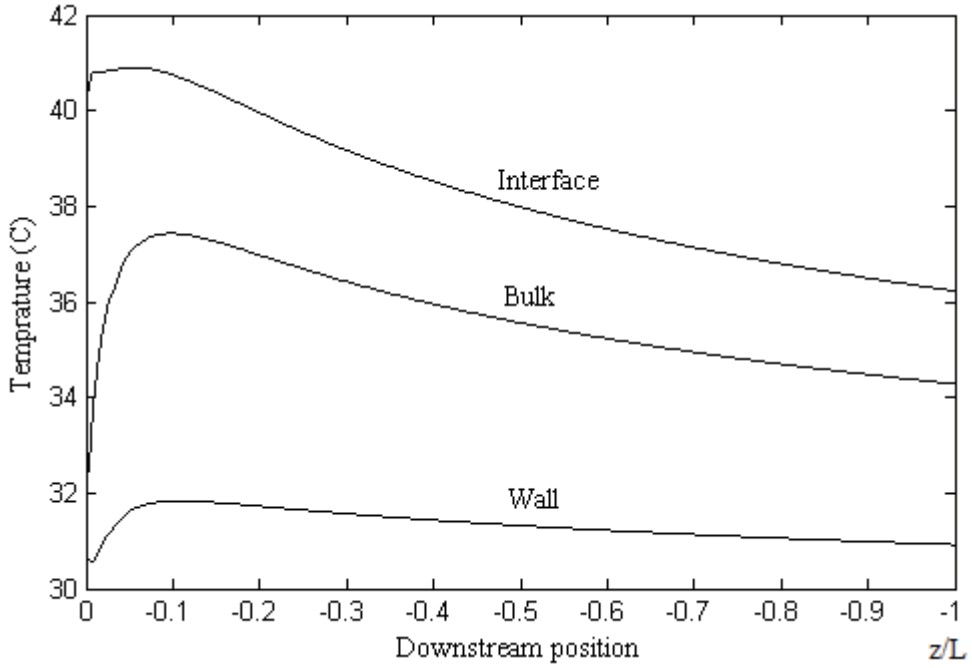

Figure 5.15 Variation of the surface, wall and bulk temperature with downstream position, low temperature inlet, vertical absorber.

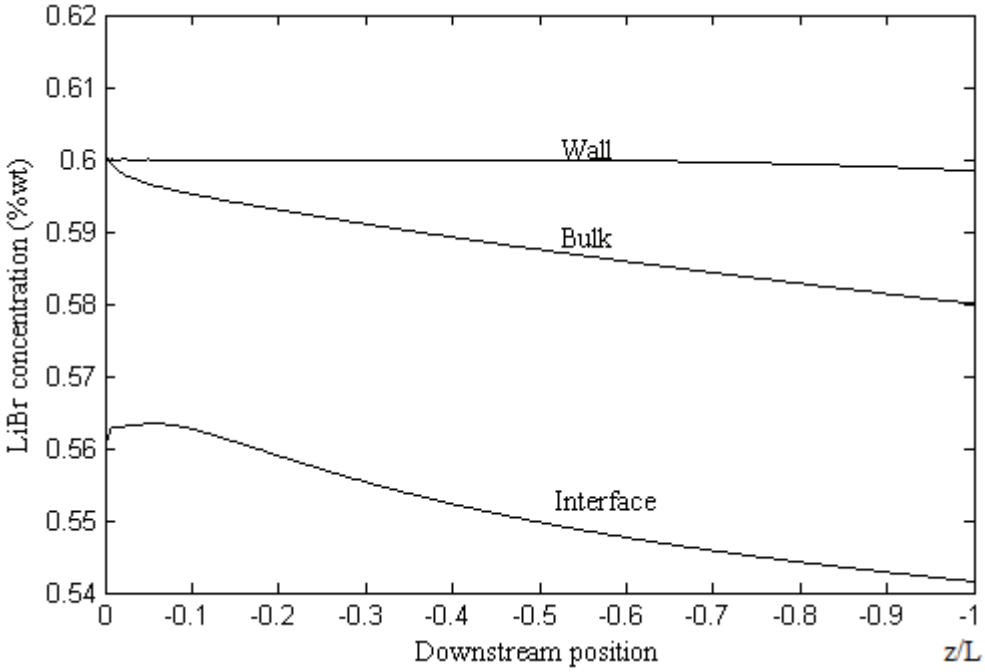

Figure 5.16 Variation of the interface, wall and bulk lithium bromide concentration with downstream position, low temperature inlet, vertical absorber.

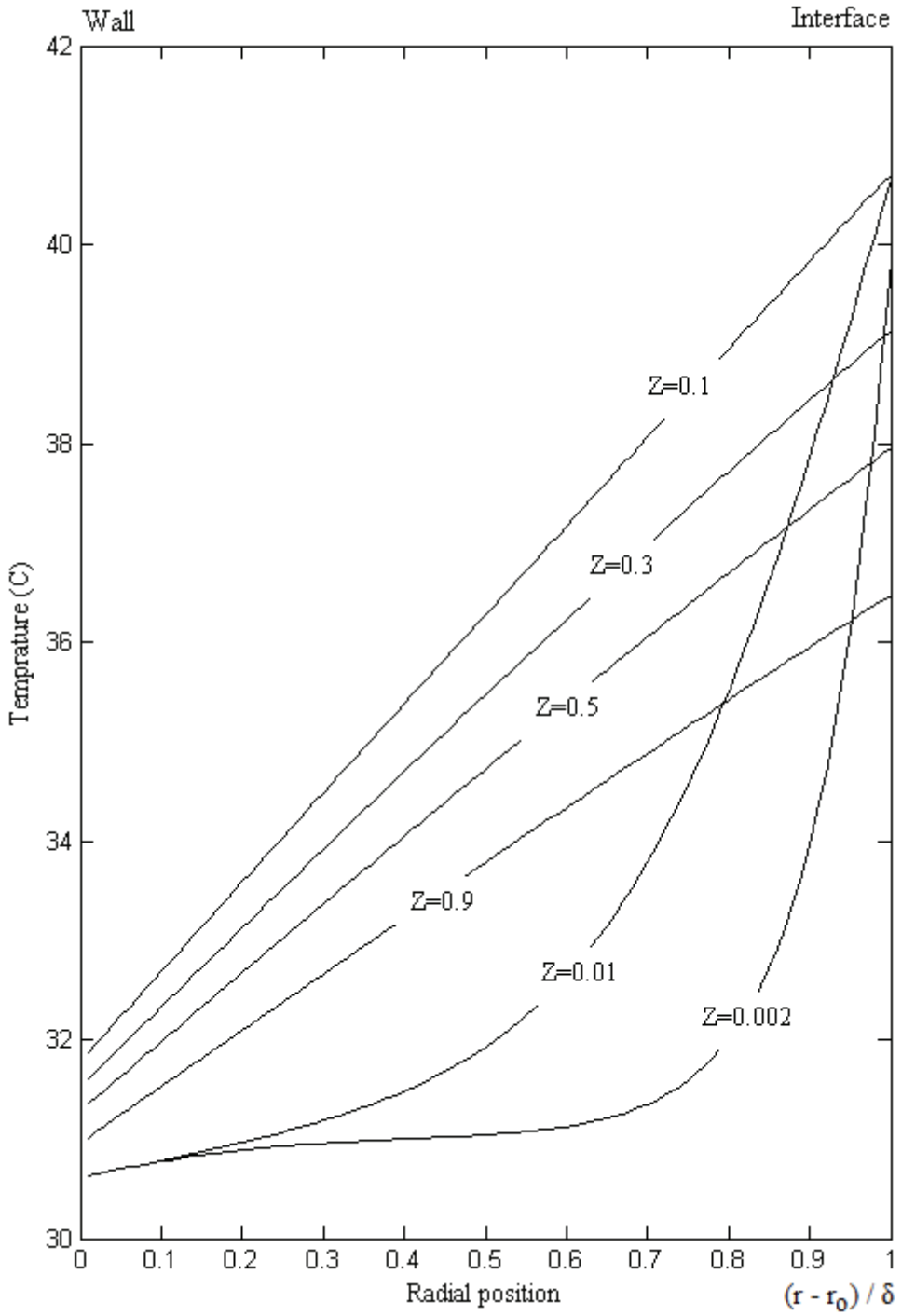

Figure 5.17 Cross stream temperature profiles at selected downstream positions, low temperature inlet, vertical absorber.

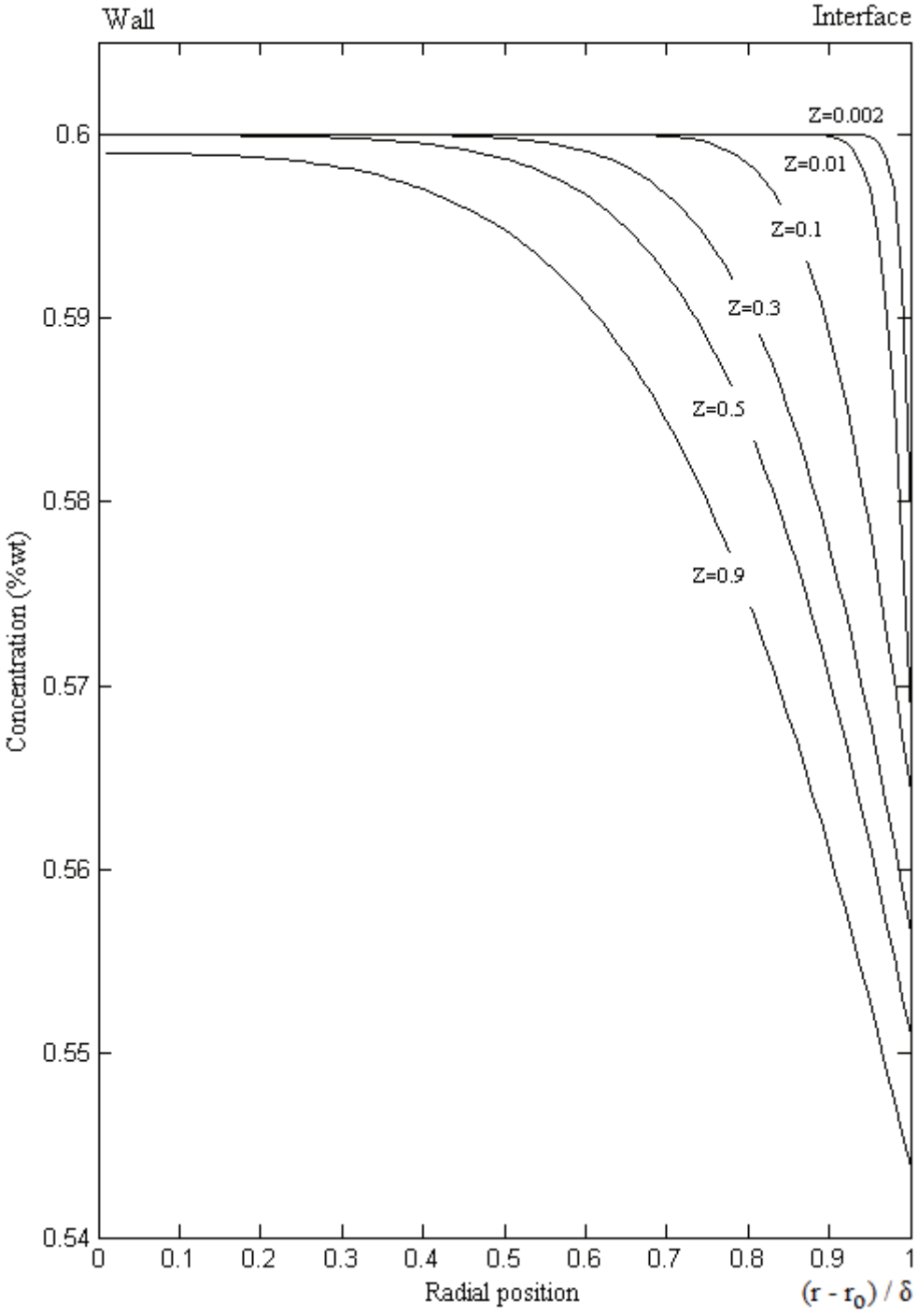

Figure 5.18 Cross stream LiBr concentration profiles at selected downstream positions, low temperature inlet, vertical absorber.

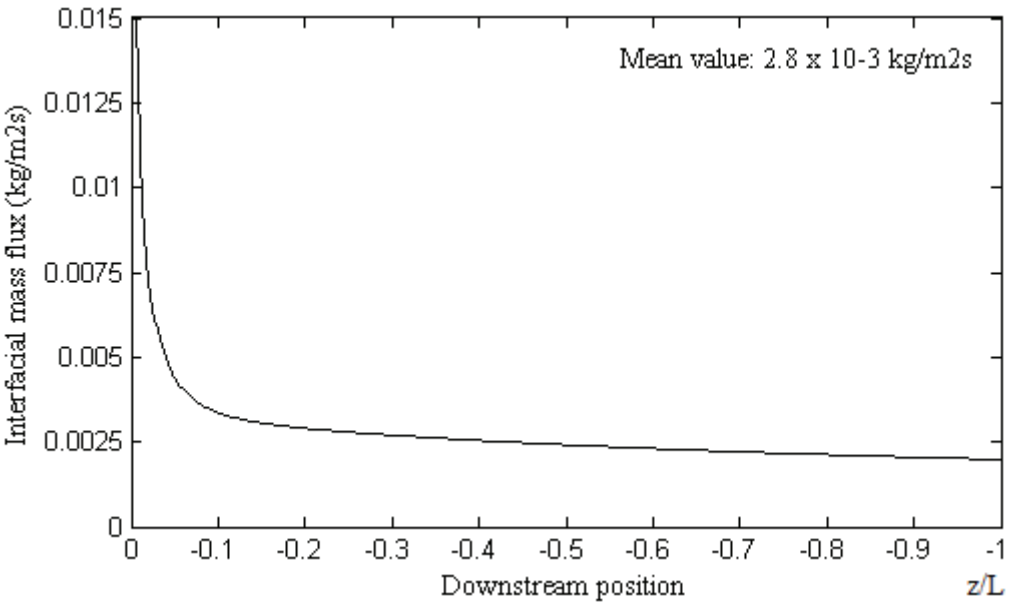

Figure 5.19 Variation of the interface vapour absorption flux with downstream position, low temperature inlet, vertical absorber.

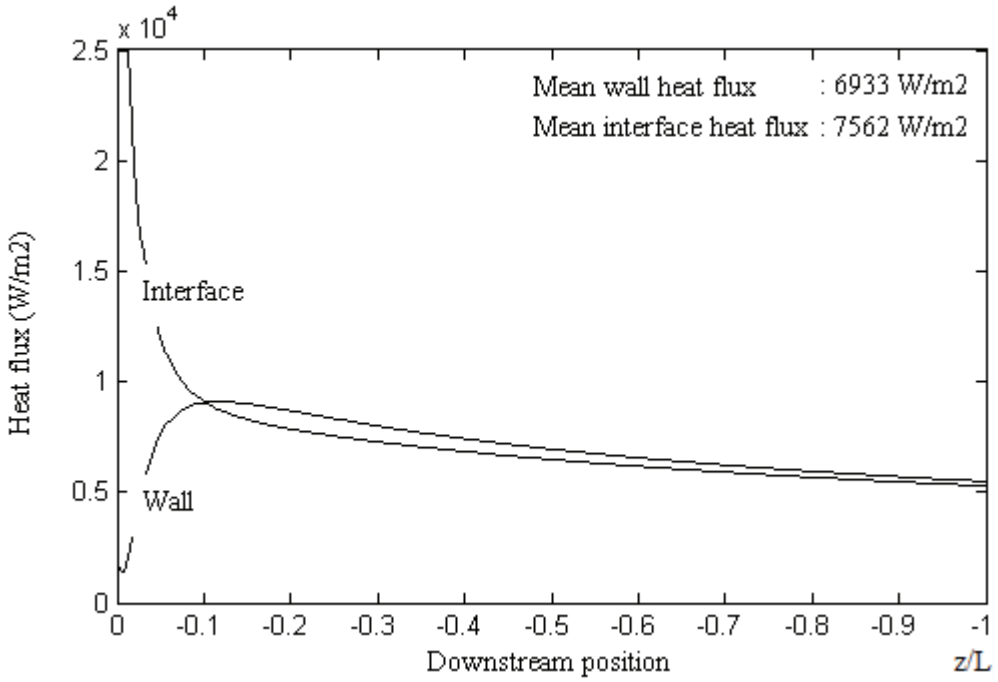

Figure 5.20 Variation of the surface and wall heat flux with downstream position, low temperature inlet, vertical absorber.

5.2.3 Effect of the Solution Inlet Temperature

There is not any huge difference between the two cases; this is partially because of low solution flow rate, hence solution temperature profile immediately develops before z/L~0.1 (see Figures 5.7 and 5.17). It is expected that if the solution flow rate is increased, the difference will become obvious. The cause of the difference is discussed in the previous section. In the low temperature solution inlet case, whole of the tube surface is used effectively for absorption, while for the high temperature solution inlet case absorption rates are smaller in the near inlet region.

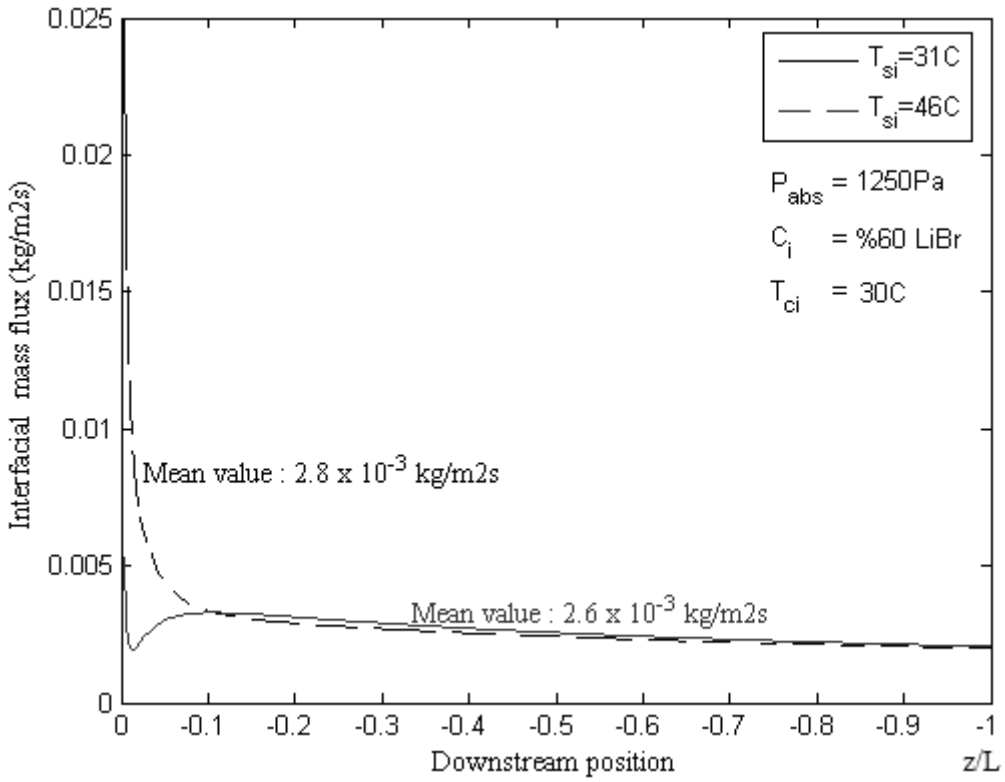

Figure 5.21 Interface vapour flux versus downstream distance, effect of the solution inlet temperature.

5.2.4 Effect of the Solution Mass Flow Rate

Increase of solution mass flow rate increases resistance for heat transfer, hence it is expected that absorption performance always increases as the resistance to heat transfer decreases. However as the resistance to heat transfer decreases, larger amount of vapour is absorbed at the regions close to inlet, which causes driving potential for absorption to decrease.

For the vertical absorber case, the second effect dominates, hence although absorption rates at the regions close to the inlet are higher for the low mass flow rate case because of low resistance to heat transfer; after the first quarter of the tube length, situation changes and local mass flow rates becomes higher for the high mass flow rate case. In the present case, the second effect dominates and overall absorption rate for the high mass flow rate is slightly higher (2.56 x 10^{-3} kg/m^2s for Re_i=45, 2.65 x 10^{-3} kg/m^2s for Re_i=67.5 and 2.66 x 10^{-3} kg/m^2s for Re_i=90). However it should be noted that bulk LiBr concentration drop is higher for the low solution case (0.563 for Re_i=45, 0.576 for Re_i=67.5 and 0,583 for Re_i=90).

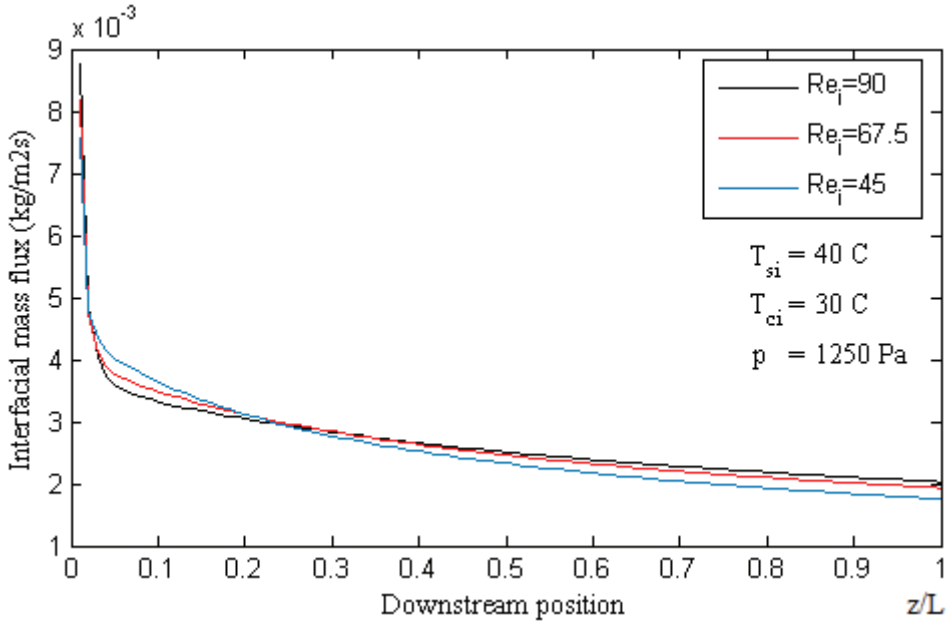

Figure 5.22 Interface vapour flux versus downstream distance, effect of the solution mass flow rate.

5.2.5 Effect of the Cooling Water Inlet Temperature

The cooling water temperature probably have the biggest effect on the absorption performance. Hence the typical mean film thickness is very small compared to the tube diameter, solution inlet temperature does not have a huge effect on the absorption performance because temperature profile immediately develops for the thin film flow. However the cooling water temperature has a much more noticable effect on the absorption performance. By decreasing the cooling water inlet temperature from 30°C to 25°C, a % 25 gain in the mean absorption performance is obtained.

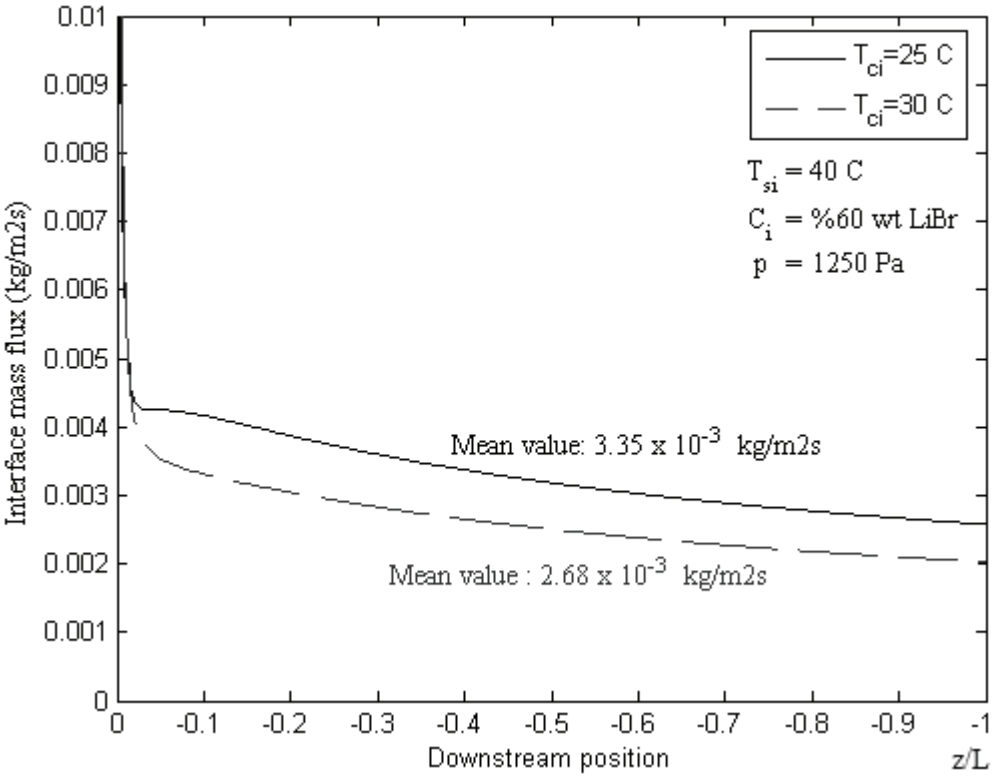

Figure 5.23 Interface vapour flux versus downstream distance, effect of the cooling water inlet temperature.

5.3 Results of the Horizontal Absorber Model

The physical geometry of the horizontal absorber considered consists of a single copper tube with an outer diameter of 19.05 mm, inner diameter of 16.6 mm and a length of 0.5 m. The LiBr / H_2O solution enters the domain from top of the tube in the form of sheet flow. This assumption is quite reasonable for interior tubes (tubes other than the tube at the top) if intentionally created by placing a thin vertical plate just below the test tube (Seol et al. (2005)). Normally the solution falls in the form of unsteady jet drainage and droplets between the tubes. The assumption of sheet drainage is questionized and verified in section 5.5.

All other parameters (including solution mass flow rate, inlet temperatures) are the same as that of vertical tube case (section 5.2). Summary of the operating parameters are presented in Table 5.3 and dimensionless inputs for the program is shown in Table 5.4 (note that definition for the Reynolds number for horizontal tube case is different from that of vertical tube case).

Table 5.3 Physical parameters which satisfies the dimensionless inputs.

	High solution inlet temperature	**Low solution inlet temperature**
T_{si}	46 ^oC	31 ^oC
C_{si}	0.6 (wt LiBr)	
m_{si}	0.00724 kg/s	
$\delta_{90i} = f(m_{si})$	0.15 mm	0.175 mm
p	1250 Pa	
r_o	9.525 mm	
r_i	8.3 mm	
L	0.5 m	
T_{ci}	30 ^oC	
m_c	0.43 kg/s	

Table 5.4 Program inputs at the inlet conditions.

	High solution inlet temperature	**Low solution inlet temperature**
T_{si}	46 ^{o}C	31 ^{o}C
C_{si}	0.6 (wt LiBr)	
p	1250 Pa	
Re_s	6.186	4.137
Pr_s	21.13	32.146
Sc_s	1812.68	2699
$\pi r_o/\delta_{90i}$	195.415	171.38
masscoef (see page 55)	16.87	17.69
CW (see page 55)	0.3428	0.2898
gradcool (see page 57)	-0.0391	-0.033

5.3.1 Results for High Temperature Solution Inlet

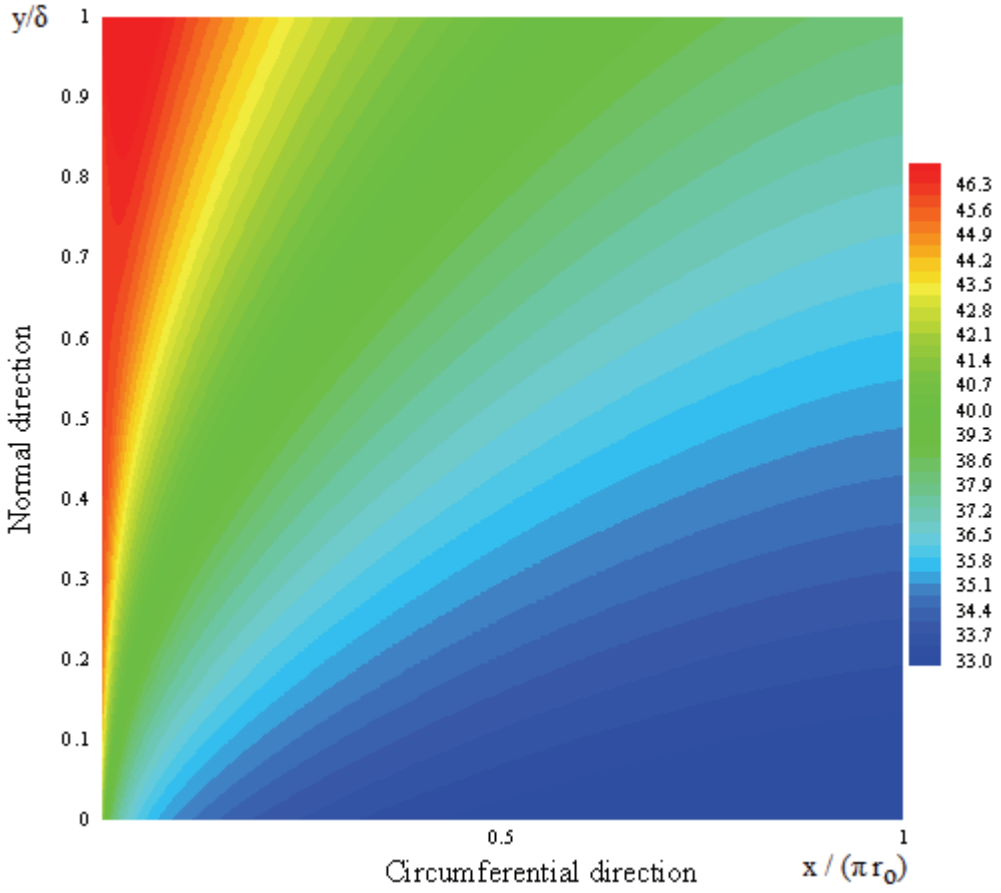

Figure 5.24 Temperature field of the falling film in dimensionless domain, high temperature inlet, horizontal absorber.

Similar observations that have already done for the vertical absorber model with high temperature inlet (Section 5.2.1) are valid for the horizontal absorber case. Hence readers are referred to this section for details of the physical behaviour. Figures 5.26, 5.27, 5.28, 5.29, 5.30 and 5.31 are horizontal absorber equivalents of Figures 5.5, 5.6, 5.7, 5.8, 5.9 and 5.10 respectively. However the film thickness distribution and the velocity fields are different than that of the vertical absorber case. Film thickness is relatively very large at the regions close to the top and bottom of the (horizontal) tube which increases resistance to heat transfer compared to that in the vertical absorber case for the same average film thickness. This can be observed in Figure 5.30, where an increase in absorption performance in the middle

region of the tube circumference (0.2<X<0.5) is obvious. This is mostly because of the decrease in film thickness.

As the temperature profile is flat at the inlet, heat of absorption generated at the film surface can not be transferred to the cooling water, which limits the absorption performance. However as the temperature profile develops to allow for a heat transfer from the film surface to cooling water (see Figure 5.28), absorption rate increases sharply (see Figure 5.30). As the vapour is absorbed in large flow rates, the surface and bulk vapour concentration starts to increase which decreases the driving potential for absorption. Hence absorption rates start to fall again gradually after %40 or the tube circumference (X>0.4). Also as the solution moves to the end of the tube, the film thickness increases which also increases the resistance to heat transfer (and so to the mass transfer). Readers are referred to Section 5.2.1 for further details.

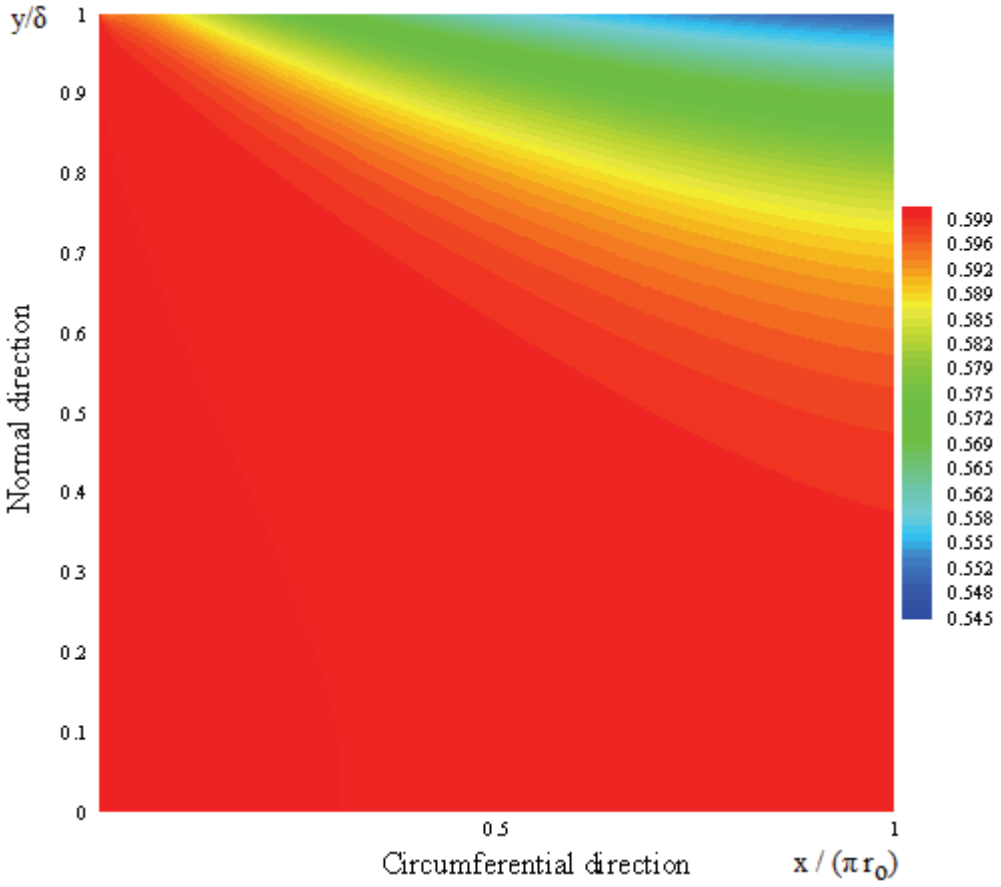

Figure 5.25 LiBr concentration field (weight ratio) of the falling film, high temperature inlet, horizontal absorber.

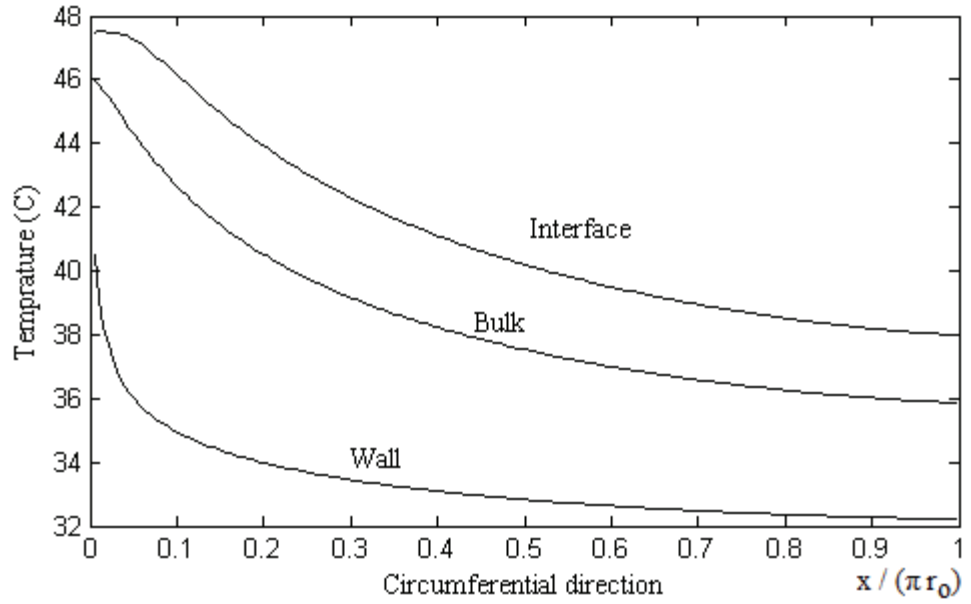

Figure 5.26 Variation of surface, wall and bulk temperature with distance around the tube, high temperature inlet, horizontal absorber.

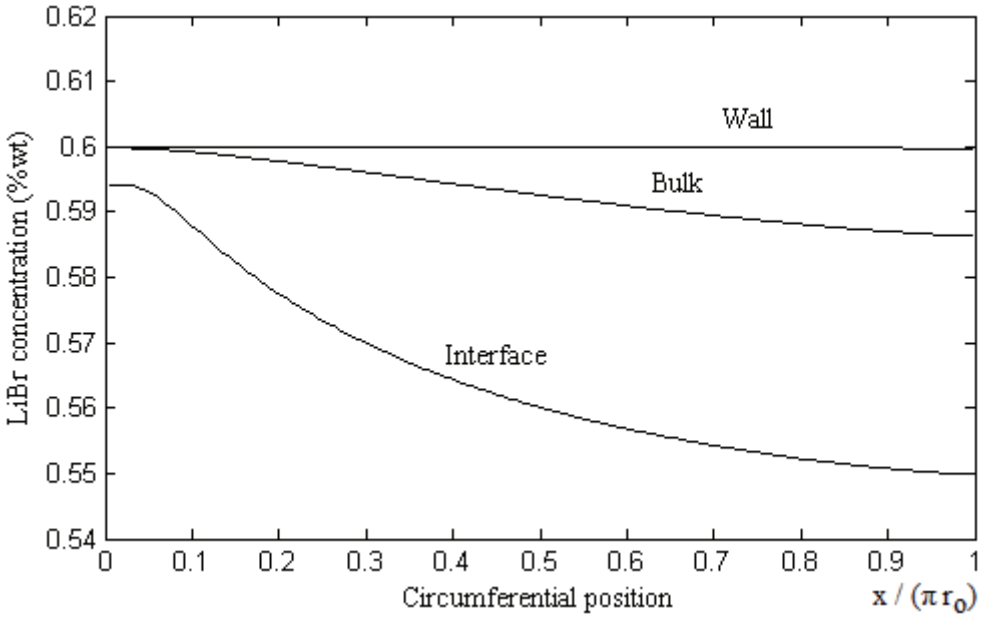

Figure 5.27 Variation of surface, wall and bulk LiBr concentration with distance around the tube, high temperature inlet, horizontal absorber.

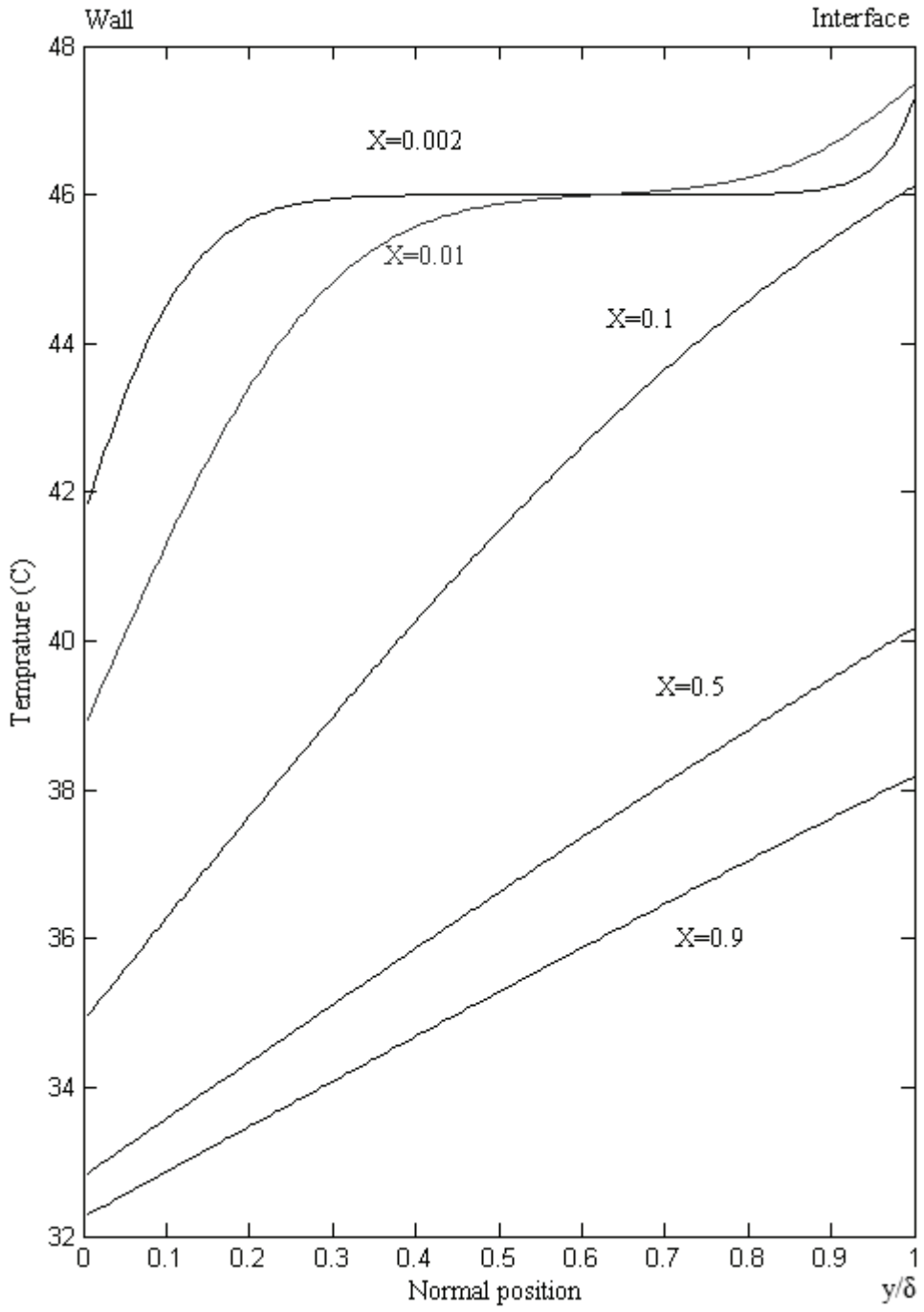

Figure 5.28 Cross stream temperature profiles at selected downstream positions, high temperature inlet, horizontal absorber.

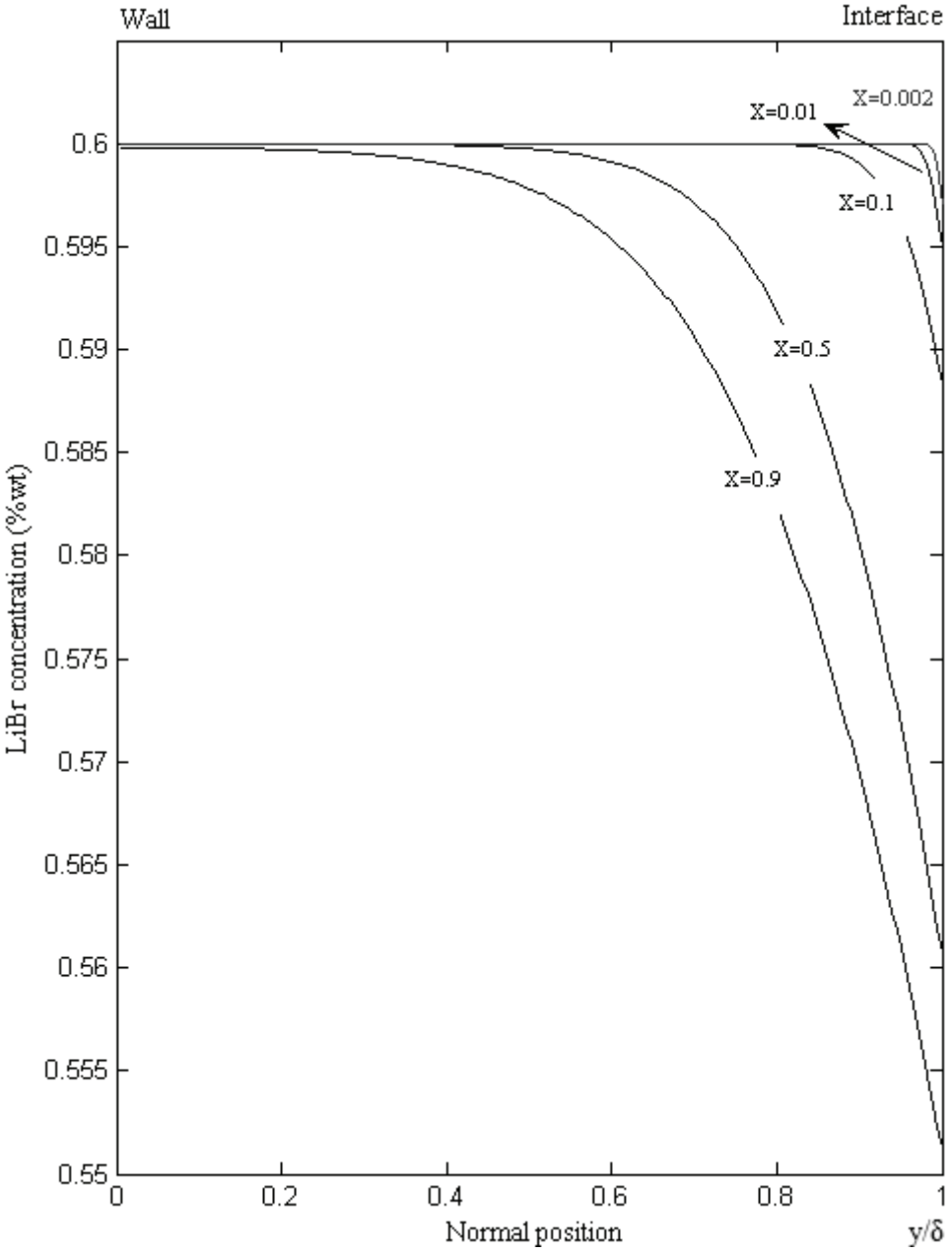

Figure 5.29 Cross stream LiBr concentration profiles at selected downstream positions, high temperature inlet, horizontal absorber.

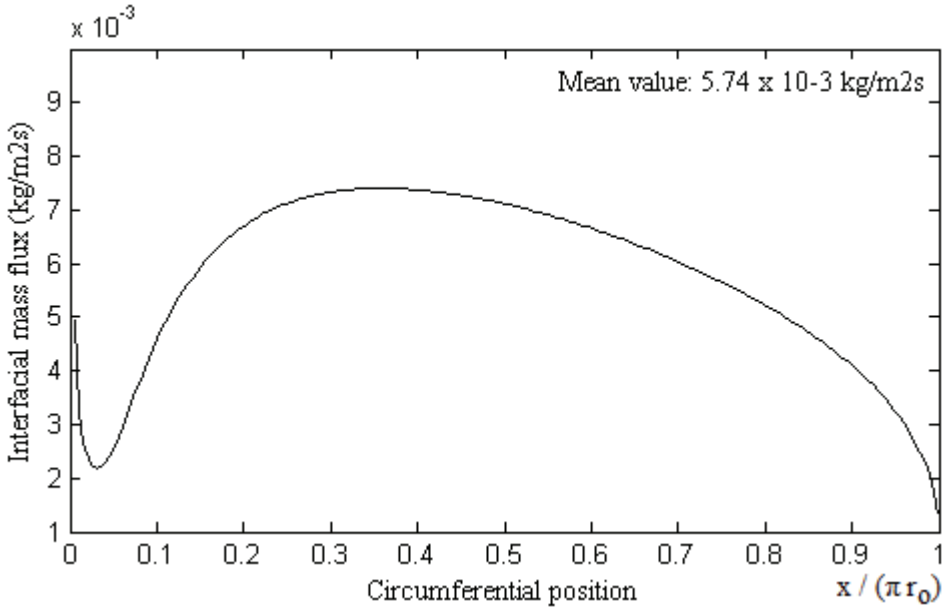

Figure 5.30 Variation of interface vapour absorption flux with distance around the tube, high temperature inlet, horizontal absorber.

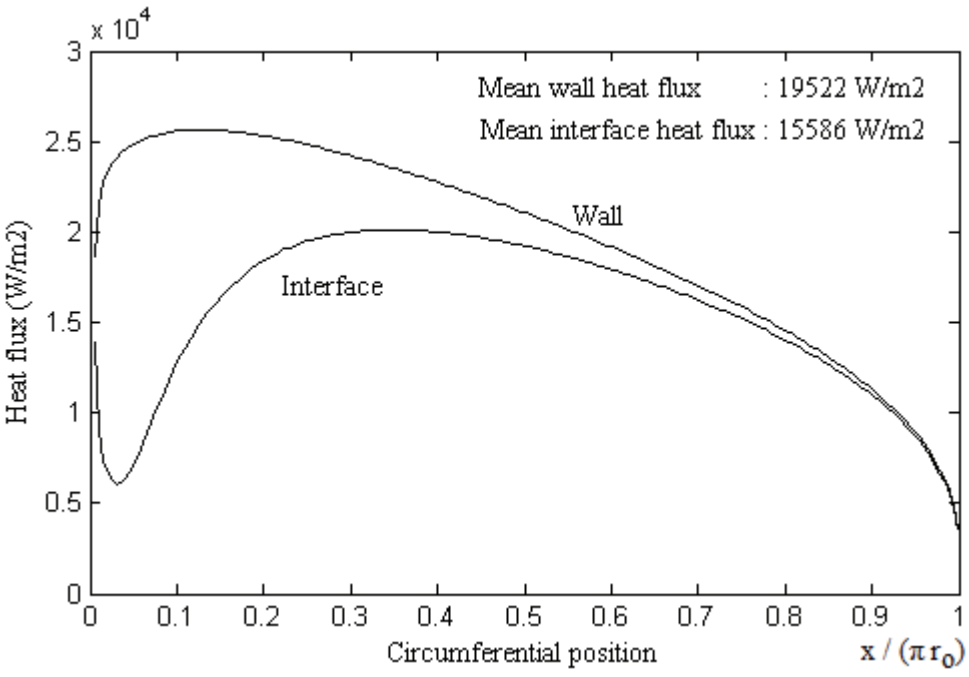

Figure 5.31 Variation of surface and wall heat flux with distance around the tube, high temperature inlet, horizontal absorber.

5.3.2 Results for Low Temperature Solution Inlet

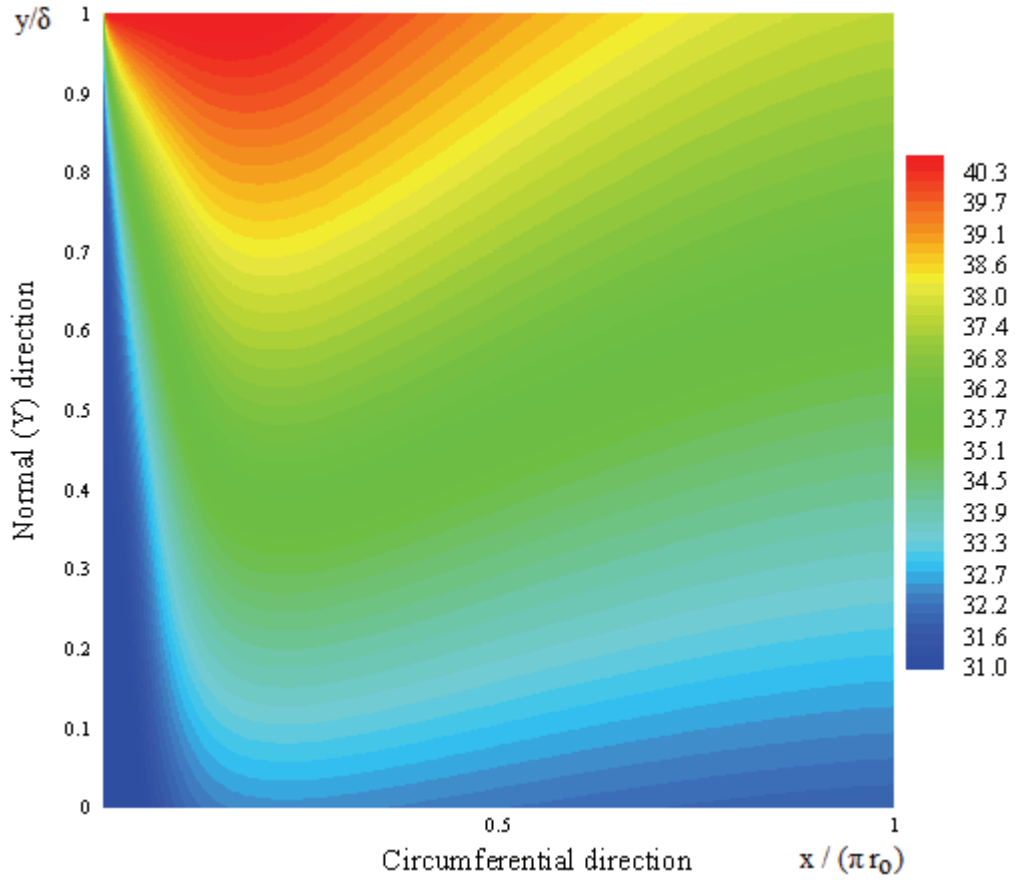

Figure 5.32 Temperature field of the falling film in dimensionless domain, low temperature inlet, horizontal absorber .

Similar observations that have already done for the vertical absorber model with low temperature inlet (Section 5.2.2) are valid for the horizontal absorber case. Hence readers are referred to this section for details of the physical behaviour. Figures 5.34, 5.35, 5.36, 5.37, 5.38 and 5.39 are horizontal absorber equivalents of Figures 5.15, 5.16, 5.17, 5.18, 5.19 and 5.20 respectively. However the film thickness distribution and the velocity fields are different than that of the vertical absorber case which makes some difference. The causes of the differences are discussed in the Section 5.3.1.

As the temperature is very low at the inlet, high amount of absorption occurs to equalize the solution vapour pressure to the absorber pressure by increasing surface temperature. However as the temperature profile is flat at the inlet, heat of absorption can not be transferred into the cooling water. As a consequence the solution bulk temperature increases sharply (see Figure 5.34). Hence absorption performance falls greatly as the solution moves around the tube (see Figure 5.38). However as the temperature profile develops to allow for a heat transfer from film surface to the cooling water (see Figure 5.36), the fall in absorption performance stops. However as the surface vapour concentration increases, the driving potential for the absorption decreases hence absorption rates starts to fall gradually as the solution moves around the tube. Readers are referred to Section 5.2.2 for further details.

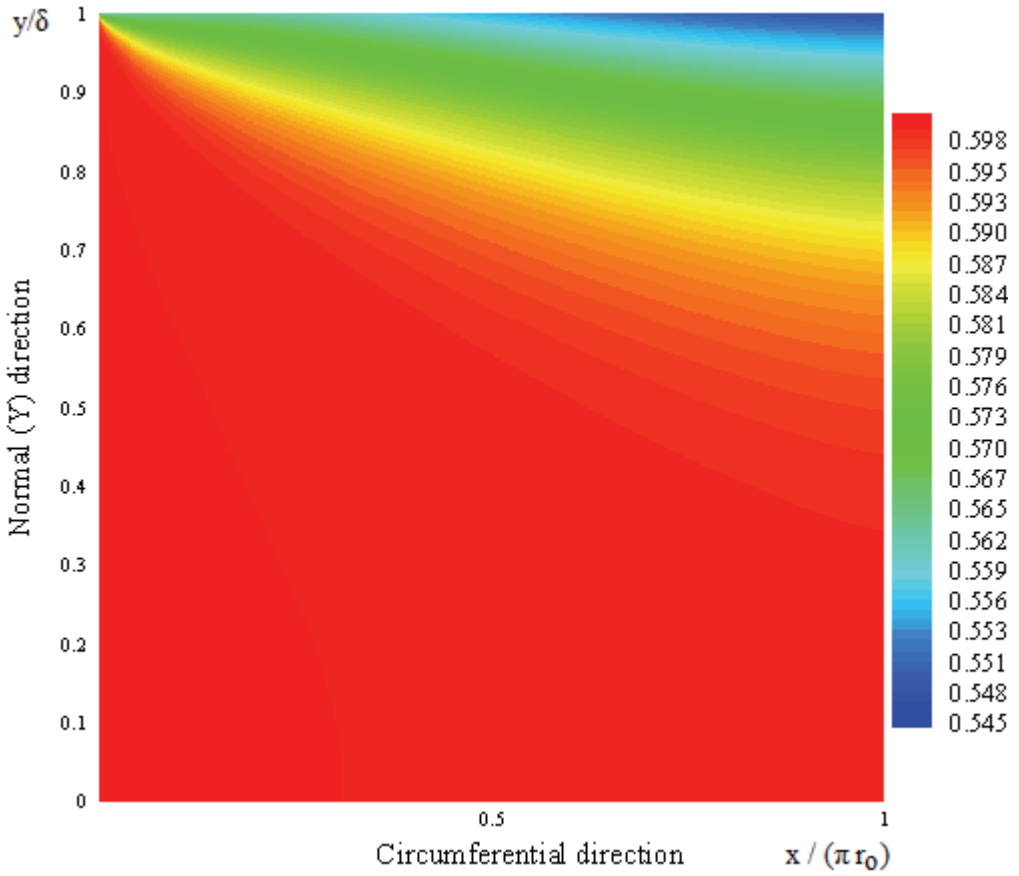

Figure 5.33 LiBr concentration field (weight ratio) of the falling film, low temperature inlet, horizontal absorber.

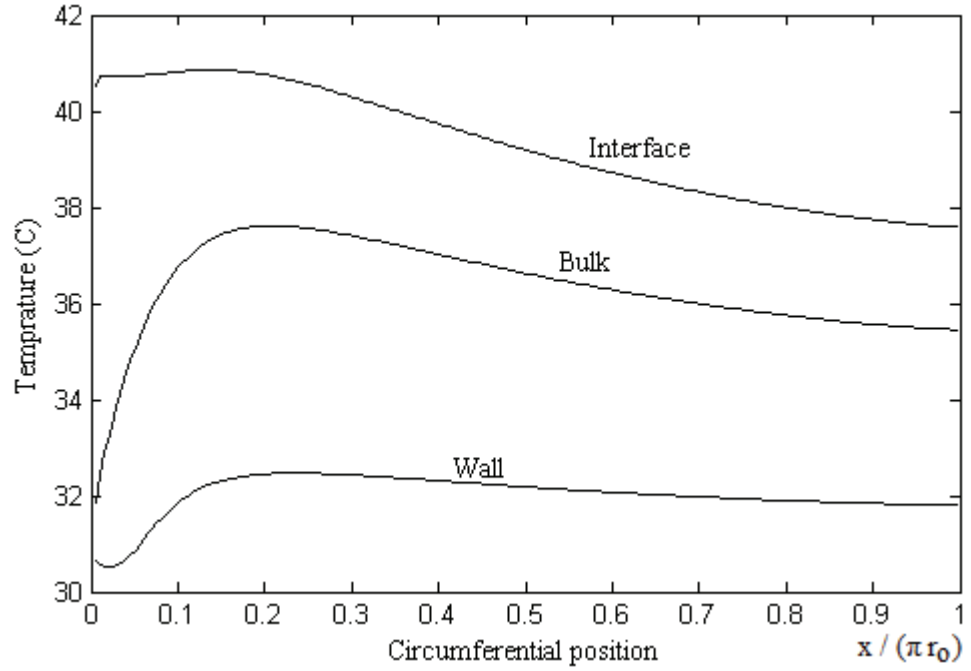

Figure 5.34 Variation of surface, wall and bulk temperature with distance around the tube, low temperature inlet, horizontal absorber.

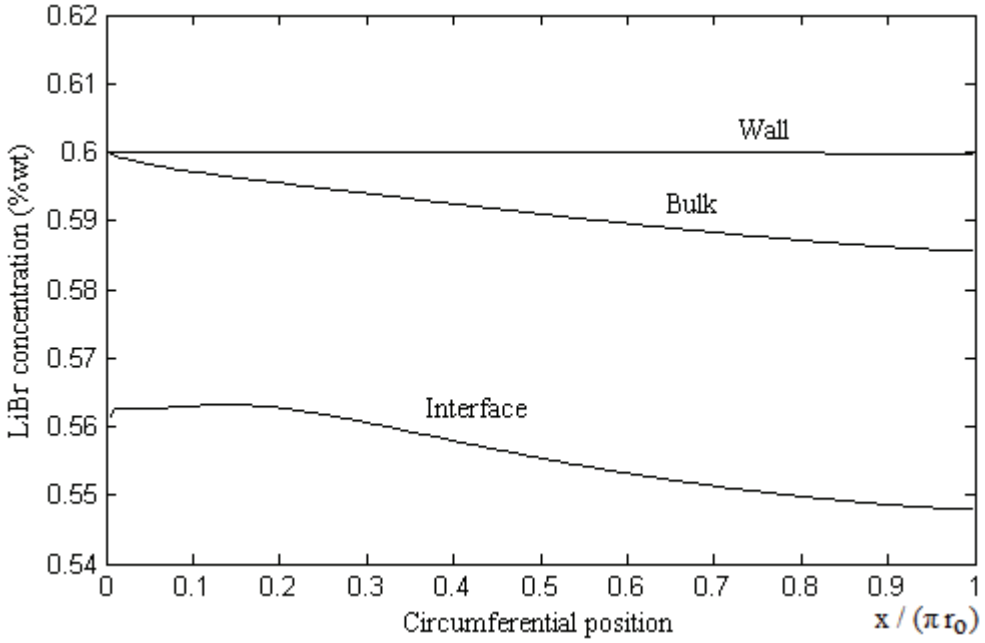

Figure 5.35 Variation of surface, wall and bulk LiBr concentration with distance around the tube, low temperature inlet, horizontal absorber.

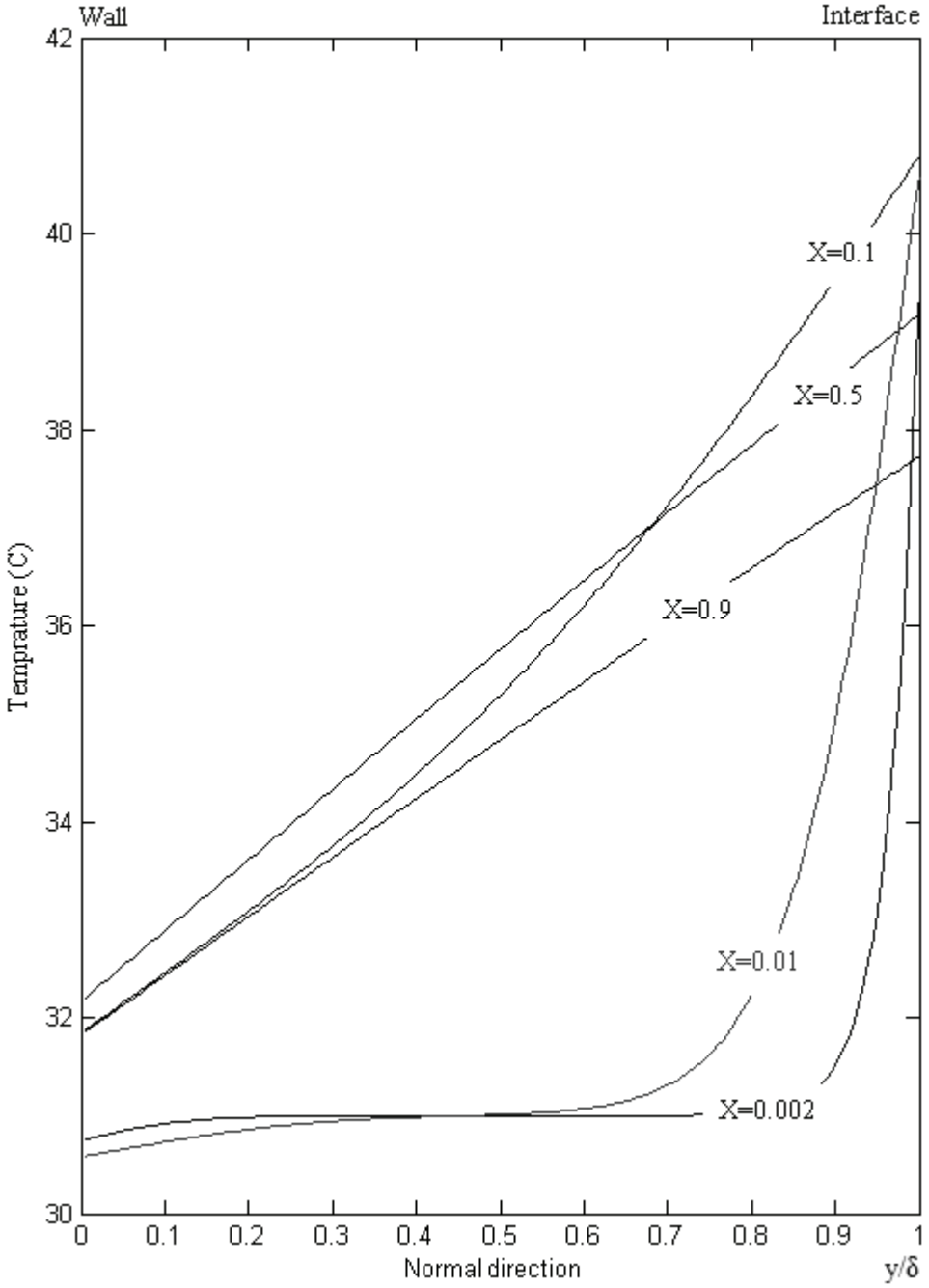

Figure 5.36 Cross stream temperature profiles at selected downstream positions, low temperature inlet, horizontal absorber.

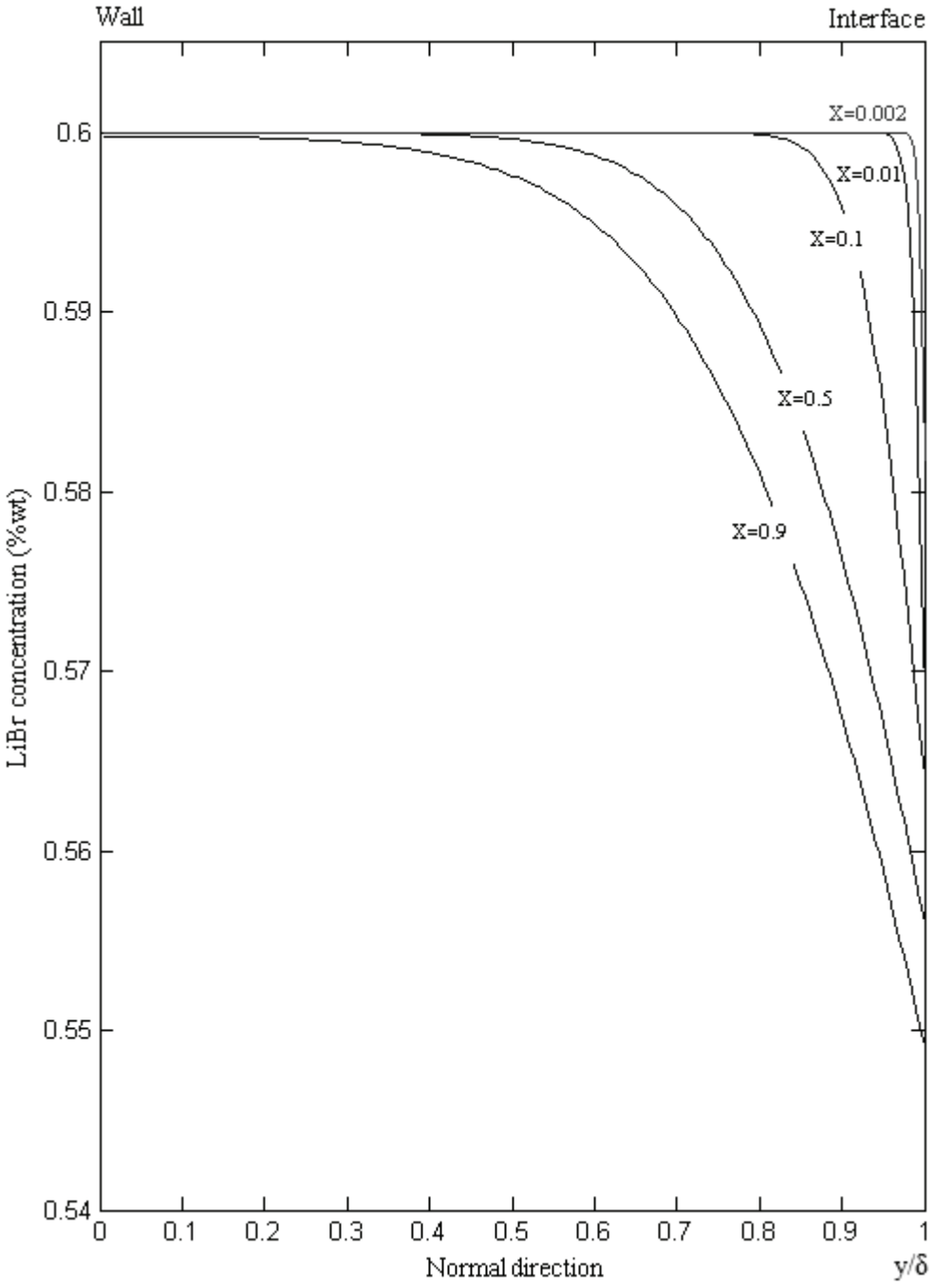

Figure 5.37 Cross stream LiBr concentration profiles at selected downstream positions, low temperature inlet, horizontal absorber.

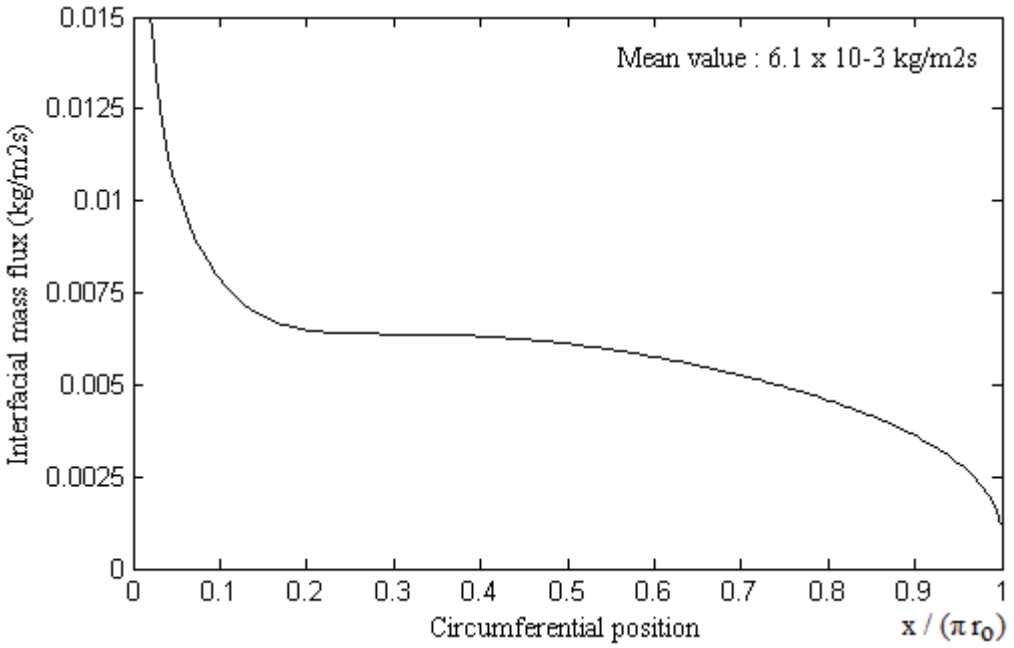

Figure 5.38 Variation of the interface vapour absorption flux with distance around the tube, low temperature inlet, horizontal absorber.

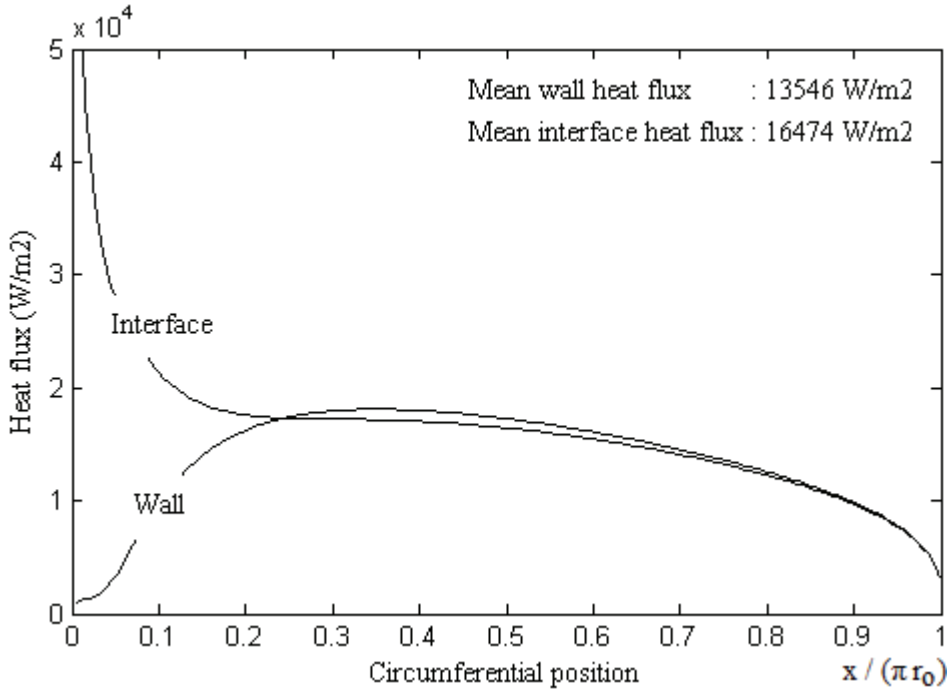

Figure 5.39 Variation of surface and wall heat flux with distance around the tube, low temperature inlet, horizontal absorber.

5.3.3 Effect of the Solution Inlet Temperature

As discussed in section 5.2.3, solution inlet temperature only effects the inlet region considerably. For the low solution inlet case, a large amount of absorption causes the bulk and surface vapour concentration to increase, hence driving potential for absorption decreases.

For the high temperature solution inlet case, absorption rates increases as the temperature profile develops to allow for a heat transfer from surface to the wall, at the most of the tube surface, the bulk and surface vapour concetration is lower than that of the low solution inlet case. As a consequence, although the low temperature solution inlet case has a great advantage at the inlet region; for the high solution inlet case, absorption rates at the regions other than the inlet is slightly higher than that of the low temperature solution inlet case. However the overall performance of the low temperature solution inlet case is % 6 higher.

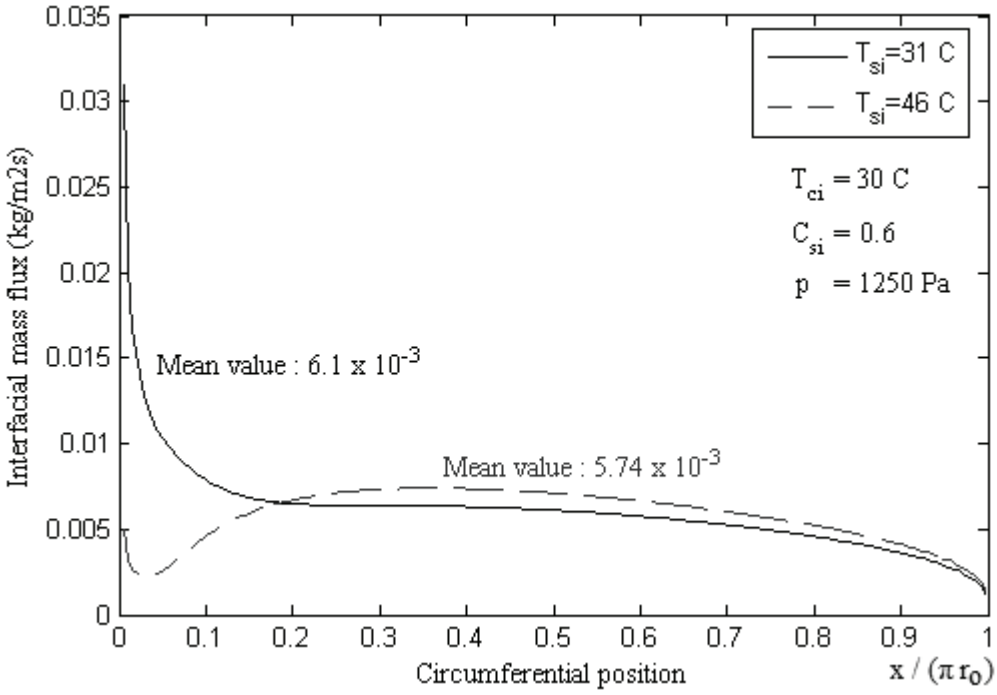

Figure 5.40 Surface vapour mass flux versus distance around the tube, effect of the solution inlet temperature.

5.3.4 Effect of the Solution Mass Flow Rate

As discussed in section 5.2.4, an increase in solution mass flow rate increases resistance to heat transfer, however this causes large amount of absorption at the entrance region which decreases driving potential for absorption as the solution flows down the tube. Contrary to vertical asborber case, the first effect dominates in the horizontal absorber case. Hence as observed in Figure 5.41, as the mass flow rate increases, absorption performance decreases. Increasing Reynolds number from 5.38 to 10.77 decreases overall absorption performance by % 2.5; increasing Reynolds number from 5.38 to 16.2 decreases overall absorption performance by % 5.26.

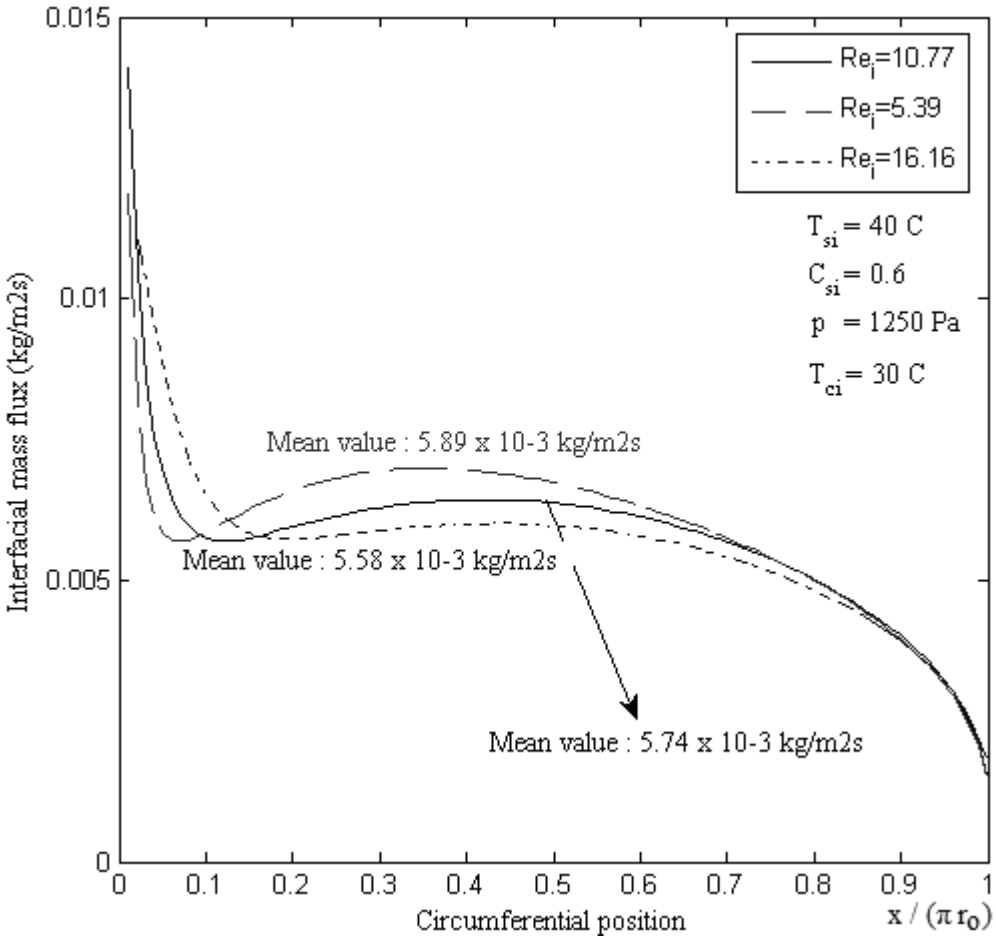

Figure 5.41 Surface vapour mass flux versus distance around the tube, effect of the solution mass flow rate.

5.3.5 Effect of the Cooling Water Inlet Temperature

Cooling water temperature probably has the biggest effect on the absorption performance, because absorption of vapour is possible only if the heat of absorption can be transferred to the cooling water. By decreasing cooling water inlet temperature from 30°C to 25°C, a % 26 increase in overall absorption performance is observed with the present parameters. However it is usually very difficult to decrease cooling water temperature economically because it should always be above the open-air temperature if cooling tower, etc. is used. In the hot regions, open air temperature is usually above 30°C, hence cooling water inlet temperature may be as high as 35°C which decreases absorption performace dramatically.

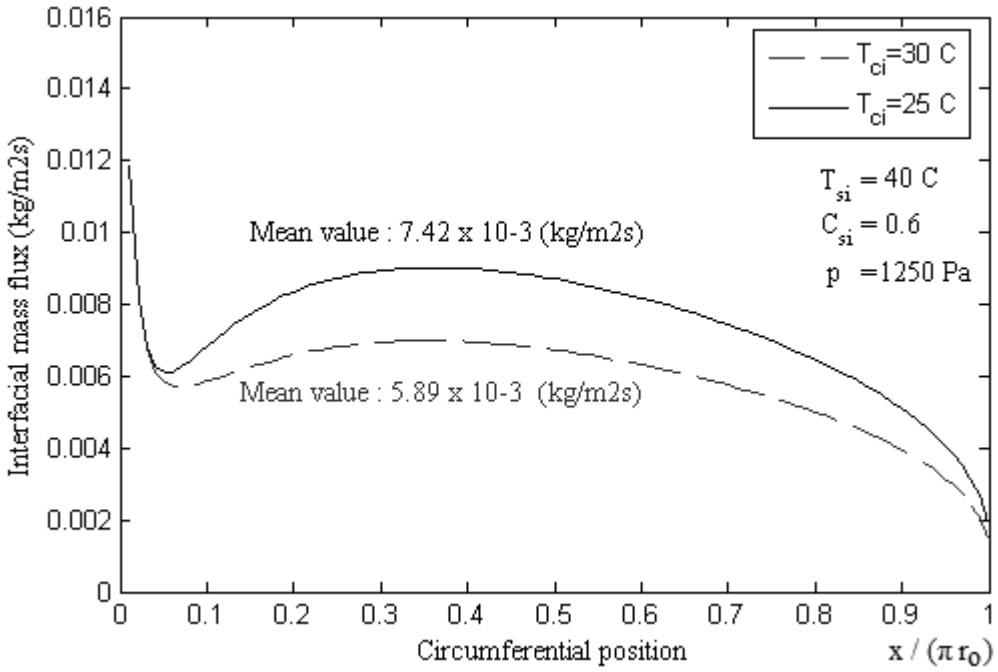

Figure 5.42 Surface vapour mass flux versus distance around the tube, effect of the cooling water inlet temperature.

5.4 Comparison of Vertical and Horizontal Absorbers

It is impossible to make a certain statement whether vertical tube geometry or horizontal geometry is better, because there are nearly infine number of parameters to consider such as dimensions, operating parameters, compability with design criterias, construction cost, maintenance easiness and costs, etc. Also the present model does not consider partial surface wetting, effect of absorption between successive horizontal tubes, time dependent random droplets between successive tubes, turbulent and wavy film hydrodynamics and effetcs of droplets on film hydrodynamics. Hence the present comparison can not state a certain criteria, however it may give a valuable idea about difference between the two absorber geometries.

Most of the parameters that have already been used in the previous analyses are again be used here, such that solution inlet temperature is taken between high and low temperatures (40^{o}C), mass flow rate is again selected as 0.007245 kg/s, the tubes are made of copper with a outer diameter of 19.05mm, a inner diameter of 16.6 mm and a length of 0.5m and 0.1m (for horizontal absorbers). Absorber pressure is selected to be 1250 Pa.

Total vapour absorption rates are be plotted as a function of different horizontal absorbes consisting of different number of tubes arranged vertically (each are 0.5 m or 0.1m in length), and different vertical absorbers each having a tube with different lengths. Apart from number of tubes and tube lengths, other parameters are fixed.

If relatively long tubes are used for the horizontal absorber (see Figures 5.43 and 5.44); the horizontal type absorber is probably advantegeous over the vertical type absorber at Reynolds numbers we studied with (Re < 100 for vertical absorber model and Re < 25 for horizontal absorber). However in actual horizontal absorbers consisting of pure horizontal tubes; droplets and long tails cause dry patches on the tube surface, hence absorption performance falls greatly (Kim, Ameel, & Wood, 1997), and the present results for the present parameters may become invalid in this

situation (see Fig. 5.47). However this situation may be prevented by placing a thin plate just below the tube which also enhances absorption performance and makes film hydrodynamics closer to the Nusselt's solution. Also relatively expensive special surfaces which increases wetting ratio are avaliable commercially (Kim et al., 1997).

On the other hand, if relatively short tubes are used for the horizontal absorber (Figures 5.43 and 5.45 reveals that); the horizontal type absorber is again advantegeous over the vertical absorber; such that 12 horizontal tubes (or 1.2m total tube length) is enough for a total mass absorption rate of 3.5×10^{-4} kg/s for the horizontal type absorber, while more than 3 m vertical tube is needed for the vertical type absorber to reach the same absorption rate. Hence much more compact designs are avaiable for the horizontal arrangement.

In summary, the horizontal geometry is probably very advantageous over the vertical tube for low flow rates. However, construction costs of horizontal absorbers are higher because they have a more complex construction.

However, things change at higher flow rates ($Re > 100$ for vertical absorber model and $Re > 25$ for horizontal absorber) such that the present model is not valid for these flow rates, hence a direct comparison cannot be made. However according to Kim et al. (1997) vertical absorber becomes advantegeous because mixing effect of the waves enhances absorption rates by moving water molecules at the surface to the bulk solution, and LiBr molecules at the bulk solution to the film surface, hence water concentration at the interface becomes lower than that of the smooth film.

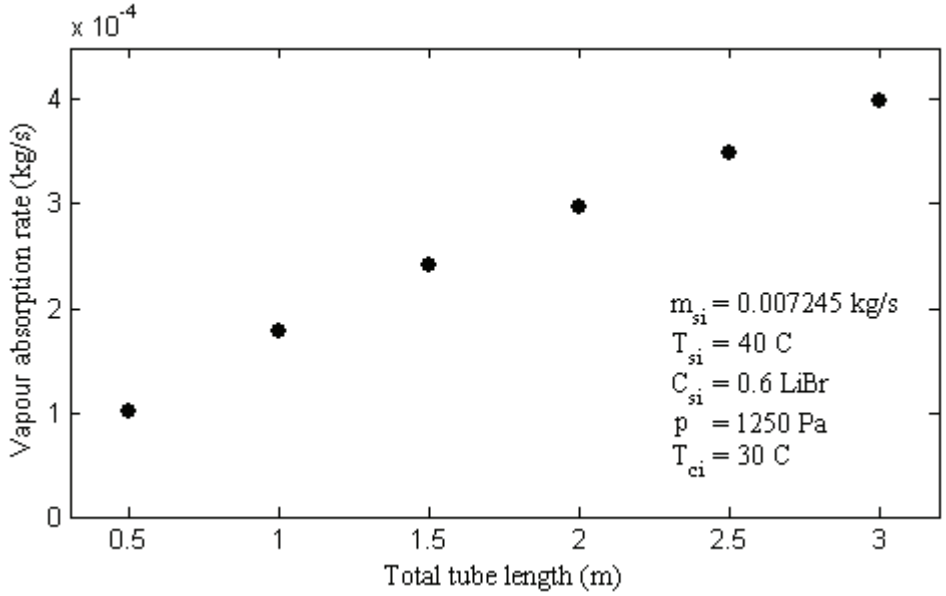

Figure 5.43 Total vapour absorption rates versus different vertical absorbers with different tube lengths.

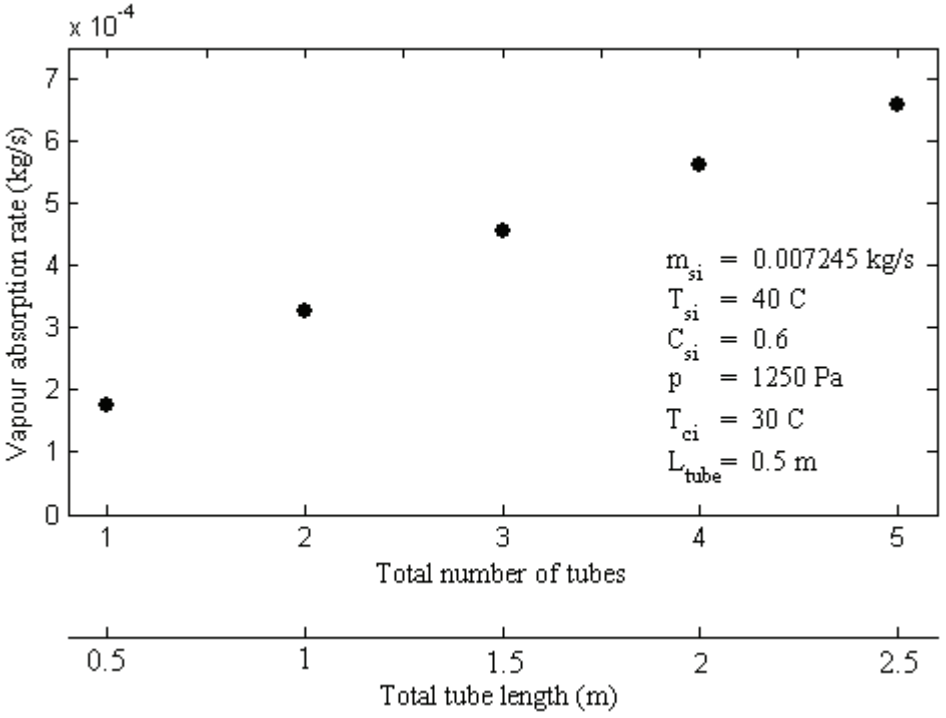

Figure 5.44 Total vapour absorption rates versus different horizontal absorbers consisting of different number of tubes arranged vertically, long tubes.

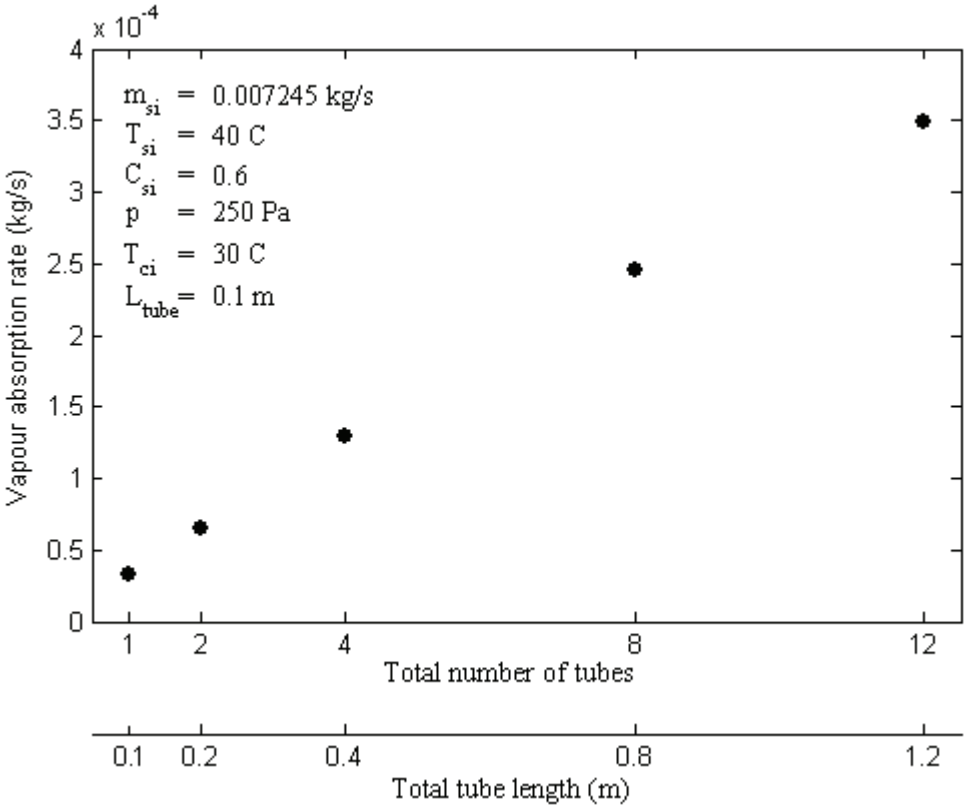

Figure 5.45 Total vapour absorption rates versus different horizontal absorbers consisting of different number of tubes arranged vertically, short tubes.

5.5 Experimental Verification

Experimental data of Kim et al. (1997) was selected to verify the present vertical absorber model. As observed in Figure 5.45, agreement between the present vertical absorber model and the experimental data of Kim et al. (1997) is very good between Reynolds numbers 30 and 100. At Reynolds number 60, agreement is excellent. These are satisfactory results because film Reynolds numbers between 30 and 100 is a common and optimum range under which actual traditional absorbers operate.

However the present model cannot predict the process at Reynolds numbers lower than 30 and higher than 100. At low flow rates, tube is not completely wetted by the aqueous solution, this is why the present model overpredicts absorption rates at Reynolds number 15. On the other hand, circulation effects of the waves enhance absorption performance at Reynolds numbers higher than 100.

Variation of average mass flux with solution inlet concentration at Reynolds number 60 is presented in Figure 5.46. Agreement with the experimental data is excellent. Although not presented here, effect of the absorber pressure, solution inlet temperature is very well simulated with the present model.

Horizontal absorber model was verified with the experimental data of Seol et al. (2005). As shown in Figure 5.47, agreement is very good for sheet flow drainage. Normally solution falls in the form of unsteady droplets or jets between two tubes, however sheet drainage is intentionally created by placing a thin plate just below the tube which ensures uniform film flow at the tube surface and increases performance for the present mass flow rate. On the other hand, the present model cannot predict the process for jet drainage because it causes time dependent and non-uniformly distributed flow at the tube surface. A more complicated time-dependent three dimensional hydrodynamic model is necessary to model these effects accurately. However because performance with the sheet drainage increases, this is not always an issue.

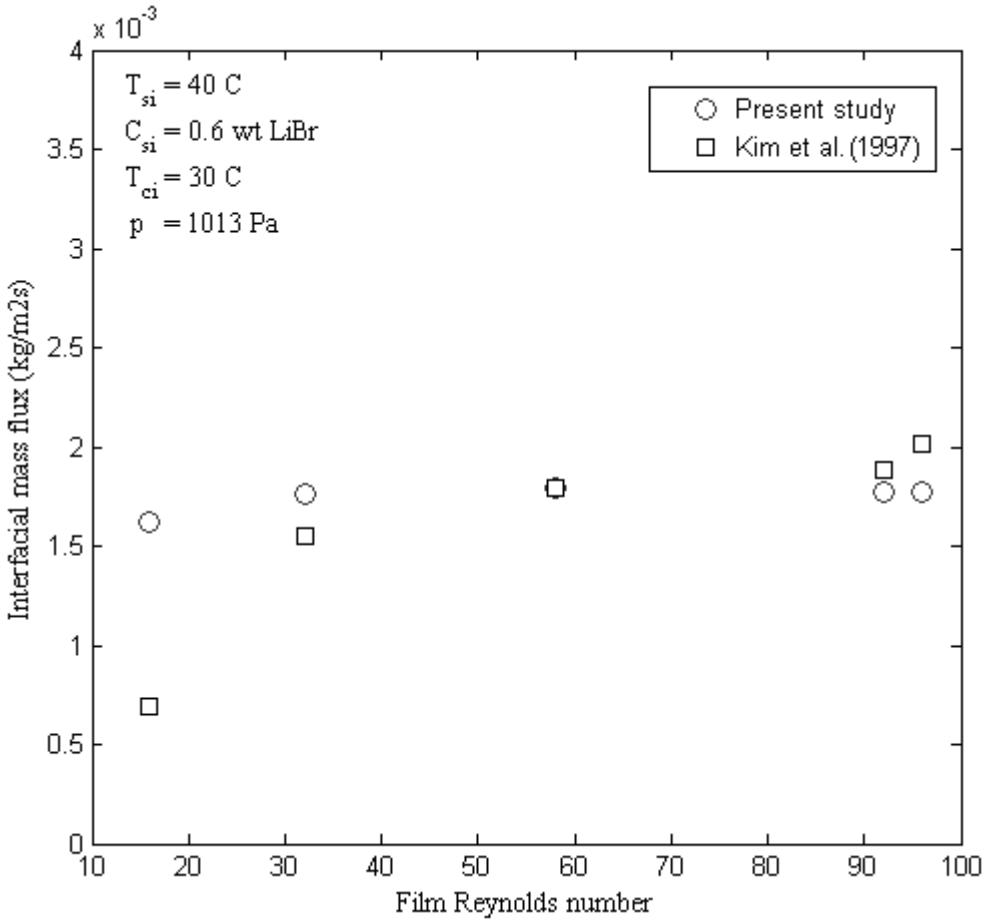

Figure 5.45 Variation of average mass flux with solution mass flow rate, comparing the present vertical absorber model with experimental data of Kim et al. (1997).

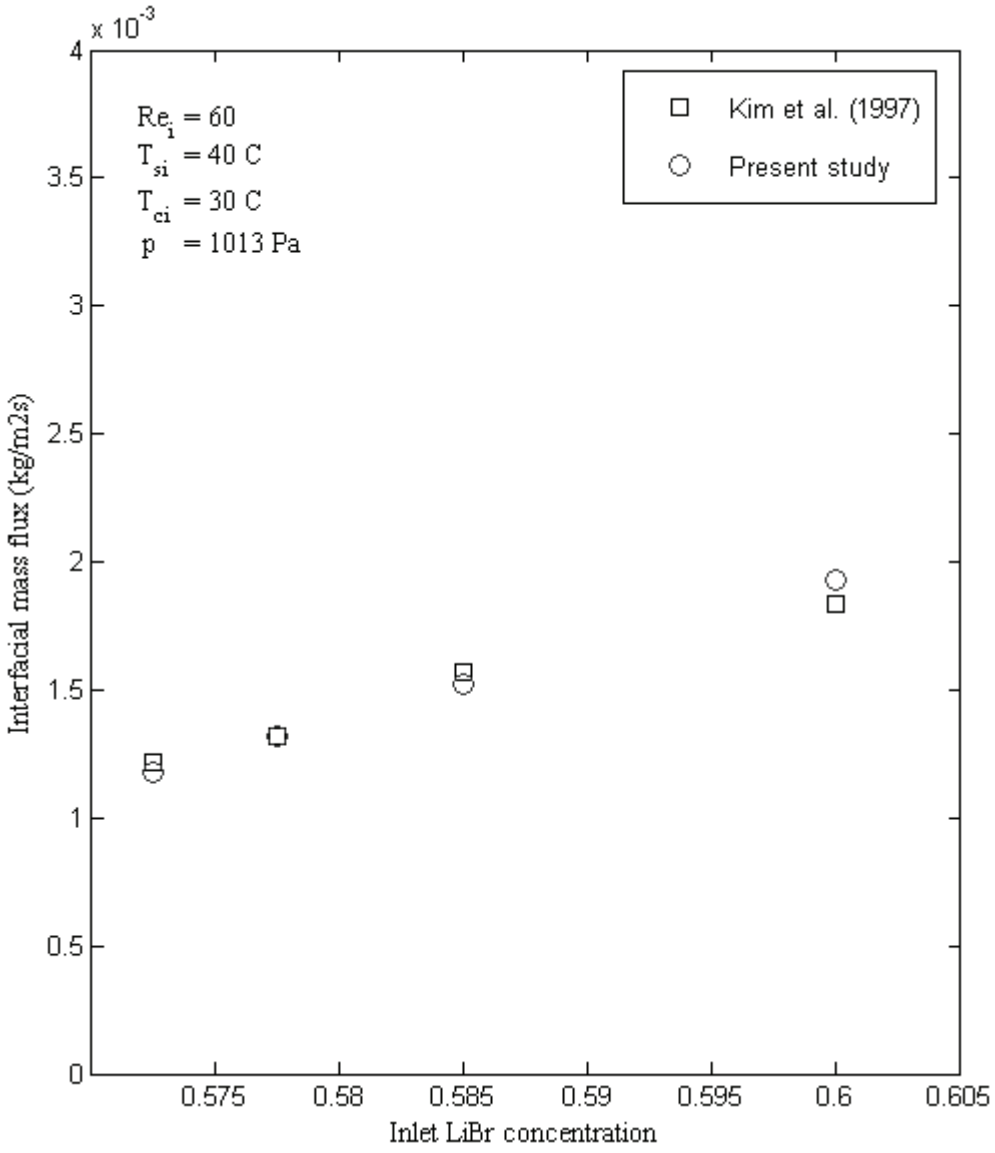

Figure 5.46 Variation of average mass flux with solution inlet concentration at Re=60, comparing the present vertical absorber model with experimental data of Kim et al. (1997).

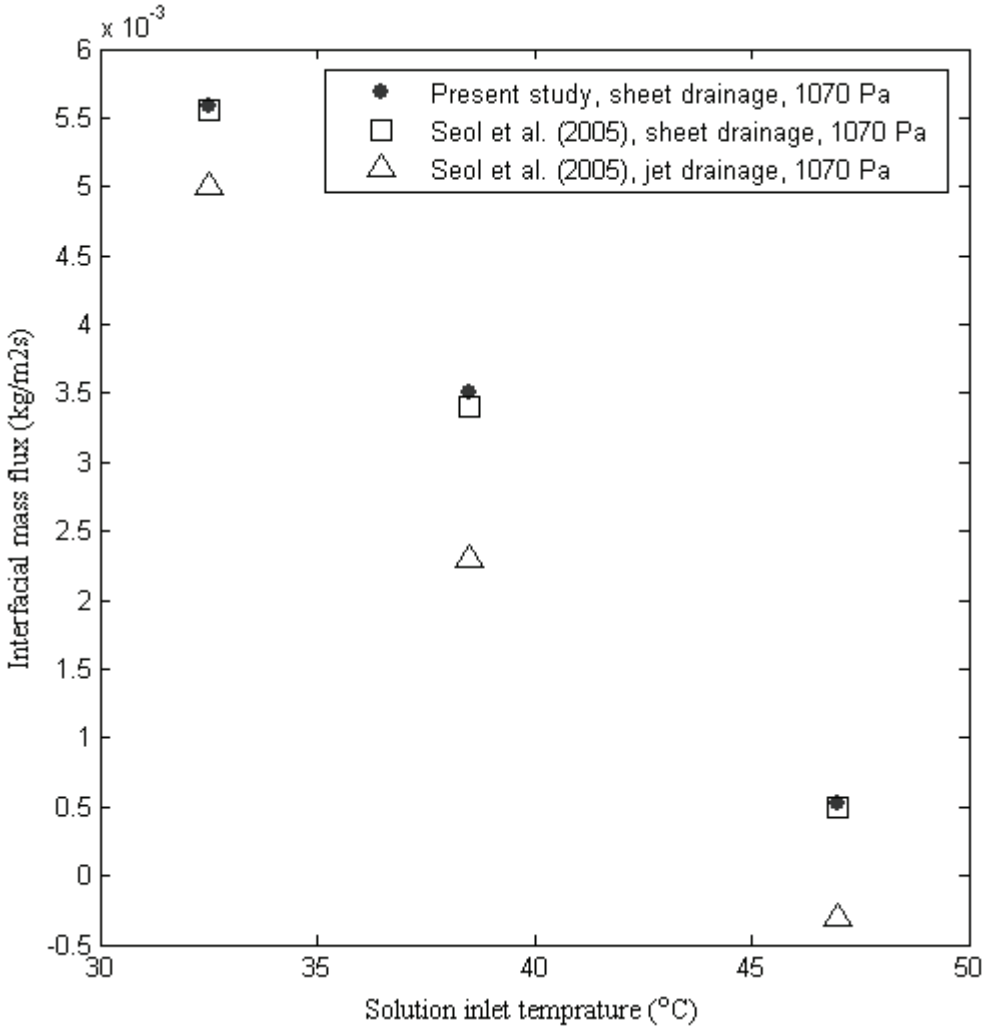

Figure 5.47 Variation of average mass flux with solution inlet temperature, comparing the present horizontal absorber model with experimental data of Seol et al. (2005).

CHAPTER SIX
CONCLUSIONS

The problem of vapour absorption of liquid films flowing over cooled vertical and horizontal tubes are analyzed numerically and verified with experimental data avaliable in the literature. The models consider energy and species transport on a differential scale. As cooling water temperature, tube wall temperature and film surface temperature distributions are unknown, a multi iterative procedure is employed. It is first assumed that cooling water and tube wall temperature distributions are known; hence based on these initial values, film surface temperature and concentration distributions are calculated iteratively. Then cooling water and tube wall temperature distributions are updated. Based on the new wall temperature distribution, film surface temperature and concentration distributions are again calculated iteratively. Low underelaxation factors are necessary for convergence. The process continues until convergence.

It is shown that absorption performance is strongly dependent on the heat transfer from the film surface to the tube wall. So as to improve vapour absorption at the film surface, the heat transfer rate from the film surface to the tube wall should be increased by means of decreasing the cooling water temprature, improving the tube surface, etc. Another mechanism that enhances absorption performance is the surface waves and effects of droplets on horizontal tubes which have a mixing effect. This mixing of solution increases driving force for absorption. At higher flow rates ($Re > 100$ for vertical absorber and $Re > 25$ for horizontal absorber) actual absorbers have better absorption performance than the results of the smooth film surface models.

Results of the present models are summarized in tables 6.1, 6.2, 6.3 and 6.4, Readers are referred to section 5 for further details.

Table 6.1 Computed and experimental average absorption fluxes for vertical absorbers.

		Vertical Absorber	
		Calculated (kg/m^2s)	**Experimental (kg/m^2s)**
Reynolds Number	**15**	1.62×10^{-3}	0.688×10^{-3}
	32	1.767×10^{-3}	1.55×10^{-3}
	60	1.788×10^{-3}	1.789×10^{-3}
	92	1.774×10^{-3}	1.887×10^{-3}
	96	1.77×10^{-3}	2.014×10^{-3}

Table 6.2 Computed and experimental average absorption fluxes for horizontal absorbers.

		Horizontal Absorber	
		Calculated (kg/m^2s)	**Experimental (kg/m^2s)**
Solution inlet temperature (°C)	**32.5**	5.59×10^{-3}	5.55×10^{-3}
	38.5	3.51×10^{-3}	3.4×10^{-3}
	47	0.52×10^{-3}	0.5×10^{-3}

Table 6.3 Vapor absorption rates for vertical and horizontal absorbers, low solution flow rate (Re < 90 for vertical absorber, Re < 25 for horizontal absorber), long tubes (0.5m) for the horizontal absorber.

Vertical tube length / Number of horizontal tubes arranged vertically	**Total vapour absorption rate x 10^3 (kg/s)**	
	Vertical absorber	**Horizontal absorber**
0.5 m / 1 (0.5m)	0.102	0.176
1 m / 2 (1m)	0.177	0.328
1.5 m / 3 (1.5m)	0.240	0.457
2 m / 4 (2m)	0.297	0.562
2.5 m / 5 (2.5m)	0.347	0.658

Table 6.4 Vapor absorption rates for vertical and horizontal absorbers, low solution flow rate (Re < 90 for vertical absorber, Re < 25 for horizontal absorber), short tubes (0.1m) for the horizontal absorber.

Vertical tube length / Number of horizontal tubes arranged vertically	**Total vapour absorption rate x 10^3 (kg/s)**	
	Vertical absorber	**Horizontal absorber**
0.5 m / 1 (0.1m)	0.102	0.0327
1 m / 2 (0.2m)	0.177	0.0657
1.5 m / 4 (0.4m)	0.240	0.129
2 m / 8 (0.8m)	0.297	0.246
2.5 m / 12 (1.2m)	0.347	0.349

6.1 Future Work

Nowadays although a lot of research have done on enhancing absorption performance, absorbers are still very ineffective due to low diffusivity of the vapour in the LiBr-H_2O solution. Improvements on heat transfer mechanisms should be done by considering different tube surface geometries, which allow complex film hydrodynamics that improve wetting ratio and convection effects from the film surface to tube wall. In numerical analysis, a three dimensional transient turbulent model with Arbitrary Lagrange-Eulerian (ALE) mesh should be employed to calculate solution-vapour interface (the film surface) accurately. In such analysis, surface effects such as waves, long tails and droplets should be considered. On the experimental side of the problem, complex surface geometries should be studied for better heat transfer mechanisms. The effect of different additives should be analysed to improve diffusivity of species in the solution, wetting ratio, solubility of water in the LiBr-H_2O solution.

REFERENCES

Ananthanarayanan, P, N., (2005). *Basic Refrigeration and Air Conditioning* (3rd Ed.). New Delhi: Tata McGraw-Hill.

Andberg, J. W., & Vliet, G. C. (1983). Nonisothermal absorption of gases into liquid films. *ASME-JSME Thermal Engineering Joint Conference Proceedings, 2*, 423-431.

Andberg, J. W., (1986). *Absorption of vapors into liquid films falling over cooled horizontal tubes*. PhD Dissertation, University of Texas, Austin.

Bejan, A., (1993). *Heat Transfer*. Singapore: John Wiley&Sons Inc.

Bourois, M., Valles, M., Medrano, M., & Coronas, A. (2005). Absorption of water vapour in the falling film of water–(LiBr+LiI+LiNO3 +LiCl) in a vertical tube at air-cooling thermal conditions. *International Journal of Thermal Sciences, 44*, 491-498.

Brauner, N., Moalem Maron, D., & Meyerson, H. (1989). Coupled heat condensation and mass absorption with comparable concentrations of absorbate and absorbent. *International Journal of Heat and Mass Transfer, 32* (10), 1897-1906.

Choudhury, S. K., Hisajima, D., Ohuchi, T., Nishiguchi, A., Fukushima, T., & Sakaguchi, S. (1993). Absorption of vapours into liquids films flowing over cooled horizontal tubes. *ASHRAE Transactions, 99* (2), 81-89.

Florides, G. A., Kalogirou, S. A., Tassou, S. A., & Wrobel, L. C. (2003). Design and construction of a LiBr–water absorption machine. *Energy Conversion and Management, 44*, 2483–2508

Grigor'eva, N. I., & Nakoryakov, V. E. (1977a). Exact solution of combined heat and mass transfer problems during film absorption. *Journal of Engineering Physics, 33* (5), 1349-1353.

Grossman, G., (1983). Simultaneous heat and mass transfer in film absorption under laminar flow. *International Journal of Heat and Mass Transfer, 26* (3), 357-371.

Incorpera, F. P., & DeWitt, D. P. (2002). *Fundamentals of Heat and Mass Transfer* (5th ed.). New York: John Wiley & Sons.

Islam, M. A., Miyara, A., & Setoguchi, T. (2009). Numerical investigation of steam absorption in falling film of LiBr aqueous solution with solitary waves. *International Journal of Refrigeration, 32*, 1597-1603.

Kakaç, S., & Liu, H. (1998). *Heat Exchangers: Selection, Rating and Thermal Design*. Boca Raton: CRC Press LLC.

Kholpanov, L. P., Malyusov, V. A., & Zhavoronkov, N. M. (1982). Hydrodynamics and heat and mass transfer in a liquid film in the presence of a gas stream or of surface tension. *Teoreticheskie Osnovy Khimicheskoi Tekhnologii, 16* (3), 201-207.

Killion, J. D., & Garimella, S. (2001). A critical review of models of coupled heat and mass transfer in falling-film absorption. *International Journal of Refrigeration, 24*, 755-797.

Kim, J. M., Ameel, T. A., & Wood, B. D. (1997). Performance evaluations of LiCl and LiBr for absorber design applications in the open-cycle absorption refrigeration system. *Journal of Solar Engineering, 119* (2), 165-173.

Kwang, J. K., (1992). *Heat and mass transfer enhancement in absorption cooling*. PhD Dissertation, Arizona State University.

Lu, Z., Li, D., Li, S., & Yu-Chi, B. (1996). A semi-empirical model of the falling film absorption outside horizontal tubes. *Proceedings of the International Ab-Sorption Heat Pump Conference, 2*, 473-480.

Nakoryakov, V. E., & Grigor'eva, N. I. (1977b). Combined heat and mass transfer during absorption in drops and films. *Journal of Engineering Physics, 32* (3), 243-247.

Nakoryakov, V. E., & Grigor'eva, N. I. (1980a). Calculation of heat and mass transfer in nonisothermal absorption of the initial portion of a downfalling film. *Teoreticheskie Osnovy Khimicheskoi Tekhnologii, 14* (4), 483-488.

Nakoryakov, V. Y., & Grigor'eva, N. I. (1980b). Combined heat and mass transfer in film absorption. *Heat Transfer-Soviet Research, 12* (3), 111-117.

Nakoryakov, V. Y., Burdukov, A. P., Bufetov, N. S., Grigor'eva N. I., & Dorokhov, A. R. (1982). Coefficient of heat and mass transfer in falling wavy liquid films. *Heat Transfer-Soviet Research, 14* (3), 6-11.

Nakoryakov, V. E., & Grigor'eva, N. I. (1995). Heat and mass transfer in film absorption with varying liquid-phase volume. *Teoreticheskie Osnovy Khimicheskoi Tekhnologii, 29* (3), 223-228.

Papaefthimiou, V. D., Karampinos, D. C., & Rogdakis, E. D. (2006). A detailed analysis of water-vapour absorption in LiBr-H_2O solution on a cooled horizontal tube. *Applied Thermal Engineering, 26*, 2095-2102.

Patankar, S. V. (1980). *Numerical Heat Transfer and Fluid Flow*. U.S.A.: Hemisphere Publishing Corporation.

Qu, M., (2008). *Model based design and performance anaysis of solar absorption cooling and heating system*. PhD Dissertation, Carnegie Mellon University.

Raisul Islam, M., Wijeysundera, N. E., & Ho, J. C. (2006). Heat and mass transfer effectiveness and correlations for counter-flow absorbers. *International Journal of Heat and Mass Transfer, 49*, 4171-4182.

Rogdakis, E. D., Papaefthimiou, V. D., & Karampinos, D. C. (2003). A realistic approach to model LiBr-H_2O smooth falling film absorption on a vertical tube. *Applied Thermal Engineering, 23*, 2269-2283.

Seol, S. S., & Lee, S. Y. (2005). Experimental study of film flow and heat/mass transfer in LiBr–H2O solution flowing over a cooled horizontal tube. *International Communications in Heat and Mass Transfer, 32*, 445-453.

Sultana, P., Wijeysundera, N. E., Ho, J. C., & Yap, C. (2007). Modeling of horizontal tube-bundle absorbers of absorption cooling systems. *International Journal of Rerigeration, 30*, 709-723.

Tsai, B., & Perez-Blanco, H. (1998). Limits of mass transfer enhancement in lithium bromide-water absorbers by active techniques. *International Journal of Heat and Mass Transfer, 41* (15), 2409-2416.

Versteeg, H. K., & Malalasekera, W., (1995). *An introduction to Computational Fluid Dynamics, The Finite Volume Method*. London: Longman Scientific & Technical.

Yüksel, M. L., & Schlünder, E. U. (1987). Heat and mass transfer in non-isothermal absorption of gases in falling films, Part II: theoretical description and numerical calculation of turbulent falling film heat and mass transfer. *Chemical Engineering and Processing, 22* (4), 203-213.

Zhang, F., Tang, D. L., Geng, J., Wang, Z. X., & Zhang, Z. B. (2008). Study on the temprature distribution of heated falling liquid films. *Physica, D237*, 867-872.

APPENDIX A
NOMENCLATURE

Variable	Description
δ	Film thickness
δ_{90}	Film thickness at theta 90^o in the horizontal absorber
p	Absorber vapour pressure
T	Temperature
C	Mass fraction of LiBr in the solution
LiBr	Lithium bromide salt
wt	Weight
a,b	Coefficients for the linearized surface pressure equilibrium function ($C_{if} = aT_{if} + b$)
r_o	Outer radius of the tube
r_i	Inner radius of the tube
L	Tube length
X	Dimensionless x coordinate
Y	Dimensionless y coordinate
R	Dimensionless r (radial) coorditane
Z	Dimensionless z (axial) coordinate
J	Conversion coefficient in the energy equation (eq. 3.4)
m	Mass flow rate (kg/s for solution, kg/m^2s for absorption)
Γ	Solution mass flow rate per tube circumference for the vertical absorber ($m/2\pi r_o$) and per side and tube length for the horizontal absorber (m/2L).
D	Mass diffusivity of any species in the solution (m^2/s)
μ	Dynamic viscosity (kg/ms)
k	Thermal conductivity (W/mK)
α	Thermal diffusivity (m^2/s)
ρ	Mass density (kg/m^3)

c_p	Specific heat capacity (J/kgK)
h_{abs}	Specific heat of absorption (J/kgK)
h	Entalphy (J/kgK)
q	Heat flux (W/m^2)
U	Overall heat transfer coefficient from the cooling water to the outer surface of the tube wall evaluated at the outer surface of the tube (W/m^2K)
Re	Film Reynolds number ($4\Gamma/\mu$)
Pr	Prandl number ($\mu c_p/k$)
Sc	Schmidt number ($\mu/\rho D$)
masscoef	A coefficient for the interface b. condition ($\rho D h_{abs}/k$)
gradcool	A coefficient that describes increase of cooling water temperature ($-2\pi(r_o+\delta)Lk / m_c c_{pc}\delta$ for the vertical absorber model, $-2\pi r_o Lk / m_c c_{pc}\delta_{mean}$ for the horizontal absorber model)
CW	A coefficient that describes the resistance to heat transfer at the tube wall ($r_o k / r_i U\delta$ for the vertical absorber model, $k / \delta_{mean} U$ for the horizontal absorber model.)

Subscripts	**Description**
s	Solution
v	Vapour
w	Water
b	Bulk
c	Cooling water
if	Solution-vapour interface
abs	Absorption or absorbed
i	Inlet
si	Solution inlet

APPENDIX B

```
'*****************************************************************
'   VERTICAL ABSORBER TEMPRATURE AND CONCENTRATION FIELD
'                        ANALYSIS CODE
'*****************************************************************

'  Properties of the model:
'  1) Physical properties vary with local temprature and concentration.
'  2) The film thickness varies with the absorption of vapour,
'     and with local bulk temprature and concentration.

'  Assumptions:
'  1) Tube is completely wetted by the solution.
'  2) At the solution-vapour interface, vapour pressure equilibrium exists.
'  3) The flow is laminar and non-wavy throughout.
'  4) No shear forces are exerted on the liquid by the vapour.
'  5) Convection in the flow direction is much more stronger than diffusion, so
'     diffusion  in the axial direction is neglected.
'  6) Heat transfer in the vapour phase is negligible compared to that in the liquid
'     phase.



'    Nomenclature:

'    Tent      =  Entrance temprature
'    Cent      =  Entrance concentration
'    Refilm    =  Film reynolds number   [4 x (massflow / pipe_circumference) / mu]
'    Pr        =  Prandl number          [mu x cp / k]
'    Sc        =  Schmidt Number         [mu/ (rho x D)]
'    thr       =  Thickness (aspect) ratio    [delta / L]
'    ftr       =  Film thickness ratio        [delta / ri]
'    masscoef  =  Species-energy eq. coupling coef.     [rho * D * habs / k]  Kelvin
'    CW        =  Coef. from cooling water en. balance  [ri / rin / Uwall * k / delta]
'    gradcool  =  Coef. from cooling water en. balance  [gradcool = -2 * pi * ro * L
'                 * k / delta / mc / cpc]
'    n         =  Number of control volumes in the radial (transverse) direction
'    m         =  Number of control volumes in the axial (downstream) direction

'          mu      =  Dynamic viscosity              [Ns/m2]
'          rho     =  Density                        [kg/m3]
'          k       =  Thermal conductivity           [W/mK]
'          D       =  Mass diffusivity               [m2/s]
'          habs    =  Heat of absorption             [j/kg]
'          Delta   =  Film thickness, a function
'                     of Renolds number, mu and rho  [m]
```

```
'           ri        =  Outer radius of the tube          [m]
'           rin       =  Inner radius of the tube          [m]
'           ro        =  Outer radius of the film          [m]
'           Cgrad()   =  1/Cinter*dC/dR

'NOTE:  'D:\results' folder must be created in order to get the results.
'           Code is set up to run on Visual Basic

Dim T() As Double, Tc() As Single, C() As Double, Tbulk() As Double
Dim Cbulk() As Double, Told() As Double, Cold() As Double
Dim coef1() As Double, coef2() As Double, coef3() As Double
Dim Tinter() As Double, Cinter() As Double, Twall() As Single, Cgrad() As Double
Dim Cgradold() As Double, grad() As Double, gradwall() As Single
Dim gradwallold() As Single, convergence() As Double, massflow() As Double
Dim dR As Double, dZ As Double, RR As Single, ZZ As Single


'Discretization Equations Coefficients

'For Energy Eq.
Dim aP() As Double, aN() As Double, aE() As Double, aW() As Double
Dim Source() As Double

'For Species Eq.
Dim aPC() As Double, aNC() As Double, aEC() As Double, aWC() As Double
Dim SourceC() As Double


'Three-Diagonal Matrix Algorithm Coefficients

'For Energy Eq.
Dim fT() As Double, eT() As Double, gT() As Double, rT() As Double

'For Species Eq.
Dim fC() As Double, eC() As Double, gC() As Double, rC() As Double
Dim delta() As Double
```

```
Private Sub Command1_Click()


'SOLVER CONSISTS OF FIVE MAIN PARTS:

' 1-DEFINING PROPERTIES
' 2-TEMPRATURE SOLVER
'     2.2.Setting up the coefficients
'     2.3.Three diagonal matrix algorithm
' 3-CONCENTRATION SOLVER
'     3.1.Setting up the coefficients
'     3.2.Three diagonal matrix algorithm
' 4-MASS-ENERGY COUPLING ITERATION ALGORITHM
' 5-COOLING WATER ENERGY BALANCE


'*********************************************************************
'*********************************************************************

'1-DEFINING PROPERTIES:


'Grid parameters

    n    =  200
    m    =  500
    dR   =  1 / n
    dZ   =  1 / m


'Inlet conditions

    ReDim Tc(m + 1) As Single
    Tent   = 40
    Cent   = 0.6
    Tc(0)  = 32          ' Exit cooling water
    Tcin   = 30          ' Inlet cooling water temprature entering from bottom
    pressure = 1000      ' Please enter a value between 800-1500 Pa


'Equilibrium coefficients (depends on absorber pressure, Cif = a * Tif + b)

    a = 4.8688 / 1000 * (pressure / 1000) ^ -0.188
    b = 0.37794 * (pressure / 1000) ^ -0.06574
```

```
'Physical properties at the inlet conditions

habs  =  habsf(Tent, Cent)
D     =  Df(Tent, Cent)
rho   =  rhof(Tent, Cent)
cp    =  cpf(Tent, Cent)
k     =  kf(Tent, Cent)
mu    =  muf(Tent, Cent)
alpha =  k / rho / cp

habsent =  habs
Dent    =  D
rhoent  =  rho
cpent   =  cp
kent    =  k
muent   =  mu


'Cooling water parameters

 mc     =  0.43
 cpc    =  4180
 Uwall =  6852


'Other parameters

ReDim massflow(m + 1) As Double
massflow(1) =  0.0050229
relax       =  0.5          'Underrelaxation factor
pi          =  3.141592653
g           =  9.81


'Physical dimensions

L  =  2.5
ri  =  19.05 / 2 / 1000
rin=  16.6 / 2 / 1000

'The film thickness at the inlet
ReDim delta(m) As Double
delta(1) = ((3 * massflow(1) * mu) / rho ^ 2 / g / 2 / pi / ri) ^ (1 / 3)
'        = (0.75 * Refilm * mu ^ 2 / rho ^ 2 / g) ^ (1 / 3)
```

```
'*********************************************************************
'*********************************************************************
'Program input at the inlet conditions

    Pr       =  mu * cp / k
    thr      =  delta(1) / L
    ftr      =  delta(1) / ri
    Refilm   =  4 * massflow(1) / 2 / pi / ri / mu
    Sc       =  mu / rho / D
    masscoef =  rho * D * habs / k

'Cooling water parameters

    CW       =  ri / rin / Uwall * k / delta(1)
    gradcool  =  -2 * pi * ri * L * k / delta(1) / mc / cpc

'*********************************************************************
'*********************************************************************

Open "d:\results\Convergence.txt"                For Output As 1
Open "d:\results\Tinter.txt"                     For Output As 2
Open "d:\results\Temprature.txt"                 For Output As 3
Open "d:\results\Concentration.txt"              For Output As 4
Open "d:\results\massabsorbed.txt"               For Output As 5
Open "d:\results\Cinter.txt"                     For Output As 6

Open "d:\results\temp_Z=0.002.txt"               For Output As 36
Open "d:\results\temp_Z=0.01.txt"                For Output As 37
Open "d:\results\temp_Z=0.1.txt"                 For Output As 7
Open "d:\results\temp_Z=0.3.txt"                 For Output As 8
Open "d:\results\temp_Z=0.5.txt"                 For Output As 9
Open "d:\results\temp_Z=0.7.txt"                 For Output As 10
Open "d:\results\temp_Z=0.9.txt"                 For Output As 11
Open "d:\results\conc_Z=0.002.txt"               For Output As 38
Open "d:\results\conc_Z=0.01.txt"                For Output As 39
Open "d:\results\conc_Z=0.1.txt"                 For Output As 12
Open "d:\results\conc_Z=0.3.txt"                 For Output As 13
Open "d:\results\conc_Z=0.5.txt"                 For Output As 14
Open "d:\results\conc_Z=0.7.txt"                 For Output As 15
Open "d:\results\conc_Z=0.9.txt"                 For Output As 16

Open "d:\results\walltemp.txt"                   For Output As 17
Open "d:\results\bulktemp.txt"                   For Output As 18
Open "d:\results\bulkcontcent.txt"               For Output As 19
Open "d:\results\exitconditions.txt"             For Output As 20
Open "d:\results\INPUTS.txt"                     For Output As 21
Open "d:\results\Sh.txt"                         For Output As 22
Open "d:\results\mSH.txt"                        For Output As 23
```

```
Open "d:\results\Nu.txt"                    For Output As 24
Open "d:\results\mNu.txt"                   For Output As 25
Open "d:\results\hm.txt"                    For Output As 26
Open "d:\results\hT.txt"                    For Output As 27
Open "d:\results\qw.txt"                    For Output As 28
Open "d:\results\qwmean.txt"                For Output As 29
Open "d:\results\Prgcont.txt"               For Output As 30
Open "d:\results\DELTA(mm).txt"             For Output As 31
Open "d:\results\qinter.txt"                For Output As 32
Open "d:\results\qintermean.txt"            For Output As 33
Open "d:\results\mass_flow_dist.txt"        For Output As 34
Open "d:\results\Cwall.txt"                 For Output As 35


ReDim T(n + 2, m + 2) As Double, C(n + 2, m + 2) As Double
ReDim Tbulk(m) As Double, Cbulk(m) As Double
ReDim Told(n + 2, m) As Double, Cold(n + 2, m) As Double
ReDim coef1(n, m) As Double, coef2(n, m) As Double, coef3(n, m) As Double
ReDim Tinter(m) As Double, Cinter(m) As Double, Twall(m + 1) As Single
ReDim Cgrad(m) As Double, Cgradold(m) As Double, grad(m) As Double
ReDim gradwall(m + 1) As Single, gradwallold(m + 1) As Single
ReDim convergence(m) As Double
ReDim fT(n) As Double, gT(n - 1) As Double, eT(n) As Double, rT(n) As Double
ReDim fC(n) As Double, gC(n - 1) As Double, eC(n) As Double, rC(n) As Double
ReDim aP(n, m) As Double, aN(n, m) As Double, aE(n, m) As Double
ReDim aW(n, m) As Double, Source(n, m) As Double
ReDim aPC(n, m) As Double, aNC(n, m) As Double, aEC(n, m) As Double
ReDim aWC(n, m) As Double, SourceC(n, m) As Double


'Initialization

For j = 1 To m
      Cgrad(j) = 5
      grad(j) = Cgrad(j) * masscoef
      Tc(j) = 30
      gradwall(j) = 0.01
      Twall(j) = Tc(j) + CW * gradwall(j)
      delta(j) = delta(1)
      massflow(j) = massflow(1)
Next j

For i = 1 To n
    For j = 1 To m
        T(i, j) = 30
        C(i, j) = 0.55
    Next j
Next i
```

```
Print #21, "Solution inlet temp    :"; Tent,
Print #21,
Print #21, "Solution inlet conc    :"; Cent,
Print #21,
Print #21, "Cooling water inlet    :"; Tcin,
Print #21,
Print #21, "Operating pressure     :"; pressure,
Print #21,
Print #21, "Refilm                 :"; Refilm,
Print #21,
Print #21, "Pr                     :"; Pr,
Print #21,
Print #21, "ftr                    :"; ftr,
Print #21,
Print #21, "thr                    :"; thr,
Print #21,
Print #21, "Sc                     :"; Sc,
Print #21,
Print #21, "masscoef               :"; masscoef,
Print #21,
Print #21, "gradcool               :"; gradcool,
Print #21,
Print #21, "CW                     :"; CW,
Print #21,
Print #21, "Cooling water flowrate :"; mc,
Print #21,
Print #21, "Uwall                  :"; Uwall,
Print #21,
Print #21,
Print #21,

Print #21, "Physical Values        :",
Print #21,
Print #21, "L                      :", L,
Print #21,
Print #21, "Tube outer diameter(mm):", ri * 1000,
Print #21,
Print #21, "Tube inner diameter(mm):", rin * 1000,
Print #21,
Print #21, "Mass flow rate         :", massflow(1),
Print #21,
Print #21, "Film Thickness (mm)    :", delta(1) * 1000,
Print #21,
Print #21,
Print #21,
Print #21, "Inlet Physical Properties :",
Print #21,
Print #21, "mu                     :", mu,
```

```
        Print #21,
        Print #21, "k                  :", k,
        Print #21,
        Print #21, "rho                :", rho,
        Print #21,
        Print #21, "cp                 :", cp,
        Print #21,
        Print #21, "habs               :", habs,
        Print #21,
        Print #21, "D                  :", D,
        Print #21,


iteration = 1

'*****************************************************************
'*****************************************************************

'2-TEMPERATURE SOLVER:


'2.1.SETTING UP THE COEFFICIENTS


5
For j = 1 To m
    Cgradold(j) = Cgrad(j)
    Tbulk(j) = 0
    Cbulk(j) = 0
Next j

'NOTE:  aS=0 because upwind differencing scheme is used
'RP = (i * 0.5 * dR)

For j = 1 To m
   For i = 1 To n

        mu = muf(T(i, j), C(i, j))
        Refilm = 4 * massflow(j) / 2 / pi / ri / mu
        Tbulk(j) = Tbulk(j) + 2 / 1.024 * pi * (ri + (i - 1) * delta(j) * dR) * delta(j) *
                   dR * mu / delta(j) * (3 / 2 * (2 * (i - 0.5) * dR - ((i - 0.5) * dR) ^ 2)
                   * Refilm / 4) * T(i, j) / massflow(j)
        Cbulk(j) = Cbulk(j) + 2 / 1.024 * pi * (ri + (i - 1) * delta(j) * dR) * delta(j) *
                   dR * mu / delta(j) * (3 / 2 * (2 * (i - 0.5) * dR - ((i - 0.5) * dR) ^ 2)
                   * Refilm / 4) * C(i, j) / massflow(j)

   Next i
Next j
```

```
For i = 1 To n
    For j = 1 To m

  If iteration < 5 Then
       cp = cpent
       k = kent
       mu = muent
       rho = rhoent
       delta(j) = delta(1)
       massflow(j) = massflow(1)
       thr = delta(j) / L
       ftr = delta(j) / ri

  Else
       mu = muf(T(i, j), C(i, j))
       mubulk = muf(Tbulk(j), Cbulk(j))
       k = kf(T(i, j), C(i, j))
       cp = cpf(T(i, j), C(i, j))
       rho = rhof(Tbulk(j), Cbulk(j))
       delta(j) = ((3 * massflow(j) * mubulk) / rho ^ 2 / g / 2 / pi / ri) ^ (1 / 3)
      '        = (0.75 * Refilm * mu ^ 2 / rho ^ 2 / g) ^ (1 / 3)
      '          Delta is a function of Reynolds number, mu and rho

       thr = delta(j) / L
       ftr = delta(j) / ri
       massflow(j + 1) = 0
       massflow(j + 1) = massflow(j) + 2 * pi * (delta(j) / ftr + delta(j)) * (delta(j) /
       thr) * dZ * (-rho * D / Cinter(j) * 2 / delta(j) * (Cinter(j) - C(n, j)) / dR)

  End If

       Refilm = 4 * massflow(j) / 2 / pi / ri / mu
       Pr = mu * cp / k

  coef1(i, j) = 3 / 8 * (2 * (i - 0.5) * dR - ((i - 0.5) * dR) ^ 2) * dR * Refilm * Pr * thr
                * 1 / dZ * ((i - 0.5) * dR * ftr + 1)
  coef2(i, j) = (i * dR * ftr + 1) / dR
  coef3(i, j) = ((i - 1) * dR * ftr + 1) / dR

    Next j
Next i
```

```
i = 1
For j = 2 To m

   aP(i, j) = coef1(i, j) + coef2(i, j) + 2 * coef3(i, j)
   aN(i, j) = coef1(i, j)
   aE(i, j) = coef2(i, j)
   aW(i, j) = 0
   Source(i, j) = 2 * coef3(i, j) * Twall(j)

Next j


i = n
For j = 2 To m

   aP(i, j) = coef1(i, j) + coef3(i, j)
   aN(i, j) = coef1(i, j)
   aE(i, j) = 0
   aW(i, j) = coef3(i, j)
   Source(i, j) = dR * coef2(i, j) * grad(j)

Next j


j = 1
For i = 2 To n - 1

   aP(i, j) = coef1(i, j) + coef2(i, j) + coef3(i, j)
   aN(i, j) = 0
   aE(i, j) = coef2(i, j)
   aW(i, j) = coef3(i, j)
   Source(i, j) = coef1(i, j) * Tent

Next i


i = 1
j = 1

  aP(i, j) = coef1(i, j) + coef2(i, j) + 2 * coef3(i, j)
  aN(i, j) = 0
  aE(i, j) = coef2(i, j)
  aW(i, j) = 0
  Source(i, j) = 2 * coef3(i, j) * Twall(j) + coef1(i, j) * Tent
```

```
i = n
j = 1

  aP(i, j) = coef1(i, j) + coef3(i, j)
  aN(i, j) = 0
  aE(i, j) = 0
  aW(i, j) = coef3(i, j)
  Source(i, j) = dR * coef2(i, j) * grad(j) + coef1(i, j) * Tent


For i = 2 To n - 1
For j = 2 To m

  aP(i, j) = coef1(i, j) + coef2(i, j) + coef3(i, j)
  aN(i, j) = coef1(i, j)
  aE(i, j) = coef2(i, j)
  aW(i, j) = coef3(i, j)
  Source(i, j) = 0

Next j
Next i


'**********************************************************************
'**********************************************************************

'2.2.THREE DIAGONAL MATRIX ALGORITHM


10
iterT = iterT + 1

For i = 1 To n
    For j = 1 To m

        Told(i, j) = T(i, j)

    Next j
Next i
```

```
For j = 1 To m

        fT(1) = aP(1, j)

    For i = 2 To n

        fT(i) = aP(i, j)
        gT(i - 1) = -aE(i - 1, j)
        eT(i) = -aW(i, j)

        eT(i) = eT(i) / fT(i - 1)
        fT(i) = fT(i) - eT(i) * gT(i - 1)

    Next i

        rT(1) = Source(1, j) + aN(1, j) * T(1, j - 1)

   For i = 2 To n

        rT(i) = Source(i, j) + aN(i, j) * T(i, j - 1) - eT(i) * rT(i - 1)

   Next i

        T(n, j) = rT(n) / fT(n)

    For i = n - 1 To 1 Step -1

        T(i, j) = (rT(i) - gT(i) * T(i + 1, j)) / fT(i)

    Next i

Next j


For i = 1 To n
    For j = 1 To m
        If Abs(T(i, j) - Told(i, j)) / T(i, j) > 10 ^ -10 Then GoTo 10
    Next j
Next i


For j = 1 To m

            Tinter(j) = grad(j) * dR / 2 + T(n, j)
            Cinter(j) = a * Tinter(j) + b

Next j
```

```
'*****************************************************************
'*****************************************************************

'3-CONCENTRATION SOLVER:


'3.1.SETTING UP THE COEFFICIENTS


For i = 1 To n
    For j = 1 To m

     If iteration < 3 Then
       mu = muent
       rho = rhoent
       k = kent
       cp = cpent
       D = Dent
     Else
       mu = muf(T(i, j), C(i, j))
       mubulk = muf(T(n / 2, j), C(n / 2, j))
       rho = rhof(T(i, j), C(i, j))
       rhobulk = rhof(T(n / 2, j), C(n / 2, j))
       k = kf(T(i, j), C(i, j))
       cp = cpf(T(i, j), C(i, j))
       D = Df(T(i, j), C(i, j))
     End If

       Refilm = 4 * massflow(j) / 2 / pi / ri / mu
       Sc = mu / rho / D
       thr = delta(j) / L
       ftr = delta(j) / ri

  coef1(i, j) = 3 / 8 * (2 * (i - 0.5) * dR - ((i - 0.5) * dR) ^ 2) * dR * Refilm * Sc * thr
                * 1 / dZ * ((i - 0.5) * dR * ftr + 1)
  coef2(i, j) = (i * dR * ftr + 1) / dR
  coef3(i, j) = ((i - 1) * dR * ftr + 1) / dR

    Next j
Next i
```

```
i = 1
For j = 2 To m

  aPC(i, j) = coef1(i, j) + coef2(i, j)
  aNC(i, j) = coef1(i, j)
  aEC(i, j) = coef2(i, j)
  aWC(i, j) = 0
  SourceC(i, j) = 0

Next j


i = n
For j = 2 To m

  aPC(i, j) = coef1(i, j) + 2 * coef2(i, j) + coef3(i, j)
  aNC(i, j) = coef1(i, j)
  aEC(i, j) = 0
  aWC(i, j) = coef3(i, j)
  SourceC(i, j) = 2 * coef2(i, j) * Cinter(j)

Next j


j = 1
For i = 2 To n - 1

  aPC(i, j) = coef1(i, j) + coef2(i, j) + coef3(i, j)
  aNC(i, j) = 0
  aEC(i, j) = coef2(i, j)
  aWC(i, j) = coef3(i, j)
  SourceC(i, j) = coef1(i, j) * Cent

Next i

i = 1
j = 1

  aPC(i, j) = coef1(i, j) + coef2(i, j)
  aNC(i, j) = 0
  aEC(i, j) = coef2(i, j)
  aWC(i, j) = 0
  SourceC(i, j) = coef1(i, j) * Cent
```

```
i = n
j = 1

  aPC(i, j) = coef1(i, j) + 2 * coef2(i, j) + coef3(i, j)
  aNC(i, j) = 0
  aEC(i, j) = 0
  aWC(i, j) = coef3(i, j)
  SourceC(i, j) = 2 * coef2(i, j) * Cinter(j) + coef1(i, j) * Cent


For i = 2 To n - 1
    For j = 2 To m

  aPC(i, j) = coef1(i, j) + coef2(i, j) + coef3(i, j)
  aNC(i, j) = coef1(i, j)
  aEC(i, j) = coef2(i, j)
  aWC(i, j) = coef3(i, j)
  SourceC(i, j) = 0

    Next j
Next i




'*********************************************************************
'*********************************************************************

'3.2.THREE DIAGONAL MATRIX ALGORITHM


20
iterC = iterC + 1

For i = 1 To n
    For j = 1 To m
          Cold(i, j) = C(i, j)
    Next j
Next i
```

```
For j = 1 To m

        fC(1) = aPC(1, j)

    For i = 2 To n

        fC(i) = aPC(i, j)
        gC(i - 1) = -aEC(i - 1, j)
        eC(i) = -aWC(i, j)

        eC(i) = eC(i) / fC(i - 1)
        fC(i) = fC(i) - eC(i) * gC(i - 1)

    Next i

        rC(1) = SourceC(1, j) + aNC(1, j) * C(1, j - 1)

    For i = 2 To n

        rC(i) = SourceC(i, j) + aNC(i, j) * C(i, j - 1) - eC(i) * rC(i - 1)

    Next i

        C(n, j) = rC(n) / fC(n)

    For i = n - 1 To 1 Step -1

        C(i, j) = (rC(i) - gC(i) * C(i + 1, j)) / fC(i)

    Next i

Next j


For i = 1 To n
    For j = 1 To m
          If Abs(C(i, j) - Cold(i, j)) / C(i, j) > 10 ^ -10 Then GoTo 20
    Next j
Next i
```

```
'*****************************************************************
'*****************************************************************

'4-MASS-ENERGY COUPLING ITERATION ALGORITHM


      For j = 1 To m
            If iteration < 3 Then
               rho = rhoent
               k = kent
               habs = habsent
               D = Dent
            Else
               rho = rhof(T(n, j), C(n, j))
               k = kf(T(n, j), C(n, j))
               habs = habsf(T(n, j), C(n, j))
               D = Df(T(n, j), C(n, j))
            End If

             masscoef = rho * D * habs / k

          Cgrad(j) = relax * (-1 / Cinter(j) * 2 * (Cinter(j) - C(n, j)) / dR) + (1 –
                     relax) * Cgradold(j)
      'If Cgrad(j) < 0 Then Cgrad(j) = -Cgrad(j)
           grad(j) = masscoef * Cgrad(j)

      Next j

iteration = iteration + 1

iterT = 0
iterC = 0

      Print #1,
      Print #1,
      Print #1, "iteration number:"; iteration

For j = 1 To m

convergence(j) = Abs(Abs(Cgrad(j) - Cgradold(j)) / Cgrad(j))

      Print #1, j, convergence(j),
      Print #1,

If convergence(j) > 10 ^ -12 Then GoTo 5

Next j
```

```
'*********************************************************************
'*********************************************************************

'5-COOLING WATER ENERGY BALANCE


For j = 1 To m

k = kf(T(1, j), C(1, j))

CW = ri / rin / Uwall * k / delta(j)
gradcool = -2 * pi * ri * L * k / delta(j) / mc / cpc

gradwallold(j) = gradwall(j)
gradwall(j) = (T(1, j) - Twall(j)) / (dR / 2)
Tc(j) = Tc(j - 1) + gradcool * gradwall(j) * dZ
Twall(j) = Tc(j) + CW * gradwall(j)
Next j

For j = 1 To m
   If Abs(gradwall(j) - gradwallold(j)) / gradwall(j) > 10 ^ -5 Then GoTo 5
Next j

If (Tc(m) - Tcin) / Tcin > 10 ^ -4 Then Tc(0) = 0.5 * (Tc(0) - (Tc(m) - Tcin)) + 0.5 *
                                        Tc(0): GoTo 5

'*********************************************************************
'*********************************************************************

For j = 1 To m
   Twall(j) = -(gradwallold(j) * dR / 2 - T(1, j))
   T(0, j) = Twall(j)
   C(0, j) = C(1, j)
   T(n + 1, j) = Tinter(j)
   C(n + 1, j) = Cinter(j)
Next j

For i = 1 To n
   T(i, 0) = Tent
   C(i, 0) = Cent
   T(i, m + 1) = T(i, m)
   C(i, m + 1) = C(i, m)
Next i

   T(0, 0) = Tent
   T(n + 1, 0) = Tent
   C(0, 0) = Cent
   C(n + 1, 0) = Cent
```

```
    T(0, m + 1) = T(0, m)
    T(n + 1, m + 1) = T(n + 1, m)
    C(0, m + 1) = C(0, m)
    C(n + 1, m + 1) = C(n + 1, m)


'Print the temprature and the concentration field

      ZZ = 0
For j = 0 To m + 1
      RR = 0
For i = 0 To n + 1

      Print #3, RR, ZZ, T(i, j),
      Print #3,
      Print #4, RR, ZZ, C(i, j),
      Print #4,

If i = 0 Or i = n Then
    delr = dR / 2
Else
    delr = dR
End If

RR = RR + delr

Next i

If j = 0 Or j = m Then
    delz = dZ / 2
Else
    delz = dZ
End If

ZZ = ZZ - delz

Next j
```

```
'Print the temperature and the concentration profiles along the transverse direction
'at selected downstream positions

For i = 1 To n

    Print #36, T(i, 1),
    Print #36,
    Print #37, T(i, m / 100),
    Print #37,
    Print #7, T(i, m / 10),
    Print #7,
    Print #8, T(i, 3 * m / 10),
    Print #8,
    Print #9, T(i, m / 2),
    Print #9,
    Print #10, T(i, 7 * m / 10),
    Print #10,
    Print #11, T(i, 9 * m / 10),
    Print #11,

    Print #38, C(i,1),
    Print #38,
    Print #39, C(i, m / 100),
    Print #39,
    Print #12, C(i, m / 10),
    Print #12,
    Print #13, C(i, 3 * m / 10),
    Print #13,
    Print #14, C(i, m / 2),
    Print #14,
    Print #15, C(i, 7 * m / 10),
    Print #15,
    Print #16, C(i, 9 * m / 10),
    Print #16,

Next i


For j = 1 To m

     Print #2, Tinter(j),
     Print #2,
     Print #6, Cinter(j),
     Print #6,
     Print #17, Twall(j),
     Print #17,
     Print #35, C(1, j),
     Print #35,
```

```
Print #18, Tbulk(j),
Print #18,
Print #19, Cbulk(j),
Print #19,

 'Thermophysical properties at the bulk conditions

      mu = muf(Tbulk(j), Cbulk(j))
      k = kf(Tbulk(j), Cbulk(j))
      Refilm = 4 * massflow(j) / 2 / pi / ri / mu

 'Thermophysical properties at the interface conditions

      rho = rhof(T(n, j), C(n, j))
      D = Df(T(n, j), C(n, j))

'Mass flux distribution

      Print #5, (-rho * D / Cinter(j) * 2 / delta(j) * (Cinter(j) - C(n, j)) / dR),
      Print #5,

'Mass transfer coefficient (hm)

      Print #26, D / delta(j) * Cgrad(j) / (Cbulk(j) - Cinter(j)),
      Print #26,

'Sherwood number distribution

      SherW = 1.1 / Refilm ^ (1 / 3) * Cgrad(j) / (Cbulk(j) - Cinter(j))
      Print #22, SherW,
      Print #22,




      meanflux = meanflux + (-rho * D / Cinter(j) * 2 / delta(j) * (Cinter(j) –
                 C(n, j)) / dR) * dZ

      mSH = mSH + SherW * dZ
```

```
'Heat transfer coefficient (hT) and wall-interface heat flux distributions

    kwall = kf(T(1, j), C(1, j))
    kinter = kf(Tinter(j), Cinter(j))

    qw = kwall * (T(1, j) - Twall(j)) / (delta(j) * dR / 2)
    qwmean = qwmean + qw * dZ
    qinter = kinter * (Tinter(j) - T(n, j)) / (delta(j) * dR / 2)
    qintermean = qintermean + qinter * dZ

    hTcoef = qw / (Tbulk(j) - Twall(j))

    Print #27, hTcoef,
    Print #27,
    Print #28, qw,
    Print #28,
    Print #32, qinter,
    Print #32,


'Nusselts number distribution

    rho = rhof(Tbulk(j), Cbulk(j))
    Nus = hTcoef * ((mu / rho) ^ 2 / g) ^ (1 / 3) / k

    Print #24, Nus,
    Print #24,

    mNu = mNu + Nus * dZ

Next j


'Mean Sherwood number
    Print #23, mSH,
    Print #23,

'Mean wall heat flux
    Print #29, qwmean,
    Print #29,

'Mean Nusselts number
    Print #25, mNu,
    Print #25,

'Mean interfacial heat flux
    Print #33, qintermean,
    Print #33,
```

```
'Verifying energy and species balance

For j = 1 To m

        k1 = kf(T(1, j), C(1, j))
        k2 = kf(T(n, j), C(n, j))
        rho = rhof(T(n, j), C(n, j))

conin = conin + k2 * 2 * pi * (ri + delta(j)) * L * dZ * grad(j) / delta(j)
conout = conout - k1 * 2 * pi * ri * L * dZ * (T(1, j) - Twall(j)) / (delta(j) * dR / 2)

Vabsorbed = Vabsorbed + 2 * pi * (ri + delta(j)) * dZ * L * (-rho * D / Cinter(j) * 2 /
                        delta(j) * (Cinter(j) - C(n, j)) / dR)

        Print #31, 1000 * delta(j),
        Print #31,
        Print #34, massflow(j),
        Print #34,

Next j

    cpent = cpf(Tent, Cent)

For i = 1 To n

    'Physical properties at the inlet conditions

    mu = muf(T(i, 1), C(i, 1))
    rho = rhof(T(i, 1), C(i, 1))
    cp = cpf(T(i, 1), C(i, 1))
    Refilm = 4 * massflow(1) / 2 / pi / ri / mu


ein = ein + rho / 1.024 * (3 / 2 * (2 * (i - 0.5) * dR - ((i - 0.5) * dR) ^ 2) * dR *
          Refilm / 4 * mu / rho / delta(1) / dR) * 2 * pi * (ri + (i - 1) * delta(1) * dR)
          * delta(1) * dR * cpent * Tent

vin = vin + rho / 1.024 * (3 / 2 * (2 * (i - 0.5) * dR - ((i - 0.5) * dR) ^ 2) * dR *
      Refilm / 4 * mu / rho / delta(1) / dR) * 2 * pi * (ri + (i - 1) * delta(1) * dR) *
      delta(1) * dR * (1 - Cent)


'Physical properties at the exit conditions

    mu = muf(T(i, m), C(i, m))
    rho = rhof(T(i, m), C(i, m))
    cp = cpf(T(i, m), C(i, m))
    Refilm = 4 * massflow(m) / 2 / pi / ri / mu
```

```
eout = eout - rho / 1.024 * (3 / 2 * (2 * (i - 0.5) * dR - ((i - 0.5) * dR) ^ 2) * dR *
        Refilm / 4 * mu / rho / delta(m) / dR) * 2 * pi * (ri + (i - 1) * delta(m) * dR) *
        delta(m) * dR * cp * T(i, m)

vout = vout - rho / 1.024 * (3 / 2 * (2 * (i - 0.5) * dR - ((i - 0.5) * dR) ^ 2) * dR *
        Refilm / 4 * mu / rho / delta(m) / dR) * 2 * pi * (ri + (i - 1) * delta(m) * dR) *
        delta(m) * dR * (1 - C(i, m))

'1.024 is the numerical correction factor

Next i

    Print #30, "net energy  :", conin + conout + ein + eout,
    Print #30,
    Print #30, "conin       :", conin,
    Print #30,
    Print #30, "conout      :", conout,
    Print #30,
    Print #30, "ein         :", ein,
    Print #30,
    Print #30, "eout        :", eout,
    Print #30,
    Print #30,
    Print #30,
    Print #30, "%err in conc:", -(vout + vin + Vabsorbed) / vout * 100,
    Print #30,
    Print #30, "vout        :", vout,
    Print #30,
    Print #30, "vin         :", vin,
    Print #30,
    Print #30, "vabsorbed   :", Vabsorbed,
    Print #30,
    Print #30,
    Print #30,

    Print #20, "Exit Bulk Temprature   :"; Tbulk(m),
    Print #20,
    Print #20, "Exit Bulk Concentration:"; Cbulk(m),
    Print #20,
    Print #20, "Mean mass flux(kg/m2s) :"; meanflux,
    Print #20,

Close #1, #2, #3, #4, #5, #6, #7, #8, #9, #10, #11, #12, #13
Close #14, #15, #16, #17, #18, #19, #20, #21, #22, #23
Close #24, #25, #26, #27, #28, #29, #30, #31, #32, #33, #34, #35, #36, #37, #38, #39


End Sub
```

```
Public Function muf(T, C)

    muf = (1 + 0.686602333 * Exp(0.107 * 100 * C) * T ^ (-1.238)) / 1000

End Function


Public Function rhof(T, C)

    rhof = 1000 * ((0.7086 + 1.691 * C) - 0.0005 * T)

End Function


Public Function cpf(T, C)

    cpf = 1000 * 19.45818349 * T ^ (0.05) * (100 * C) ^ (-0.609)

End Function


Public Function habsf(T, C)

    habsf = 2.5124 * 10 ^ 6 - (283.3 + 1177 * T) + 20152 * (1660.47 * C ^ 7 - 2550 *
            C ^ 8 + 1410.1 * C ^ 9)

End Function


Public Function Df(T, C)

    Df = 10^9*(0.9622+0.435*(0.01151*rhof(T(i,j),C(i,j))*C(i,j))^0.414) *
         ((273+T(i,j))/298)*(muf(25,C(i,j))/ muf(T(i,j),C(i,j)))

End Function


Public Function kf(T, C)

    kf = 1.163 * (0.4945 + 0.002052 * T - 0.000015 * T ^ 2 - 0.31 * C)

End Function
```

APPENDIX C

```
'*****************************************************************
' HORIZONTAL ABSORBER TEMPRATURE AND CONCENTRATION FIELD
'                          ANALYSIS CODE
'*****************************************************************


'Properties of the model:
'   1)  Physical properties vary with local temprature and concentration.
'   2)  The film thickness varies with the absorption of vapour,
'       and with local bulk temprature and concentration.


'Assumptions to run the model
'   1)  Tube is completely wetted by the solution.
'   2)  At the solution-vapour interface, vapour pressure equilibrium exists.
'   3)  The flow is laminar and non-wavy throughout.
'   4)  No shear forces are exerted on the liquid by the vapour.
'   5)  Convection in the flow direction is much more stronger than diffusion,
'       so diffusion in the flow direction is neglected.
'   6)  Heat transfer in the vapour phase is negligible compared to that in the liquid
'       phase



'Nomenclature:

'    Tent          =  Entrance temprature
'    Cent          =   Entrance concentration
'    Refilm        =   Film reynolds number                  [4 x (massflow / '
                                                             pipe_length) / mu]
'    Pr            =  Prandl number                          [mu x cp / k]
'    Sc            =  Schmidt Number                         [mu/ (rho x D)]
'    ftr           =  Film thickness ratio                   [pi x ro / delta90]
'    masscoef      =  Species-energy eq. coupling coef.      [rho * D * habs / k]
'    CW            =  Coef. from cooling water en. balance   [k / deltamean / Uwall]
'    gradcoolcoef  =  Coef. from cooling water en. balance   [2 * pi * ro * L * k / mc /
'                                                             cpc / deltamean]
'    n             =  Number of control volumes in the downstream (X) direction
'    m             =  Number of control volumes in the transverse (Y) direction
'    nt            =  Number of horizontal tubes arranged vertically

'          mu      =  Dynamic viscosity          [Ns/m2]
'          rho     =  Density                    [kg/m3]
'          k       =  Thermal conductivity       [W/mK]
'          D       =  Mass diffusivity           [m2/s]
'          habs    =  Heat of absorption         [j/kg]
```

```
'           Delta90 =  Film thickness at theta=90    [m]
'           ro      =  Outer diameter of the tube    [m]
'           Cgrad() =  1/Cinter*dC/dY

'NOTE:  'D:\results' folder must be created in order to get the results.
'           Code is set up to run on Visual Basic

Dim T() As Double, C() As Double, Tbulk() As Single, Cbulk() As Single
Dim Told() As Double, Cold() As Double, coef1() As Double, coef2() As Double
Dim Tinter() As Double, Cinter() As Double, Cgrad() As Double
Dim Cgradold() As Double, grad() As Double
Dim convergence() As Double, Twall() As Double, Twallold() As Double
Dim Ux() As Double, mcell() As Double
Dim dX As Double, dY As Double, XX() As Single, YY() As Single,
Dim XXX As Single, YYY As Single


'Discretised Governing Equation Coefficients

'For Energy Eq.
Dim aP() As Double, aN() As Double, aST() As Double, aE() As Double, aW() As
Double, Source() As Double


'For Species Eq.
Dim aPC() As Double, aNC() As Double, aSC() As Double, aEC() As Double,
aWC() As Double, SourceC() As Double


'Three-Diagonal Matrix Algorithm Coefficients

'For Energy Eq.
Dim fT() As Double, eT() As Double, gT() As Double, rT() As Double

'For Species Eq.
Dim fC() As Double, eC() As Double, gC() As Double, rC() As Double
```

```
Private Sub Command1_Click()


'SOLVER CONSISTS OF FIVE MAIN PARTS:

' 1 - DEFINING PROPERTIES
' 2 - TEMPRATURE SOLVER
'    2.2  - Setting up the coefficients
'    2.3  - Three diagonal matrix algorithm
' 3 - CONCENTRATION SOLVER
'    3.1  - Setting up the coefficients
'    3.2  - Three diagonal matrix algorithm
' 4 - MASS-ENERGY COUPLING ITERATION ALGORITHM
' 5 - COOLING WATER ENERGY BALANCE


'*****************************************************************
'*****************************************************************

'1-DEFINING PROPERTIES:


'Grid parameters

n  = 500
m = 200

Xin =  0.001
Xout =   0.999

dX  =  (Xout - Xin) / n
dY  =  1 / m
nt  =  1


ReDim Twall(n + 2, nt + 1) As Double, Twallold(n) As Double
ReDim Tent(nt + 1) As Double, Cent(nt + 1) As Double

'Initial&boundary conditions

Tent(1) = 31
Cent(1) = 0.6
Tcoutestimate = 30.2
pressure = 1250   'Please enter a value between 800-1500 Pa
```

```
'Equilibrium coefficients (depends on absorber pressure, Cif=a * Tif+ b)

    a = 4.8688 / 1000 * (pressure / 1000) ^ -0.188
    b = 0.37794 * (pressure / 1000) ^ -0.06574


'Physical properties at the inlet conditions

 habs   =  habsf(Tent(1), Cent(1))
 D      =  Df(Tent(1), Cent(1))
 rho    =  rhof(Tent(1), Cent(1))
 cp     =  cpf(Tent(1), Cent(1))
 k      =  kf(Tent(1), Cent(1))
 mu     =  muf(Tent(1), Cent(1))
 alpha  =  k / rho / cp


'Cooling water parameters

 mc = 0.43
 cpc = 4180
 Uwall = 6852


'Other parameters

 massflow = 0.00724522
 relax = 0.1        'Underrelaxation factor
 pi = 3.141592653
 g = 9.81


'Physical dimensions
 L   =  0.5
 ro  =  9.525 / 1000

'Film thickness at theta=pi/2 at the inlet conditions
 delta90 = ((3 * massflow / 2 * mu) / rho ^ 2 / g / L) ^ (1 / 3)
 deltamean = 1.2 * delta90
```

```
'*********************************************************************
'*********************************************************************
'Nondimensional input at the inlet conditions
   Pr         =  mu * cp / k
   ftr        =  pi * ro / delta90
   Refilm     =  4 * massflow / 2 / L / mu
   Sc         =  mu / rho / D
   masscoef =  rho * D * habs / k

'For cooling water modeling
   CW             =  k / deltamean / Uwall
   gradcoolcoef  =  -2 * pi * ro * L * k / mc / cpc / deltamean

'*********************************************************************
'*********************************************************************


ReDim T(n + 2, m + 2) As Double, C(n + 2, m + 2) As Double
ReDim Tbulk(n) As Single, Cbulk(n) As Single
ReDim Told(n, m) As Double, Cold(n, m) As Double, coef1(n, m) As Double
ReDim coef2(n, m) As Double
ReDim Tinter(n) As Double, Cinter(n) As Double, Cgrad(n) As Double
ReDim Cgradold(n) As Double, grad(n) As Double
ReDim convergence(n) As Double, Ux(m) As Double, mcell(m) As Double
ReDim XX(n) As Single, YY(m) As Single, fT(m) As Double, gT(m - 1) As Double
ReDim eT(m) As Double, rT(m) As Double
ReDim fC(m) As Double, gC(m - 1) As Double, eC(m) As Double, rC(m) As Double
ReDim aP(n, m) As Double, aN(n, m) As Double, aST(n, m) As Double
ReDim aE(n, m) As Double, aW(n, m) As Double, Source(n, m) As Double
ReDim aPC(n, m) As Double, aNC(n, m) As Double, aSC(n, m) As Double
ReDim aEC(n, m) As Double
ReDim aWC(n, m) As Double, SourceC(n, m) As Double


'Initialization

        For i = 1 To n

          For j = 1 To m
               T(i, j) = Tent(1) - 2
               C(i, j) = Cent(1) - 0.01
          Next j

          For ntu = 0 To nt
               Twall(i, ntu) = 30
           Next ntu

        Next i
```

```
        Tcout = Tcoutestimate

        masscoef = rho * D * habs / k  'initial value

        For i = 1 To n
            Cgrad(i) = 0.0016
            grad(i) = Cgrad(i) * masscoef
        Next i

iteration = 1

Open "d:\results\CWater.txt"                For Output As 7
Open "d:\results\averagefluxes.txt"         For Output As 11
Open "d:\results\INPUTS.txt"                For Output As 12
Open "d:\results\meansherwood.txt"          For Output As 21
Open "d:\results\meannusselts.txt"          For Output As 23
Open "d:\results\delta90.txt"               For Output As 25
Open "d:\results\progcontrol.txt"           For Output As 26
Open "d:\results\qwallmean.txt"             For Output As 29
Open "d:\results\qintermean.txt"            For Output As 30
Open "d:\results\Mass flow rate.txt"        For Output As 31
Open "d:\results\conver.txt"                For Output As 50
Open "d:\results\Twallcontrol.txt"          For Output As 51


      Print #7, "Tube No", "Tcout", "Tcin", "Twall", "Texit", "Cexit", "Tent", "Cent",
      Print #7,

      Print #12, "Solution inlet temp    :"; Tent(1),
      Print #12,
      Print #12, "Solution inlet conc    :"; Cent(1),
      Print #12,
      Print #12, "Cooling water inlet    :"; Tcin,
      Print #12,
      Print #12, "Operating pressure     :"; pressure,
      Print #12,
      Print #12, "Refilm                 :"; Refilm,
      Print #12,
      Print #12, "Pr                     :"; Pr,
      Print #12,
      Print #12, "ftr                    :"; ftr,
      Print #12,
      Print #12, "Sc                     :"; Sc,
      Print #12,
      Print #12, "masscoef               :"; masscoef,
      Print #12,
      Print #12, "gradcoolcoef           :"; gradcoolcoef,
      Print #12,
```

```
Print #12, "CW                    :"; CW,
Print #12,
Print #12, "Cooling water flowrate :"; mc,
Print #12,
Print #12, "Uwall                 :"; Uwall,
Print #12,
Print #12,
Print #12,
Print #12,
Print #12, "Physical Variables     :",
Print #12,
Print #12, "L                     :", L,
Print #12,
Print #12, "ro (mm)               :", ro * 1000,
Print #12,
Print #12, "total massflow        :", massflow,
Print #12,
Print #12, "Initial delta90 (mm)   :", delta90 * 1000,
Print #12,
Print #12,
Print #12,
Print #12, "Initial physical prop  :",
Print #12,
Print #12, "k                     :", k,
Print #12,
Print #12, "mu                    :", mu,
Print #12,
Print #12, "cp                    :", cp,
Print #12,
Print #12, "habs                  :", habs,
Print #12,
Print #12, "D                     :", D,
Print #12,
Print #12, "rho                   :", rho,
Print #12,
Print #12, "alpha                 :", alpha,
Print #12,
```

```
For ntu = 1 To nt 'Calculating solution for each tube

Open "d:\results\convergence\Convergence(" & ntu & ").txt"          For Output As 1
Open "d:\results\Tinter\Tinter(" & ntu & ").txt"                    For Output As 2
Open "d:\results\Temprature\Temprature(" & ntu & ").txt"            For Output As 3
Open "d:\results\Concentration\Concentration(" & ntu & ").txt"      For Output As 4
Open "d:\results\massabsorbed\massabsorbed(" & ntu & ").txt"        For Output As 5
Open "d:\results\Cinter\Cinter(" & ntu & ").txt"                    For Output As 6

Open "d:\results\bulk\Tbulk(" & ntu & ").txt"                       For Output As 8
Open "d:\results\bulk\Cbulk(" & ntu & ").txt"                       For Output As 9
Open "d:\results\bulk\Twall(" & ntu & ").txt"                       For Output As 10

Open "d:\results\profiles\T_X_0.002(" & ntu & ").txt"               For Output As 52
Open "d:\results\profiles\T_X_0.01(" & ntu & ").txt"                For Output As 53
Open "d:\results\profiles\T_X_0.1(" & ntu & ").txt"                 For Output As 13
Open "d:\results\profiles\T_X_0.5(" & ntu & ").txt"                 For Output As 14
Open "d:\results\profiles\T_X_0.9(" & ntu & ").txt"                 For Output As 15

Open "d:\results\profiles\C_X_0.002(" & ntu & ").txt"               For Output As 54
Open "d:\results\profiles\C_X_0.01(" & ntu & ").txt"                For Output As 55
Open "d:\results\profiles\C_X_0.1(" & ntu & ").txt"                 For Output As 16
Open "d:\results\profiles\C_X_0.5(" & ntu & ").txt"                 For Output As 17
Open "d:\results\profiles\C_X_0.9(" & ntu & ").txt"                 For Output As 18

Open "d:\results\massabsorbed\hm(" & ntu & ").txt"                  For Output As 19
Open "d:\results\massabsorbed\Sherwood(" & ntu & ").txt"            For Output As 20
Open "d:\results\Nu\Nu(" & ntu & ").txt"                            For Output As 22
Open "d:\results\Nu\hT(" & ntu & ").txt"                            For Output As 24

Open "d:\results\Nu\qwall(" & ntu & ").txt"                         For Output As 27
Open "d:\results\Nu\qinter(" & ntu & ").txt"                        For Output As 28
Open "d:\results\bulk\Cwall(" & ntu & ").txt"                       For Output As 32
```

```
'*****************************************************************
'*****************************************************************

'2-TEMPRATURE SOLVER:


'2.1.SETTING UP THE COEFFICIENTS


5
For i = 1 To n
Cgradold(i) = Cgrad(i)
Next i

  'Calculation of the film thickness at theta=pi/2
  'using the mean physical properties of each tube,
  'depending on the delta90, the film thickness distribution
  'will be calculated by delta(X) = delta90 / sin(pi.X) ^ (1/3)
        Tmean = Tent(ntu) - 0.5
        Cmean = Cent(ntu) - 0.002
        mumean = muf(Tmean, Cmean)
        rhomean = rhof(Tmean, Cmean)
        kmean = kf(Tmean, Cmean)
        delta90 = ((3 * massflow / 2 * mumean) / rhomean ^ 2 / g / L) ^ (1 / 3)
        deltamean = 1.2 * delta90
        Remean = 4 * massflow / 2 / L / mumean

       'For cooling water modeling
        CW = kmean / deltamean / Uwall
        gradcoolcoef = -2 * pi * ro * L * kmean / mc / cpc / deltamean

For i = 1 To n
          XX(i) = Xin + (i - 0.5) * dX
    For j = 1 To m
          YY(j) = (j - 0.5) * dY

        mu = muf(T(i, j), C(i, j))
        rho = rhof(T(i, j), C(i, j))
        k = kf(T(i, j), C(i, j))
        cp = cpf(T(i, j), C(i, j))
        D = Df(T(i, j), C(i, j))
```

```
  'Program Input
    Refilm = 4 * massflow / 2 / L / mu
    Pr = mu * cp / k
    ftr = pi * ro / delta90

    coef1(i, j) = 0
    coef2(i, j) = 1 / dY * 8 * ftr * (Sin(pi * XX(i))) ^ (1 / 3) / (3 * Refilm * Pr * (2 *
                  YY(j) - YY(j) ^ 2))

    Next j
Next i


j = 1
For i = 2 To n

   aP(i, j) = dY / dX + coef1(i, j) / 2 + 3 * coef2(i, j)
   aN(i, j) = coef2(i, j) - coef1(i, j) / 2
   aST(i, j) = 0
   aE(i, j) = 0
   aW(i, j) = dY / dX
   Source(i, j) = (coef1(i, j) + 2 * coef2(i, j)) * Twall(i, ntu)

Next i


j = m
For i = 2 To n

   aP(i, j) = dY / dX + coef1(i, j) / 2 + coef2(i, j)
   aN(i, j) = 0
   aST(i, j) = coef1(i, j) / 2 + coef2(i, j)
   aE(i, j) = 0
   aW(i, j) = dY / dX
   Source(i, j) = (coef2(i, j) - coef1(i, j) / 2) * dY * grad(i)

Next i
```

```
i = 1
For j = 2 To m - 1

   aP(i, j) = dY / dX + 2 * coef2(i, j)
   aN(i, j) = coef2(i, j) - coef1(i, j) / 2
   aST(i, j) = coef2(i, j) + coef1(i, j) / 2
   aE(i, j) = 0
   aW(i, j) = 0
   Source(i, j) = dY / dX * Tent(ntu)

Next j


i = 1
j = 1

   aP(i, j) = dY / dX + coef1(i, j) / 2 + 3 * coef2(i, j)
   aN(i, j) = coef2(i, j) - coef1(i, j) / 2
   aST(i, j) = 0
   aE(i, j) = 0
   aW(i, j) = 0
   Source(i, j) = (coef1(i, j) + 2 * coef2(i, j)) * Twall(i, ntu) + dY / dX * Tent(ntu)


i = 1
j = m

   aP(i, j) = dY / dX + coef1(i, j) / 2 + coef2(i, j)
   aN(i, j) = 0
   aST(i, j) = coef1(i, j) / 2 + coef2(i, j)
   aE(i, j) = 0
   aW(i, j) = 0
   Source(i, j) = (coef2(i, j) - coef1(i, j) / 2) * dY * grad(i) + dY / dX * Tent(ntu)


For i = 2 To n
For j = 2 To m - 1

   aP(i, j) = dY / dX + 2 * coef2(i, j)
   aN(i, j) = -coef1(i, j) / 2 + coef2(i, j)
   aST(i, j) = coef1(i, j) / 2 + coef2(i, j)
   aE(i, j) = 0
   aW(i, j) = dY / dX
   Source(i, j) = 0

Next j
Next i
```

```
'*****************************************************************
'*****************************************************************

'2.2.THREE DIAGONAL MATRIX ALGORITHM


10
iterT = iterT + 1

For i = 1 To n
    For j = 1 To m
        Told(i, j) = T(i, j)
    Next j
Next i


For i = 1 To n

        fT(1) = aP(i, 1)

   For j = 2 To m

        fT(j) = aP(i, j)
        gT(j - 1) = -aN(i, j - 1)
        eT(j) = -aST(i, j)

        eT(j) = eT(j) / fT(j - 1)
        fT(j) = fT(j) - eT(j) * gT(j - 1)

   Next j

        rT(1) = Source(i, 1) + aW(i, 1) * T(i - 1, 1)

   For j = 2 To m

        rT(j) = Source(i, j) + aW(i, j) * T(i - 1, j) - eT(j) * rT(j - 1)

   Next j

        T(i, m) = rT(m) / fT(m)

   For j = m - 1 To 1 Step -1

        T(i, j) = (rT(j) - gT(j) * T(i, j + 1)) / fT(j)

   Next j

Next i
```

```
For i = 1 To n
   For j = 1 To m
         If Abs(T(i, j) - Told(i, j)) / T(i, j) > 10 ^ -10 Then GoTo 10
   Next j
Next i

      For i = 1 To n

            Tinter(i) = grad(i) * dY / 2 + T(i, m)
            Cinter(i) = a * Tinter(i) + b

      Next i


'*****************************************************************
'*****************************************************************

'3-CONCENTRATION SOLVER:


'3.1.SETTING UP THE COEFFICIENTS


For i = 1 To n
For j = 1 To m

      mu = muf(T(i, j), C(i, j))
      rho = rhof(T(i, j), C(i, j))
      k = kf(T(i, j), C(i, j))
      cp = cpf(T(i, j), C(i, j))
      D = Df(T(i, j), C(i, j))

  'Program Input
   Refilm = 4 * massflow / 2 / L / mu
   ftr = pi * ro / delta90
   Sc = mu / rho / D

   coef1(i, j) = 0
   coef2(i, j) = 1 / dY * 8 * ftr * (Sin(pi * XX(i))) ^ (1 / 3) / (3 * Refilm * Sc * (2 *
                 YY(j) - YY(j) ^ 2))
Next j
Next i
```

```
j = 1
For i = 2 To n

   aPC(i, j) = dY / dX - coef1(i, j) / 2 + coef2(i, j)
   aNC(i, j) = coef2(i, j) - coef1(i, j) / 2
   aSC(i, j) = 0
   aEC(i, j) = 0
   aWC(i, j) = dY / dX
   SourceC(i, j) = 0

Next i


j = m
For i = 2 To n

   aPC(i, j) = dY / dX - coef1(i, j) / 2 + 3 * coef2(i, j)
   aNC(i, j) = 0
   aSC(i, j) = coef1(i, j) / 2 + coef2(i, j)
   aEC(i, j) = 0
   aWC(i, j) = dY / dX
   SourceC(i, j) = (2 * coef2(i, j) - coef1(i, j)) * Cinter(i)

Next i


i = 1
For j = 2 To m - 1

   aPC(i, j) = dY / dX + 2 * coef2(i, j)
   aNC(i, j) = coef2(i, j) - coef1(i, j) / 2
   aSC(i, j) = coef2(i, j) + coef1(i, j) / 2
   aEC(i, j) = 0
   aWC(i, j) = 0
   SourceC(i, j) = dY / dX * Cent(ntu)

Next j


i = 1
j = 1

   aPC(i, j) = dY / dX - coef1(i, j) / 2 + coef2(i, j)
   aNC(i, j) = coef2(i, j) - coef1(i, j) / 2
   aSC(i, j) = 0
   aEC(i, j) = 0
   aWC(i, j) = 0
   SourceC(i, j) = dY / dX * Cent(ntu)
```

```
i = 1
j = m

   aPC(i, j) = dY / dX - coef1(i, j) / 2 + 3 * coef2(i, j)
   aNC(i, j) = 0
   aSC(i, j) = coef1(i, j) / 2 + coef2(i, j)
   aEC(i, j) = 0
   aWC(i, j) = 0
   SourceC(i, j) = (2 * coef2(i, j) - coef1(i, j)) * Cinter(i) + dY / dX * Cent(ntu)


For i = 2 To n
  For j = 2 To m - 1

   aPC(i, j) = dY / dX + 2 * coef2(i, j)
   aNC(i, j) = -coef1(i, j) / 2 + coef2(i, j)
   aSC(i, j) = coef1(i, j) / 2 + coef2(i, j)
   aEC(i, j) = 0
   aWC(i, j) = dY / dX
   SourceC(i, j) = 0

  Next j
Next i









'*********************************************************************
'*********************************************************************

'3.2.THREE DIAGONAL MATRIX ALGORITHM


20
iterC = iterC + 1

For i = 1 To n
    For j = 1 To m
          Cold(i, j) = C(i, j)
    Next j
Next i
```

```
For i = 1 To n

        fC(1) = aPC(i, 1)

    For j = 2 To m

        fC(j) = aPC(i, j)
        gC(j - 1) = -aNC(i, j - 1)
        eC(j) = -aSC(i, j)

        eC(j) = eC(j) / fC(j - 1)
        fC(j) = fC(j) - eC(j) * gC(j - 1)

    Next j

        rC(1) = SourceC(i, 1) + aWC(i, 1) * C(i - 1, 1)

    For j = 2 To m

        rC(j) = SourceC(i, j) + aWC(i, j) * C(i - 1, j) - eC(j) * rC(j - 1)

    Next j

        C(i, m) = rC(m) / fC(m)

    For j = m - 1 To 1 Step -1

        C(i, j) = (rC(j) - gC(j) * C(i, j + 1)) / fC(j)

    Next j

Next i


For i = 1 To n
    For j = 1 To m
            If Abs(C(i, j) - Cold(i, j)) / C(i, j) > 10 ^ -10 Then GoTo 20
    Next j
Next i
```

```
'*****************************************************************
'*****************************************************************

'4-MASS-ENERGY COUPLING ITERATION ALGORITHM


        For i = 1 To n

                rho = rhof(T(i, m), C(i, m))
                k = kf(T(i, m), C(i, m))
                habs = habsf(T(i, m), C(i, m))
                D = Df(T(i, m), C(i, m))

            masscoef = rho * D * habs / k

            Cgrad(i) = relax * (-1 / Cinter(i) * 2 * (Cinter(i) - C(i, m)) / dY) +
                        (1 – relax) * Cgradold(i)
        'If Cgrad(i) < 0 Then Cgrad(i) = -Cgrad(i)
            grad(i) = masscoef * Cgrad(i)

        Next i


iteration = iteration + 1

iterT = 0
iterC = 0

     Print #1,
     Print #1,
     Print #1, "iteration number:"; iteration

For i = 1 To n

convergence(i) = Abs(Cgrad(i) - Cgradold(i)) / Cgrad(i)
     Print #1, i, convergence(i),
     Print #1,
If convergence(i) > 10 ^ -10 Then GoTo 5

Next i
```

```
'*****************************************************************
'*****************************************************************

'5-COOLING WATER ENERGY BALANCE


If parameter = 1 Then GoTo 50
  'Cooling water temprature gradient is assumed to be constant in the axial direction,
  'If wall temprature and wall heat flux at inlet converges,
  'parameter=1 means directly go to the middle of the tube,
  'and assume the same wall heat flux and calculate mean tube wall temprature at
  'z=L/2.

gradwall = 0
For i = 1 To n
  'Mean solution temprature gradient at the wall
    gradwall = gradwall + (T(i, 1) - Twall(i, ntu)) / (dY / 2) / n
Next i

Tc = 0.5 * gradcoolcoef * gradwall + Tcout
  'Average cooling water temprature is calculated at axial position L/2,
  '0,5 stands for indicating half of the tube in the non-dimensional form Z=z/L.
Tcin = 1 * gradcoolcoef * gradwall + Tcout

      Print #51,
      Print #51,

For i = 1 To n

      Twallold(i) = Twall(i, ntu)
      gradwall = (T(i, 1) - Twall(i, ntu)) / (dY / 2)
      Twall(i, ntu) = 0.2 * (CW * gradwall + Tc) + 0.8 * Twallold(i)

      Print #51, i, Twall(i, ntu),
      Print #51,

Next i

      Print #50,
      Print #50,
```

```
For i = 1 To n

    Print #50, i, Abs(Twall(i, ntu) - Twallold(i)) / Twall(i, ntu),
    Print #50,

    If Abs(Twall(i, ntu) - Twallold(i)) / Twall(i, ntu) > 10 ^ -5 Then GoTo 5

Next i

parameter = 1
'Now use this mean wall temprature and skip above iteration.
GoTo 5

'*********************************************************************
'*********************************************************************

50
For i = 1 To n
   T(i, 0) = Twall(i, ntu)
   C(i, 0) = C(i, 1)
   T(i, m + 1) = Tinter(i)
   C(i, m + 1) = Cinter(i)
Next i

For j = 1 To m
   T(0, j) = Tent(ntu)
   C(0, j) = Cent(ntu)
   T(n + 1, j) = T(n, j)
   C(n + 1, j) = C(n, j)
Next j

   T(0, 0) = Tent(ntu)
   T(0, m + 1) = Tent(ntu)
   C(0, 0) = Cent(ntu)
   C(0, m + 1) = Cent(ntu)

   T(n + 1, 0) = T(n, 0)
   T(n + 1, m + 1) = T(n, m + 1)
   C(n + 1, 0) = C(n, 0)
   C(n + 1, m + 1) = C(n, m + 1)
```

```
YYY = 0

For j = 0 To m + 1

XXX = Xin

For i = 0 To n + 1

      Print #3, XXX, YYY, T(i, j),
      Print #3,
      Print #4, XXX, YYY, C(i, j),
      Print #4,

If i = 0 Or i = n Then
   delx = dX / 2
Else
   delx = dX
End If

XXX = XXX + delx

Next i

If j = 0 Or j = m Then
   dely = dY / 2
Else
   de ly = dY
End If

YYY = YYY + dely

Next j


For i = 1 To n
For j = 1 To m

       Tmean = Tent(ntu) - 0.5
       Cmean = Cent(ntu) - 0.002
       mu = muf(Tmean, Cmean)
       rho = rhof(Tmean, Cmean)
       k = kf(Tmean, Cmean)
       cp = cpf(Tmean, Cmean)
       Refilm = 4 * massflow / 2 / L / mu

 Ux(j) = rho * g / mu * (YY(j) - 0.5 * YY(j) ^ 2) * delta90 ^ 2 * (Sin(pi * XX(i))) ^
         (1 / 3)
 mcell(j) = rho * Ux(j) * L * dY * delta90 / (Sin(pi * XX(i))) ^ (1 / 3) / 1.000045
```

```
 'The coefficient 1.00045 is the correction factor for the numerical error.
  Tbulk(i) = Tbulk(i) + T(i, j) * mcell(j) / (massflow / 2)
  Cbulk(i) = Cbulk(i) + C(i, j) * mcell(j) / (massflow / 2)
Next j

       mu = muf(T(i, m), C(i, m))
       rho = rhof(T(i, m), C(i, m))
       Refilm = 4 * massflow / 2 / L / mu

      Print #5, rho * D * (-1 / Cinter(i) * 2 * (Cinter(i) - C(i, m)) / dY) / delta90 *
                (Sin(pi * XX(i))) ^ (1 / 3),
      Print #5,

     'Interface mass transfer coefficient distribution
      Print #19, D * (Sin(pi * XX(i))) ^ (1 / 3) / delta90 * Cgrad(i) / (Cbulk(i) –
                 Cinter(i)),
      Print #19,

     'Interface Sherwood number distribution
      Print #20, 1.1 * (Sin(pi * XX(i))) ^ (1 / 3) / Refilm ^ (1 / 3) * Cgrad(i) /
                 (Cbulk(i) - Cinter(i)),
      Print #20,

     'Wall heat transfer coefficient distribution
     '     k2 is the heat conduction coefficient at the wall surface conditions
           k2 = kf(T(i, 1), C(i, 1))
           qw = k2 * 2 * (T(i, 1) - Twall(i, ntu)) / (dY * delta90 / Sin(pi * XX(i)) ^ (1 /
                3))
           qwmean = qwmean + qw / n

     '     k1 is the heat conduction coefficient at the interfacial conditions
           k1 = kf(T(i, m), C(i, m))
           qinter = k1 * 2 * (Tinter(i) - T(i, m)) / (dY * delta90 / Sin(pi * XX(i)) ^ (1 /
                    3))
           qintermean = qintermean + qinter / n

           hTcoef = qw / (Tbulk(i) - Twall(i, ntu))

      Print #24, hTcoef,
      Print #24,

      Print #27, qw,
      Print #27,
      Print #28, qinter,
      Print #28,
```

```
'Wall Nusselts number distribution

    Nus = hTcoef / k2 * ((mu / rho) ^ 2 / g) ^ (1 / 3)

Print #22, Nus,
Print #22,


'Mean mass flux at the interface

  meanflux = meanflux + rho * D * (-1 / Cinter(i) * 2 * (Cinter(i) - C(i, m)) / dY) /
             delta90 * (Sin(pi * XX(i))) ^ (1 / 3) / n

'Mean Sherwood number

   mSH = mSH + 1.1 * (Sin(pi * XX(i))) ^ (1 / 3) / Refilm ^ (1 / 3) * Cgrad(i) /
         (Cbulk(i) - Cinter(i)) / n


'Mean Nusselts number

   mNu = mNu + Nus / n

  Print #2, Tinter(i),
  Print #2,
  Print #6, Cinter(i),
  Print #6,
  Print #8, Tbulk(i),
  Print #8,
  Print #9, Cbulk(i),
  Print #9,
  Print #10, Twall(i, ntu),
  Print #10,
  Print #32, C(i, 1),
  Print #32,

Next i


'Print mean values for mass flux, Sherwood and Nusselts numbers.
Print #11, meanflux,
Print #11,
Print #21, mSH,
Print #21,
Print #23, mNu,
Print #23,
```

```
'Selected temprature and concentraion profiles in the transverse direction.

For j = 1 To m

    Print #52, T(1, j),
    Print #52,
    Print #53, T(n / 100, j),
    Print #53,
    Print #13, T(n / 10, j),
    Print #13,
    Print #14, T(n / 2, j),
    Print #14,
    Print #15, T(9 * n / 10, j),
    Print #15,

    Print #54, C(1, j),
    Print #54,
    Print #55, C(n / 100, j),
    Print #55,
    Print #16, C(n / 10, j),
    Print #16,
    Print #17, C(n / 2, j),
    Print #17,
    Print #18, C(9 * n / 10, j),
    Print #18,
Next j

Texit = Tbulk(n)
Cexit = Cbulk(n)

    Print #7, ntu, Tcout, Tcin, Twall(i, ntu), Texit, Cexit, Tent(ntu), Cent(ntu),
    Print #7,
```

```
'Energy-Mass balance control

For i = 1 To n

      'Physical properties at the wall and the interface are evaluated to obtain fluxes
       k1 = kf(Tinter(i), Cinter(i))
       k2 = kf(Twall(i, ntu), C(i, 1))
       rho = 1000 * ((0.7086 + 1.691 * C(i, m)) - 0.0005 * T(i, m))

conin = conin + L * k1 * pi * ro * dX * grad(i) / (delta90 / Sin(pi * XX(i)) ^ (1 / 3))
conout = conout - L * k2 * pi * ro * dX * 2 * (T(i, 1) - Twall(i, ntu)) / (dY * delta90
                        / Sin(pi * XX(i)) ^ (1 / 3))

vabsorbed = vabsorbed + rho * D * Cgrad(i) / delta90 * (Sin(pi * XX(i))) ^ (1 / 3) *
                    L * pi * (ftr * delta90 / pi + delta90 / (Sin(pi * XX(i))) ^ (1 / 3)) * dX

Next i

       cp = cpf(Tent(ntu), Cent(ntu))

  ein = massflow / 2 * cp * Tent(ntu)
  vin = massflow / 2 * (1 - Cent(ntu))

For j = 1 To m
       cp = cpf(T(n, j), C(n, j))
  eout = eout - mcell(j) * cp * T(n + 1, j)
  vout = vout - mcell(j) * (1 - C(n + 1, j))
Next j

      Print #26, "net energy  :", ntu, conin + conout + ein + eout,
      Print #26,
      Print #26, "conin       :", ntu, conin,
      Print #26,
      Print #26, "conout      :", ntu, conout,
      Print #26,
      Print #26, "ein         :", ntu, ein,
      Print #26,
      Print #26, "eout        :", ntu, eout,
      Print #26,
      Print #26,
      Print #26,
      Print #26,

      Print #26, "%err in conc:", ntu, -(vout + vin + vabsorbed) / vout * 100,
      Print #26,
      Print #26, "vout        :", ntu, vout,
      Print #26,
      Print #26, "vin         :", ntu, vin,
```

```
        Print #26,
        Print #26, "vabsorbed   :", ntu, vabsorbed,
        Print #26,
        Print #26,
        Print #26,
        Print #31, massflow,
        Print #31,

  massflow = massflow + 2 * vabsorbed

conin = 0
conout = 0
vabsorbed = 0
ein = 0
vin = 0
eout = 0
vout = 0

        'Print the delta at theta=pi/2 for each tube
         Print #25, delta90 * 1000,
         Print #25,
         Print #29, qwmean,
         Print #29,
         Print #30, qintermean,
         Print #30,

Close #1, #2, #3, #4, #5, #6, #8, #9, #10, #13, #14, #15, #16, #17, #18, #19, #20,
#22, #24, #27, #28, #32, #52, #53, #54, #55

  Tcout = Tcin
  Tent(ntu + 1) = Texit
  Cent(ntu + 1) = Cexit
  parameter = 0
  meanflux = 0
  qwmean = 0
  qintermean = 0
  mSH = 0
  mNu = 0

  For i = 1 To n
  Tbulk(i) = 0
  Cbulk(i) = 0
  Next i

Next ntu
Close #7, #11, #12, #21, #23, #25, #26, #29, #30, #31, #50, #51

End Sub
```

```
Public Function rhof(TT, CC)

    rhof = 1000 * ((0.7086 + 1.691 * CC) - 0.0005 * TT)

End Function


Public Function kf(TT, CC)

    kf = 1.163 * (0.4945 + 0.002052 * TT - 0.000015 * TT ^ 2 - 0.31 * CC)

End Function


Public Function cpf(TT, CC)

    cpf = 1000 * 19.45818349 * TT ^ (0.05) * (100 * CC) ^ (-0.609)

End Function


Public Function muf(TT, CC)

    muf = (1 + 0.686602333 * Exp(0.107 * 100 * CC) * TT ^ (-1.238)) / 1000

End Function


Public Function Df(TT, CC)

    Df = 10^9*(0.9622+0.435*(0.01151*rhof(T(i,j),C(i,j))*C(i,j))^0.414) *
         ((273+T(i,j))/298)*(muf(25,C(i,j))/ muf(T(i,j),C(i,j)))

End Function


Public Function habsf(TT, CC)

habsf = 2.5124 * 10 ^ 6 - (283.3 + 1177 * TT) + 20152 * (1660.47 * CC ^ 7 - 2550 *
        CC ^ 8 + 1410.1 * CC ^ 9)

End Function
```